Improving Blood Brain Barrier Permeation of Small Molecules Exhibiting Chemotherapeutic and Neuroprotective Effects

By

Kelly E. Desino

B.S., Biology, University of Michigan, Ann Arbor, MI, 1998
M.S., Pharmaceutical Chemistry, The University of Kansas, Lawrence, KS 2006

Submitted to the Department of Pharmaceutical Chemistry and the faculty of the Graduate School of The University of Kansas in partial fulfillment of the requirements for the degree of Doctor of Philosophy.

_____
Chairperson

Dissertation committee:

_____

_____

_____

_____

Dissertation Defense: April 24, 2008

This dissertation is dedicated to my daughter Lilly, may she grow up in a world where we don't have to watch loved ones suffer from diseases like Alzheimer's and cancer.

ABSTRACT

The blood brain barrier is the body's natural defense system for limiting the brain's exposure to potentially harmful xenobiotics. This barrier exists between the blood of the systemic circulation and the brain and is made up of brain endothelial cells which have tight junctions, reduced pinocytosis, minimal fenestration and increased expression of metabolizing enzymes and membrane transporters capable of efflux. Estimates predict that the blood brain barrier may be capable of limiting up to 98% of all drugs from entering the brain and is therefore a major obstacle in drug delivery. The research presented herein highlights several small molecules that possess chemotherapeutic and neuroprotective properties. These molecules also represent various strategies for improving blood brain barrier penetration. Derivatives of the microtubule stabilizing agent paclitaxel were investigated in which chemical modification was employed to reduce interaction with the efflux transporter P-glycoprotein, which is critical in limiting paclitaxel's entry into the brain. TH-237A, another microtubule stabilizing agent that is structurally very different from paclitaxel was also characterized and was shown to have excellent blood brain barrier penetration. Additionally, derivatives of the monoamine oxidase inhibitor tranylcypromine were explored that have fatty acid and lipoamino acid chains of varying length attached to improve blood brain barrier permeability. In order for these compounds to exert their mechanism of action as either chemotherapeutic or neuroprotective agents, they must be able to penetrate the blood brain barrier. The specific objective of this project was to explore various chemical approaches to improving blood brain barrier permeability using pharmacologically relevant molecules.

ACKNOWLEDGEMENTS

I would like to thank my research advisor, Dr. Kenneth L. Audus for his support and guidance throughout my graduate career. Ken, I appreciate everything you have done for me and although I didn't see you very often, I always knew you were just an email or a phone call away. I also want to thank you for being so supportive in my decision to start a family while in graduate school. I truly appreciate it.

I would also like to thank my dissertation committee: Dr. Ronald T. Borchardt, Dr. Sue M. Lunte, Dr. Teruna J. Siahaan and Dr. Mary Lou Michaelis. I know all of you have very busy schedules and I appreciate you taking the time to serve on my committee. I especially want to thank Drs. Lunte and Siahaan for their helpful and insightful comments as readers.

There are many great scientists with whom I collaborated with that I would also like to thank. Dr. Gunda Georg and her medicinal chemistry students and post-docs for all their efforts in synthesizing many of the small molecules described in this dissertation. Thank you to Dr. Jared T. Spletstoser, Dr. Brandon J. Turunen, Dr. Haibo Ge, Dr. Jariat Oyetunji, Dr. Emily Reiff, and Dr. Hanumaiah Telikepalli. Also, a thank you to Dr. Mary Lou Michaelis and Dr. Sabah Ansar for their work with the neuroprotection assays. Thank you to Dr. Brian J. Blagg and his laboratory for their collaboration on the Hsp90 inhibitor project. Thank you to Dr. Salvatore Guccione for the wonderful opportunity to visit your laboratory in Catania, Italy and work with you on multiple projects. I would also like to thank the graduate students and post-docs in the Department of

Pharmaceutical Chemistry who helped me in the lab. Thank you to Dr. Veena Vasandani, Dr. Erik Rytting, Dr. Amber Young, Dr. Arvind Chappa, Dr. Daniel Mudra, Pallabi Mitra, and Courtney Kuhnline.

My time here would not have been nearly as enjoyable if it were not for all the wonderful friendships I made. I especially want to thank Diana Sperger, Courtney Kuhnline, Becky Bross, Dan Mudra, Joe Lubach, Bill Marinaro, Kevin Head, Dave Fischer, Ben Nelson, Allyn Kaufmann, Bob Berendt, Natalie Ciaccio, Maria Thorson, Laura Peek and Nancy Helm for their friendships. A special thank you is also in order to Dan Mudra and Dave Fischer who were immensely helpful while studying for prelims. I don't know how I would have made it through without you guys! Also, thank you to Pallabi Mitra, my one and only labmate over the past couple years and all the members of the Krise lab for making the lab a fun and enjoyable place to work.

Thank you to the following organizations for funding throughout my graduate career: The NIGMS Biotechnology Training Grant, the National Cancer Institute (1 RO1 CA82801), the Novartis Fellowship and the Department of Pharmaceutical Chemistry.

Last, but certainly not least, I would like to thank my family. Thank you to my parents, Larry and Kathy Rizor for instilling in me a love of learning and for teaching me to always challenge myself. I wouldn't be where I am today without your wonderful parenting and constant support. Thank you to my brother Derek, who always knows how to make me laugh. Most of all, thank you to my husband Jason and my precious daughter

Lilly. Lilly you are the light of my life and you remind me every day what the truly important things in life are. Jason you are the best friend, colleague, father and husband anyone could ask for. Your support during graduate school has been phenomenal and I don't know if I could have done it without you. I love you very much. Thank you!

Improving Blood Brain Barrier Permeability of Small Molecules Exhibiting Chemotherapeutic and Neuroprotective Effects

Table of Contents

1. Introduction

The delivery of pharmaceutical agents to the brain remains one of the greatest challenges in drug delivery. The central nervous system has evolved many biological mechanisms to protect the brain from circulating toxins, including the blood brain barrier. This protective barrier is formed by the brain capillary endothelial cells that are characterized by tight junctions, reduced pinocytosis and minimal fenestration (Reese and Karnovsky, 1967; Brightman and Reese, 1969). Additionally, these brain endothelial cells have increased expression of transport proteins capable of drug efflux (Hegmann *et al*., 1992; Tatsuta *et al*., 1992; Huai-Yun *et al*., 1998) as well as metabolizing enzymes (Spatz and Mrsula, 1982). In order for drugs to reach specific targets within the brain for treatment of diseases such as cancer, Alzheimer's, etc. the molecules must be able to circumvent these barriers. Current strategies for delivery of drugs to the brain vary and each has its own individual successes and failures.

1.1 Strategies for drug delivery to the brain

A variety of delivery strategies exist for achieving drug exposure within the central nervous system, and many of these have arisen from a need for successful treatment options for patients with primary and metastatic brain tumors. Current strategies include, but are not limited to, osmotic and chemical disruption of the blood brain barrier, direct injection or infusion into the brain, concurrent administration of drug efflux inhibitors,

targeting of endogenous uptake transporters expressed at the brain endothelium, and chemical modification of existing pharmacologic agents (Groothuis, 2000).

The idea of transient disruption of the blood brain barrier has been around for some time, first proposed by Rapoport *et al.* in the 1970's (Rapoport and Thompson, 1973). This method involves the infusion of a hyperosmolar solution, usually mannitol, into a cerebral artery resulting in a transient increase in permeability due to osmotic shrinkage of the endothelial cells. The use of pharmacologic agents as transient disruptors has also been explored. Lobradimil (Cereport, RMP-7) is a bradykinin analog that has been clinically tested as a CNS enhancing agent (Bartus *et al*., 1996). Interestingly, it was found that the disruption caused by lobradimil was more pronounced in brain-tumor vasculature than in normal brain tissue which could be beneficial in the treatment of primary and metastatic brain tumors. This method of delivery, however, has obvious disadvantages, including its invasive nature as well as its transient effect. Furthermore, during this disruption, the BBB is not able to preserve the delicate homeostasis it has been designed to maintain, and this can potentially result in a host of complications.

Direct injection or infusion is one of the less elegant, but nevertheless effective methods of drug delivery into the brain. In this case, the blood brain barrier is bypassed completely and close to 100% of the administered dose can be delivered. Administration can be intrathecal, intratumoral, or intraventricular, but the principal disadvantages are the same- unpredictable distribution relying solely on diffusion, highly invasive nature, and risk for neurotoxicity in healthy tissue (Groothuis, 2000). Recently, the technique of

convection-enhanced therapy (CED) has been developed in an attempt to overcome the diffusion problem (Morrison *et al*., 1999; Croteau *et al*., 2005). This is a technique in which the therapeutic agent is pumped into the target tissue with a pressure differential. Although some efficacy has been observed in preclinical trials (Kaiser *et al*., 2000; Degen *et al*., 2003), the potential for success in humans has yet to be seen.

Exclusion of drugs caused by efflux proteins (eg: P-gp, MRP, BCRP) expressed at the blood brain barrier presents an additional challenge, and inhibition of these protein systems has been explored (Nobili *et al*., 2006; O'Connor, 2007). Clinical trials of molecules designed to inhibit P-glycoprotein are ongoing and include inhibitors such as cyclosporine A and PSC833 (Sikic *et al*., 1997). To date the results have not been too promising and the failure is most likely due to their nonspecific affinity to the efflux protein as well as the redundant mechanisms of exclusion that exist at the BBB. The risk of drug-drug interactions is also a concern with the use of these inhibitors and could have major effects on pharmacokinetics and toxicity of the parent compound.

Targeting of endogenous uptake transporters expressed at the brain endothelium has not been commonly pursued, but has been explored in other fields with some success. The intestinal permeation of the antiviral drug acyclovir was enhanced by attaching a valine moiety to the drug. The new prodrug, valacyclovir, had increased permeability due to its recognition by an endogenous peptide transporter (de Vrueh *et al*., 1998). Interestingly enough, it was not due to recognition by an amino acid transporter as might have been expected. This strategy, while more commonly seen when attempting to improve

intestinal permeability may be a feasible strategy in improving delivery across the BBB. Sakaeda *et al.* showed that the blood brain barrier permeability of an analogue of the antitumor agent D-Mephalan, could be increased by conjugation with L-glutamate (Sakaeda *et al*., 2000). Additionally, Walker *et al.* showed that the permeability of the antiviral agent phosphonoformate could be improved across porcine brain microvessel endothelial cells following conjugation with L-Tyrosine (Walker *et al*., 1994). Capillary endothelial cells are known to express carriers for the uptake of essential substances such as amino acids, monocarboxylic acids, amines and biotin (Pardridge and Oldendorf, 1977; Pardridge, 1986). Studies investigating the attachment of nutrient groups including succinate and biotin derivatives in an attempt to improve blood brain barrier permeability have been performed in our laboratory and will be discussed herein.

Chemical modification of existing drugs may be one of the best strategies for improving delivery across the BBB and extensive work in this area has been done in our laboratory. Chemical modifications that retain potency but improve the overall physicochemical characteristics of the molecule, or eliminate recognition elements which cause the molecule to be excluded by efflux proteins, may hold the most promise. Furthermore, it should not be overlooked that the principle route by which most molecules cross the blood brain barrier is by passive diffusion. Thus the incorporation of favorable physicochemical properties or discovery of new molecules with inherently good physicochemical properties may be the most successful approach, as was demonstrated with the novel small molecule agents described in Chapters 3 and 4.

1.2 Disease states of the central nervous system

A large number of CNS diseases exist and their treatment remains a great challenge to the pharmaceutical industry. Treatment is often complicated by the very restrictive nature of the blood brain barrier.

Although the incidence of primary brain tumor is relatively low compared to other types of cancer, the prognosis is quite bleak. Chemotherapeutics, such as paclitaxel, that are effective in combating other cancers, cannot be used to treat tumors within the CNS due to their inability to cross the BBB (Fellner *et al*., 2002). Treatment of neurodegenerative diseases such as Alzheimer's has also been hampered by an inability to achieve therapeutic levels of drug at the site of action (Jolliet-Riant and Tillement, 1999; Bodor and Buchwald, 2002). Interestingly, research detailed in the following chapters describes compounds with potentially good blood brain permeability that have the unique feature of being both chemotherapeutic as well as neuroprotective against the β-amyloid induced neurodegeneration that occurs in Alzheimer's disease. These molecules include structural analogues of paclitaxel, a novel small molecule called TH-237A and a novel Hsp90 inhibitor, A4. These compounds have been shown to stabilize microtubules. It is via this mechanism that they are purported to induce cell death in cancer cells as well as maintain the integrity of the cytoskeletal network which may help neurons survive the toxic effects of β-amyloid (Michaelis *et al*., 2005). Additionally, the blood brain barrier permeability of TCP-FA4 is described, and this is a derivative of the monoamine oxidase inhibitor tranylcypromine. Although TCP-FA4 could be potentially neuroprotective it

does not demonstrate the dual function of being chemotherapeutic like the other compounds described.

1.3 Techniques for studying blood brain barrier permeability

A variety of techniques exist for studying the permeability of pharmaceuticals across the blood brain barrier. Although no one technique is perfect, these methods are invaluable tools for helping researchers understand the complex biology of the blood brain barrier. Used together these various *in vitro* and *in situ* models can be used to predict the likelihood of a pharmaceutical agent crossing the blood brain barrier and are, therefore, essential to the drug discovery process when the site of action lies within the central nervous system.

1.3.1 Cell culture models

It is widely accepted that cell culture is among the most suitable of the models used to predict blood brain barrier permeability. Brain microvessel endothelial cells (BBMECs) grown in culture offer a brain-derived, primary cell line with many of the physiological characteristics of the blood brain barrier including minimal fenestra and reduced pinocytic vesicles (Audus and Borchardt, 1987). Additionally, many enzymes associated with the blood brain barrier are expressed in the BBMEC system including alkaline phosphatase, angiotensin-converting enzyme and monoamine oxidase (Audus and Borchardt, 1987). The existence of membrane proteins responsible for both efflux and

uptake of molecules has also been shown in BBMECs. These include the efflux transporters P-glycoprotein (Fontaine *et al*., 1996) and multidrug resistance-associated protein (MRP) (Huai-Yun *et al*., 1998). Additionally, nutrient uptake transporters have been characterized in BBMECs including a biotin uptake system (Shi *et al*., 1993) and evidence exists for monocarboxylic acid, dipeptide and neutral amino acid transporters (Audus and Borchardt, 1986). Since the BBMECs are a primary cell line that does not retain their morphological features upon repeated passage, there have been attempts to establish an immortalized cell line.

TBMECs are an immortalized cell line in which brain microvessel endothelial cells are transfected with a plasmid containing the middle-T antigen gene from polyoma virus (Yazdanian and Bormann, 2000). They grow monolayers in culture and maintain an endothelial cell phenotype after repeated passages. Although the TBMECs express functional P-gp, as evidenced by an increase in cellular uptake of P-gp substrates such as rhodamine 123 in the presence of P-gp inhibitors, they lack asymmetry in the efflux of P-gp substrates as compared to primary BBMECs (Rice, 2002). Therefore, their utility in studying efflux transporters is limited to studying cellular uptake. However, these cells have the advantage over primary BBMECs that it is not necessary to perform repeated isolations and confluent monolayers form more rapidly (7 days versus 14 days for primary BBMECs).

1.3.2 Side-bi-Side™ diffusion chambers

BBMECs grown on permeable filters or filter inserts allow one to study the transport properties of various molecules across the cell monolayer. Although the convenient and disposable Transwell® insert system can be used for BBMECs, the cells tend to not grow as well at the edges of the filter and this phenomenon results in a leakier monolayer as evidenced by increased flux of low permeability markers. Additionally the Transwell® system lacks convenient temperature control and agitation of the unstirred water layer can be challenging. Therefore, a Side-bi-Side™ diffusion apparatus (Crown Glass, Inc. Somerville, NJ) was used for the permeability studies described in the following chapters. This set up consists of two glass chambers surrounded by thermal jackets which are maintained by a circulating water bath. BBMECs are grown on polycarbonate membranes (13 mm diameter, 0.4 μm pore size) which are mounted horizontally between the two chambers. Chambers are filled with an aqueous buffer solution which is stirred by magnetic stir bars driven by and external drive console (Figure 1.1).

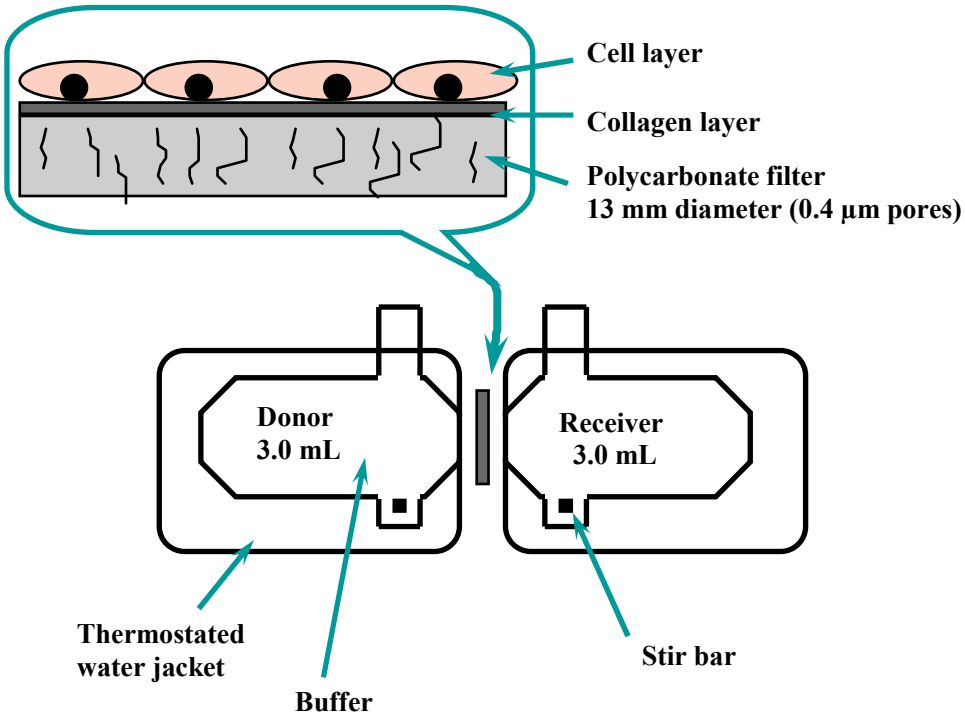

Figure 1.1 Schematic of the Side-bi-Side™ diffusion apparatus (Ho *et al*., 1999)

Permeability studies are conducted by filling the donor (luminal) and receiver (abluminal) chambers with PBSA (phosphate buffered saline supplemented with $CaCl_2$, $MgSO_4$, glucose and L-ascorbic acid) pre-warmed to 37 degrees C. The donor side is then spiked with test compound at the desired concentration (typically 5-10 µM) and stirring of the chambers begins. Aliquots are removed from the donor chambers at time zero to establish concentration and subsequently from the receiver chambers at various time points. The removal of each aliquot from the receiver chamber is followed by replacement with blank PBSA pre-warmed to 37 degrees C, which eliminates any volume differences between the chambers that could affect flux. Upon completion of the study,

[^{14}C]-sucrose, a low permeability paracellular marker, is added to the donor chamber in trace quantities and aliquots are removed from the receiver chamber at 10, 20 and 30 minutes. Samples are analyzed by liquid scintillation counting and the permeability of sucrose is calculated. This exercise serves as a control to insure that monolayer integrity has not been disrupted throughout the course of the study. A sucrose permeability of approximately 5 x 10^{-5} cm/sec is expected if the monolayer has remained intact.

Modifications to this experimental setup can offer additional information. For example, studies can be performed to monitor the asymmetric transport of compounds by spiking the receiver solution and calculating flux in the abluminal to luminal direction. Also, the temperature of the chambers can be reduced to 4 degrees to determine the effects of a reduction in ATP activity. Furthermore, the determination of a compound's permeability at a range of temperatures can be used to generate an Arrhenius plot from which an activation energy of transport can be calculated.

1.3.3 Rhodamine 123 uptake assay

Another *in vitro* assay utilizing BBMECs can be used for prediction of a drug's interaction with the efflux transporter P-glycoprotein. In this cellular uptake assay, the fluorescent dye, rhodamine 123 is used as a surrogate P-gp substrate (Fontaine *et al*., 1996). The effect of the test compound on intracellular accumulation of rhodamine 123 is determined by monitoring intracellular fluorescence (excitation λ: 485, emission λ: 530). If the test compound is a substrate for P-gp, then addition of the compound will

increase rhodamine 123 uptake relative to the negative control. This *in vitro* assay was used extensively for the work described in upcoming chapters in which structurally modified analogues of paclitaxel were screened for interaction with P-gp. Observation by confocal microscopy confirms that there is minimal rhodamine 123 accumulation in BBMECs following incubation with a 5 μM solution of rhodamine 123. However, in the presence of 10 μM paclitaxel, another known substrate for P-gp, the intracellular accumulation of rhodamine 123 is greatly increased and is distributed throughout the cell (Figure 1.2).

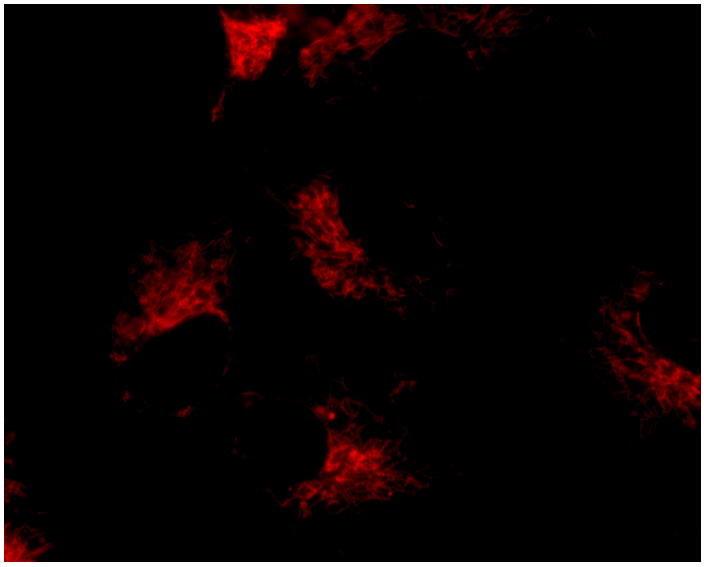

Figure 1.2.1 Rhodamine 123 accumulation in BBMECs after treatment with 5 μM rhodamine 123.

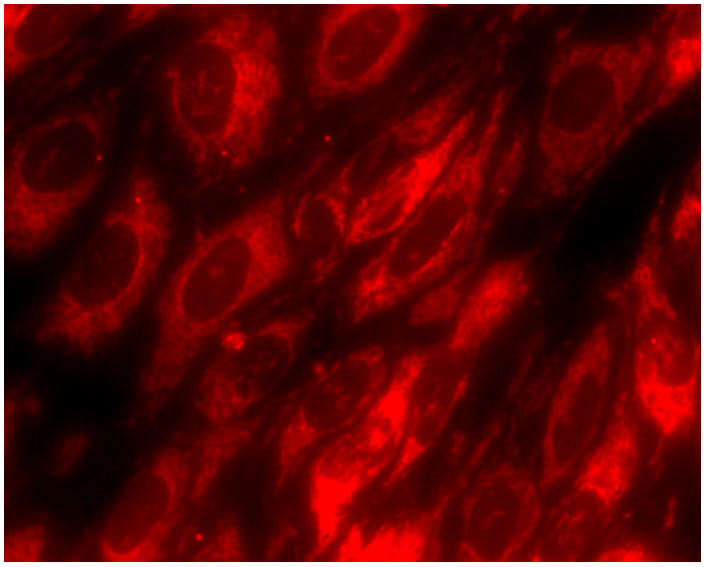

Figure 1.2.2 Rhodamine 123 accumulation in BBMECs after treatment with 5 μM rhodamine 123 in the presence of 10 μM paclitaxel.

1.3.4 In situ *rat brain perfusion*

Unfortunately, cell culture models do not fully incorporate the complexity of the *in vivo* situation, and therefore additional methods must sometimes be used for validation of the *in vitro* findings. A commonly used technique is the *in situ* rat brain perfusion in which a solution containing test compound is delivered directly into the brain via the carotid artery (Smith, 1996). This technique allows investigators to control both the concentration and time of drug administeration. Furthermore, since the compound is not exposed to peripheral metabolizing enzymes, the complexity of the system is minimized. Brain uptake kinetics can be examined and permeability constants can be calculated.

1.4 Specific objectives

Researchers are investigating a variety of approaches to improve the brain penetration of molecules that have a site of action within the CNS. The research within our laboratory has focused on several approaches for improving the blood brain barrier permeability of molecules that are chemotherapeutic as well as neuroprotective. These molecules could hold promise for the treatment of primary brain tumors as well as neurological disorders. The specific objective of this project was to explore various chemical approaches to improving blood brain barrier permeability using pharmacologically relevant molecules.

***Specific Aim 1**: Characterize the permeability of structurally modified paclitaxel derivatives as well as their recognition by P-glycoprotein* in vitro.

Derivatives of paclitaxel in which one or more functional groups have been altered were synthesized by the Medicinal Chemistry Department at The University of Kansas. These analogues were designed with the goal of reducing their recognition by the efflux transporter P-gp while maintaining their chemotherapeutic effect. To determine if the modifications resulted in changes in recognition by P-gp, an indirect measure of P-gp interaction was performed using the rhodamine 123 uptake assay described earlier. Compounds showing reduced interaction with P-gp were then monitored for increased permeability across BBMECs monolayers to determine if the modification translated into improved permeability.

***Specific Aim 2**: Characterize the blood brain barrier permeability of the novel neuroprotective agent TH-237A.*

GS-164, a microtubule stabilizing compound, which is purported to have a mechanism of action similar to that of paclitaxel (Shintani *et al*., 1997) was found to be not only chemotherapeutic but also neuroprotective against the β-amyloid induced neurodegeneration that is seen with Alzheimer's disease. A variety of GS-164 stereoisomers were then synthesized and the stereomerically pure *cis*-isomer TH-237A was characterized to determine its ability to cross the blood brain barrier. Experiments include *in vitro, in situ* and *in vivo* methods.

***Specific Aim 3**: Characterize the blood brain barrier permeability of the tranylcypromine derivative TCP-FA4.*

Derivates of the monoamine oxidase inhibitor (MAO inhibitor) tranylcypromine were synthesized in an attempt to increase blood brain barrier permeability. The derivatives contained lipoamino acids or fatty acids which can ideally enhance the lipophilicity of the parent compound and result in improved permeability. The derivative TCP-FA4, containing a four carbon fatty acid chain, showed good permeability and its mode of transport was investigated. Additionally, the ability of this compound to be neuroprotective was explored and may be linked to its ability to regulate the expression of brain derived neurotrophic factor.

1.5 References

Audus KL and Borchardt RT (1986) Characteristics of the large neutral amino acid transport system of bovine brain microvessel endothelial cell monolayers. *J Neurochem* **47**:484-488.

Audus KL and Borchardt RT (1987) Bovine brain microvessel endothelial cell monolayers as a model system for the blood-brain barrier. *Ann N Y Acad Sci* **507**:9-18.

Bartus R, Elliott P, Hayward N, Dean R, McEwan E and Fisher S (1996) Permeability of the blood brain barrier by the bradykinin agonist RMP-7: Evidence for a sensitive, auto-regulated, receptor mediated system. *Immunopharmacology* **33**:270-278.

Bodor N and Buchwald P (2002) Barriers to remember: brain-targeting chemical delivery systems and Alzheimer's disease. *Drug Discov Today* **7**:766-774.

Brightman MW and Reese TS (1969) Junctions between intimately apposed cell membranes in the vertebrate brain. *J Cell Biol* **40**:648-677.

Croteau D, Walbridge S, Morrison PF, Butman JA, Vortmeyer AO, Johnson D, Oldfield EH and Lonser RR (2005) Real-time in vivo imaging of the convective distribution of a low-molecular-weight tracer. *J Neurosurg* **102**:90-97.

de Vrueh RL, Smith PL and Lee CP (1998) Transport of L-valine-acyclovir via the oligopeptide transporter in the human intestinal cell line, Caco-2. *J Pharmacol Exp Ther* **286**:1166-1170.

Degen JW, Walbridge S, Vortmeyer AO, Oldfield EH and Lonser RR (2003) Safety and efficacy of convection-enhanced delivery of gemcitabine or carboplatin in a malignant glioma model in rats. *J Neurosurg* **99**:893-898.

Fellner S, Bauer B, Miller DS, Schaffrik M, Fankhanel M, Spruss T, Bernhardt G, Graeff C, Farber L, Gschaidmeier H, Buschauer A and Fricker G (2002) Transport of paclitaxel (Taxol) across the blood-brain barrier *in vitro* and *in vivo*. *J Clin Invest* **110**:1309-1318.

Fontaine M, Elmquist WF and Miller DW (1996) Use of rhodamine 123 to examine the functional activity of P-glycoprotein in primary cultured brain microvessel endothelial cell monolayers. *Life Sci* **59**:1521-1531.

Groothuis DR (2000) The blood-brain and blood-tumor barriers: a review of strategies for increasing drug delivery. *Neuro Oncol* **2**:45-59.

Hegmann EJ, Bauer HC and Kerbel RS (1992) Expression and functional activity of P-glycoprotein in cultured cerebral capillary endothelial cells. *Cancer Res* **52**:6969-6975.

Ho N, Raub T, Burton P, Barsuhn C, Adson A, Audus K and Borchardt R (1999) *Transport Processes in Pharmaceutical Systems*. Marcel Dekker, New York.

Huai-Yun H, Secrest DT, Mark KS, Carney D, Brandquist C, Elmquist WF and Miller DW (1998) Expression of multidrug resistance-associated protein (MRP) in brain microvessel endothelial cells. *Biochem Biophys Res Commun* **243**:816-820.

Jolliet-Riant P and Tillement JP (1999) Drug transfer across the blood-brain barrier and improvement of brain delivery. *Fundam Clin Pharmacol* **13**:16-26.

Kaiser MG, Parsa AT, Fine RL, Hall JS, Chakrabarti I and Bruce JN (2000) Tissue distribution and antitumor activity of topotecan delivered by intracerebral clysis in a rat glioma model. *Neurosurgery* **47**:1391-1398; discussion 1398-1399.

Michaelis ML, Ansar S, Chen Y, Reiff ER, Seyb KI, Himes RH, Audus KL and Georg GI (2005) β-Amyloid-induced neurodegeneration and protection by structurally diverse microtubule-stabilizing agents. *J Pharmacol Exp Ther* **312**:659-668.

Morrison PF, Chen MY, Chadwick RS, Lonser RR and Oldfield EH (1999) Focal delivery during direct infusion to brain: role of flow rate, catheter diameter, and tissue mechanics. *Am J Physiol* **277**:R1218-1229.

Nobili S, Landini I, Giglioni B and Mini E (2006) Pharmacological strategies for overcoming multidrug resistance. *Curr Drug Targets* **7**:861-879.

O'Connor R (2007) The pharmacology of cancer resistance. *Anticancer Res* **27**:1267-1272.

Pardridge WM (1986) Receptor-mediated peptide transport through the blood-brain barrier. *Endocr Rev* **7**:314-330.

Pardridge WM and Oldendorf WH (1977) Transport of metabolic substrates through the blood-brain barrier. *J Neurochem* **28**:5-12.

Rapoport SJ and Thompson HK (1973) Osmotic opening of the blood-brain barrier in the monkey without associated neurological deficits. *Science* **180**:971.

Reese TS and Karnovsky MJ (1967) Fine structural localization of a blood-brain barrier to exogenous peroxidase. *J Cell Biol* **34**:207-217.

Rice AH (2002) Taxanes: Identification of Structures that Elude P-glycoprotein Efflux at the Blood Brain Barrier, in *Department of Pharmaceutical Chemistry* p 133, The University of Kansas, Lawrence.

Sakaeda T, Siahaan TJ, Audus KL and Stella VJ (2000) Enhancement of transport of D-melphalan analogue by conjugation with L-glutamate across bovine brain microvessel endothelial cell monolayers. *J Drug Target* **8**:195-204.

Shi F, Bailey C, Malick AW and Audus KL (1993) Biotin uptake and transport across bovine brain microvessel endothelial cell monolayers. *Pharm Res* **10**:282-288.

Shintani Y, Tanaka T and Nozaki Y (1997) GS-164, a small synthetic compound, stimulates tubulin polymerization by a similar mechanism to that of Taxol. *Cancer Chemother Pharmacol* **40**:513-520.

Sikic B, Fisher GA, Lum BL, Halsey J, Beketic-Oreskovic L and Chen G (1997) Modulation and prevention of multidrug resistance by inhibitors of P-glycoprotein. *Cancer Chemother Pharmacol* **40 (suppl)**:S13-S19.

Smith QR (1996) Brain perfusion systems for studies of drug uptake and metabolism in the central nervous system. *Pharm Biotechnol* **8**:285-307.

Spatz M and Mrsula B (1982) Progress in cerebral microvascular studies related to the function of the blood-brain barrier. *Adv Cell Neurobiol* **3**:311–337.

Tatsuta T, Naito M, Oh-hara T, Sugawara I and Tsuruo T (1992) Functional involvement of P-glycoprotein in blood-brain barrier. *J Biol Chem* **267**:20383-20391.

Walker I, Nicholls D, Irwin WJ and Freeman S (1994) Drug delivery via active transport at the blood–brain barrier: affinity of a prodrug of phosphonoformate for the large amino acid transporter. *International Journal of Pharmaceutics* **104**:157-167.

Yazdanian M and Bormann BJ (2000) Immortalized brain endothelial cells, patent number 6093553, Boehringer Ingelheim Pharmaceuticals, Inc., United States.

Chapter 2: Improving the Blood-Brain Barrier Permeation of Paclitaxel

Chapter 2: Improving the Blood-Brain Barrier Permeation of Paclitaxel

2.1 Introduction

Although the incidence of primary brain tumor is relatively low, the prognosis is often poor. There are several challenges in treating cancers of the CNS. First, as with any cancer there is the issue of drug resistance. This phenomenon is due to the overexpression of efflux transporters that essentially act as pumps to remove xenobiotics from the cancer cells (Dano, 1973; Juliano and Ling, 1976). Delivery of anticancer agents is further complicated within the brain because the blood brain barrier expresses these same efflux transporters creating a dual barrier to drug delivery. Paclitaxel, one of the leading anticancer drugs on the market is subject to removal by efflux transporters (Fellner *et al*., 2002) . Specifically, it is a known substrate for P-glycoprotein (P-gp), one of the most well known and well studied of the efflux proteins. P-gp is a member of the ATP-binding cassette (ABC) family. It has a molecular weight of 170 kDa and consists of six transmembrane domains (Juliano and Ling, 1976). Studies using knockout mice show that concentrations of paclitaxel in the brain after IV administration are 12-fold higher in P-gp knockout mice compared to wild type (van Asperen *et al*., 1997). This suggests that P-gp is very much responsible for limiting paclitaxel's entry into the brain. One approach to overcome paclitaxel's poor blood brain barrier permeability is to synthesize paclitaxel analogues that retain their pharmacological effect but are no longer substrates for P-gp. Designing a rationale for the synthesis of compounds that will circumvent P-gp is quite challenging as the substrate specificity of the protein is still

quite poorly understood. Nevertheless, structure activity relationship (SAR) studies have offered some insight into possible recognition elements.

One of the most specific and detailed SAR studies on P-gp was performed by Seelig. Her results suggest that the specific, spatial arrangement of electron-donating groups are a feature recognized by P-gp (Seelig, 1998). Briefly, Type I units consist of electron-donating groups separated by 2.5 ± 0.3 Å and Type II units consist of electron-donating groups separated by 4.6 ± 0.6 Å with a possible third electron-donating group existing between the outer two. When paclitaxel is examined for these recognition elements, one finds it possesses several of these motifs (Figure 2.1). This is not surprising as Seelig postulates that most P-gp substrates contain at least four of these recognition elements and essentially all P-gp substrates contain a Type II unit, which proves true for paclitaxel as well.

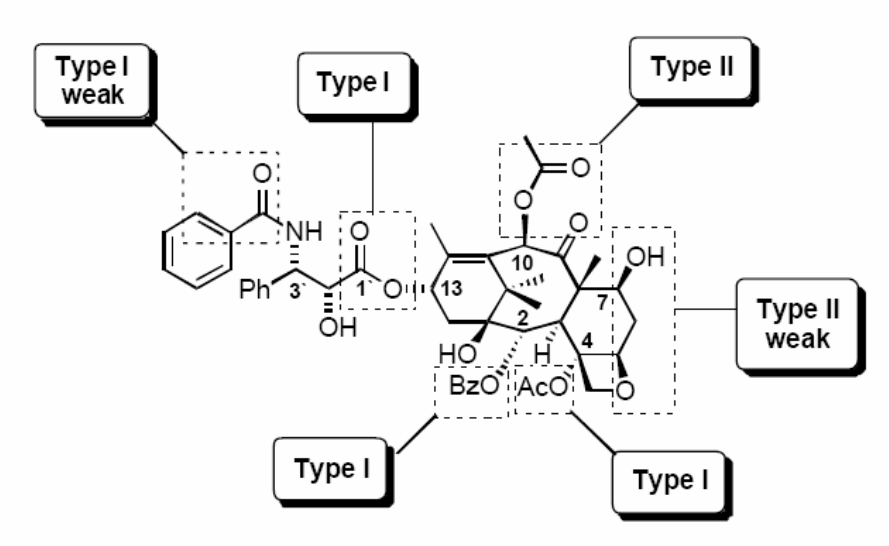

Figure 2.1 P-gp recognition elements on paclitaxel (Spletstoser *et al*., 2006)

In addition to considering which substituents are being recognized by P-gp, one must also consider which substituents are essential for the chemotherapeutic effect, as these must be preserved. Paclitaxel, works by binding to microtubules within the cell (Jordan *et al*., 1993). Therefore, the features that ensure this binding cannot be altered in the search for new analogues possessing reduced interaction with P-gp. According to prior SAR studies, the C7 and C10 positions on paclitaxel are not essential for binding to microtubules (Georg *et al*., 1995). Therefore, these two positions, which are also Type II recognition elements, are a logical choice for modification. Over 70 analogues of paclitaxel were synthesized and a variety of modifications were made, but for simplicity, the following chapter will detail three strategies employed for reducing interaction with P-gp. These strategies include: 1) spatial rearrangement at the C10 position via epimerization, 2) addition of nutrient-like groups at the C7 and C10 position and 3) modification of the C13 side chain to enhance potency combined with strategies one and two.

The rhodamine 123 uptake assay using bovine brain microvessel endothelial cells (BBMECs) was used as an *in vitro* model to determine the novel paclitaxel analogues' interaction with P-gp. Furthermore, permeability studies using BBMECs mounted in Side-bi-Side™ chambers were used to predict an analogue's potential for crossing the blood brain barrier if it demonstrated reduced interaction with P-gp.

2.2 Experimental

2.2.1 Isolation and maintenance of BBMECs

Bovine brain microvessel endothelial cells (BBMECs) were isolated from the gray matter of bovine cerebral cortices by enzymatic digestion followed by centrifugation and then seeded as primary cultures following methods described by Audus *et al*. (Audus and Borchardt, 1987).

BBMECs were grown at 37 degrees C in an atmosphere of 5% CO_2 and 95% relative humidity. The cells were grown in 50% Minimal Essential Medium and 50% Ham's F12 supplemented with 100 μg/mL streptomycin, 100 μg/mL penicillin G, 13 mM sodium bicarbonate, 10% platelet poor horse serum, 0.5% endothelial cell growth supplement (ECGS), and adjusted to pH 7.4 with 10 mM HEPES. Cells were seeded on polycarbonate 24-well cell culture plates pre-coated with rat tail collagen and fibronectin or 0.4μm polycarbonate membranes with the same treatment. The cells were seeded at a density of approximately 25,000-50,000 cells/cm^2.

2.2.2 Rhodamine 123 uptake assay

BBMECs were seeded onto 24-well cell culture plates at a density of approximately 50,000 cells/cm^2. The culture medium was changed every other day starting 72 hours after seeding until a confluent monolayer was observed as determined by light

microscopy. Experiments were performed in phosphate-buffered saline supplemented with $CaCl_2$, $MgSO_4$, glucose and ascorbic acid (PBSA), pH 7.4. The growth medium was first aspirated off and then the cells were rinsed three times with pre-warmed (37 degrees C) PBSA. The monolayers were then equilibrated in 0.5 mL of PBSA for 10 minutes at 37 degrees C. Paclitaxel analogues (final concentration: 10 μM) were then added to the wells and allowed to equilibrate for 30 minutes. No analogues were added to the control wells. Rhodamine 123 (final concentration: 5 μM) was then added to all wells and allowed to incubate for 2 hours. Cyclosporin A (CsA, 5 μM), and paclitaxel (10 μM) known P-glycoprotein inhibitors, were used as positive controls. At the end of the experiment, the substrate solution was removed by aspiration, and the monolayers were immediately rinsed three times with ice-cold PBS. Each monolayer was solubilized for at least 30 minutes (37 degrees C) with 0.5 mL of lysing solution (0.5% v/v Triton X-100 in 0.2 N NaOH). Cell lysates were assayed using a microplate fluorescence reader (Bio-Tek Instruments, Winooski, VT) at excitation/emission wavelengths of 485 nm/530 nm and then quantified against standard curves of rhodamine 123 in lysing solution. The fluorescence of the cell lysates was corrected for autofluorescence of untreated cells. The protein content of each monolayer was then determined using a Pierce BCA protein assay reagent kit (Pierce, Rockford, IL). Results were expressed as nmol of rhodamine 123 accumulated per mg of cellular protein.

2.2.3 Paclitaxel analogue permeability

BBMECs were grown on 0.4 μm polycarbonate membranes in a petri dish coated with rat tail collagen and fibronectin. Once cells had formed a confluent monolayer as determined by light microscopy, the membranes were transferred to Side-bi-Side™ diffusion chambers as previously described by Audus *et al.* (Audus and Borchardt, 1987). Briefly, each chamber was filled with 3 mL of PBSA and the donor chamber included 10 μM of test compound. A temperature of 37 degrees C was maintained with an external circulating water bath and chamber contents were stirred with Teflon coated magnetic stir bars driven by an external console. At the various time points (5, 15, 30, 45 and 90 minutes), 200 μL aliquots were removed from the receiver side and replaced with 200 μL of blank PBSA warmed to 37 degrees C. Samples of the donor solution were also taken for analysis. All samples were analyzed for concentration by LC/MS/MS. The integrity of the cell monolayer was tested post experiment by monitoring the permeability of [^{14}-C]-sucrose, a low permeability paracellular marker which should not readily cross the cell monolayer. Radioactive samples were analyzed by liquid scintillation counting.

2.2.4 Sample preparation for LC/MS/MS analysis

Aliquots taken during the permeability studies were aqueous and contained high salt concentrations so it was necessary to clean up the samples prior to analysis by LC/MS/MS. Aliquots of 190 μL were taken at the various time points and extracted using tert-butylmethylether (t-BME) liquid-liquid extraction. To each aliquot, 10 μL of

docetaxel was added to serve as an internal standard. To start the extraction, 1.0 mL of t-BME was added to all samples. Samples were then vortexed for approximately 10 minutes followed by a 5 minute centrifugation at 4500 rpm and 4 degrees C. Samples were then placed in a – 80 degrees C freezer and allowed to freeze for at least 15 minutes. After freezing of the aqueous portion of the sample, 800 µL of the organic phase was transferred to new microcentrifuge tubes and dried in a concentrator under vacuum. If the samples were not immediately analyzed, they were stored at – 80 degrees C until analysis. Before analysis, samples were reconstituted in 200 µL of acetonitrile (60%, v/v) containing 0.1% (v/v) formic acid and vortexed.

As part of the method development, the percent solute recovery when using this liquid-liquid extraction method was determined for paclitaxel as well as docetaxel, the internal standard. Aqueous buffer (PBSA) was spiked with various concentrations of paclitaxel and docetaxel at a concentration of 0.5 µg/mL/sample. Percent recovery values were then calculated by comparing the solute peak areas from extracted samples to the peak areas from samples spiked directly into mobile phase (60% acetonitrile (v/v) containing 0.1% formic acid (v/v)). The average percent recovery for paclitaxel was 59% and 67% for docetaxel (Figure 2.2.4.1). Percent solute recovery was not calculated for every single paclitaxel analogue and the assumption was made that the percent recovery for the analogues would be similar to that of paclitaxel and docetaxel. Standards generated from extracted buffer samples showed good linearity over a calibration range of 5-5000 ng/mL and this was consistent for the various paclitaxel analogues as well. Figure 2.2.4.2 is a calibration curve for paclitaxel and Figure 2.2.4.3 is a representative calibration curve of

one of the paclitaxel analogues (TX-297), showing linearity was achieved for the analogues as well.

	% solute recovery	
conc (ng/mL)	Paclitaxel in buffer	Docetaxel (0.5µg/mL/sample) in buffer
5	62%	69%
10	59%	70%
50	61%	65%
100	67%	67%
500	58%	60%
1000	43%	65%
2500	61%	66%
5000	58%	74%

Figure 2.2.4.1 Percent solute recovery for paclitaxel and docetaxel after sample preparation by liquid-liquid extraction with t-BME. (n=3, all %RSD < 10%)

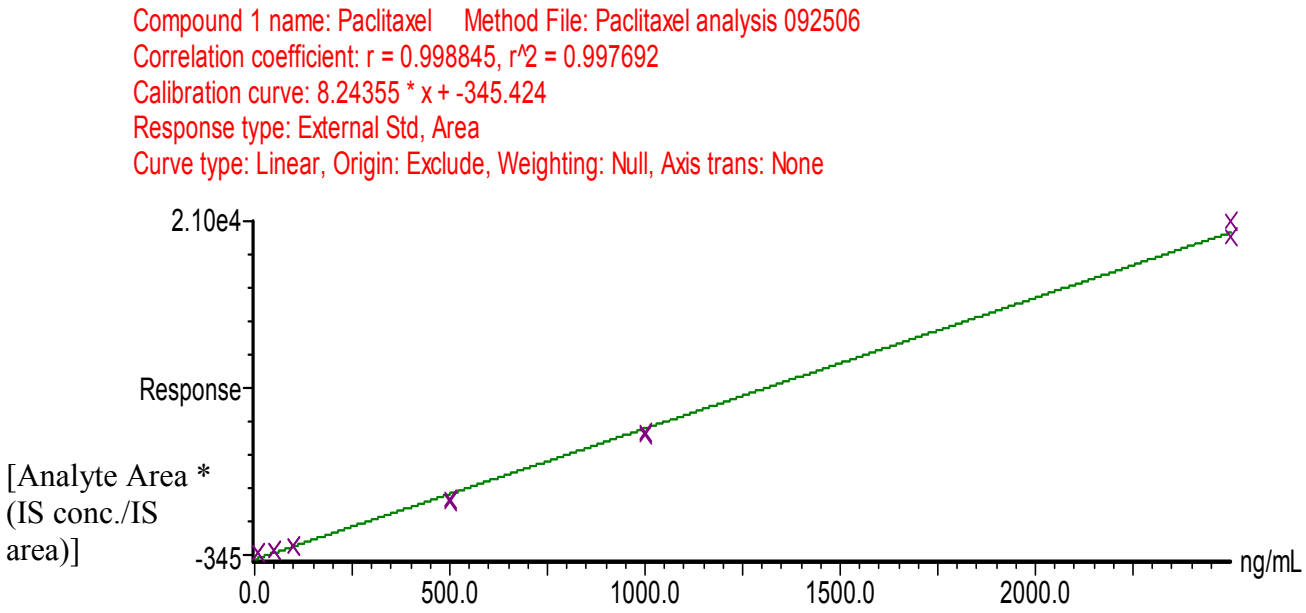

Figure 2.2.4.2 Typical calibration curve for paclitaxel extracted from aqueous buffer (PBSA) using liquid-liquid extraction. Linearity seen from 5 – 5000 ng/mL. (R^2 = 0.998)

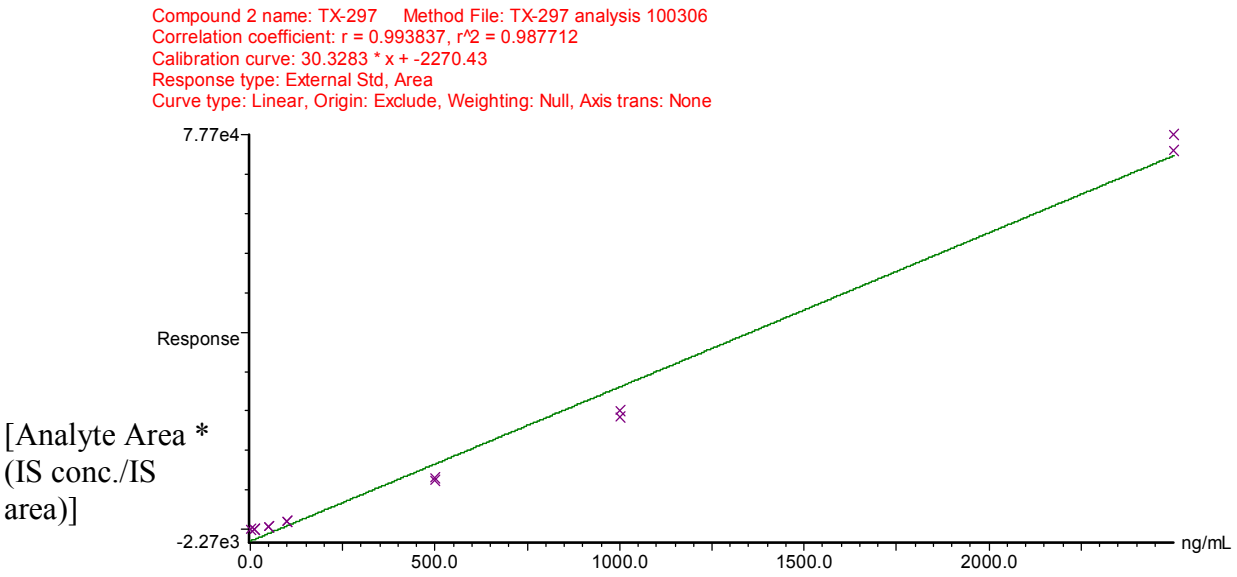

Figure 2.2.4.3 Representative calibration curve of a paclitaxel derivative (TX-297) extracted from aqueous buffer (PBSA) using liquid-liquid extraction. Linearity seen from 5 – 5000 ng/mL. ($R^2 = 0.988$)

2.2.5 Sample analysis by LC/MS/MS

Samples of 20 µL were chromatographed by a Waters 2690 HPLC system using a Zorbax Eclipse XDB-C8 column (2.1 x 50 mm, 5 micron) and then directed into the mass spectrometer (Micromass™ triple quadrupole) and detected by tandem mass spectrometry in positive ion mode using electrospray ionization.

A solvent gradient program was selected for the HPLC analyses as there was minimal peak tailing as compared to an isocratic method. Furthermore, the increased retention obtained with a gradient method allowed a diversion of the HPLC eluent between 0 and 5 minutes which reduced the exposure of the mass spectrometer to possible cellular contaminants not eliminated by the sample cleanup procedure. For the gradient parameters, Solvent A was 0.1 % formic acid in nanopure water and Solvent B was 0.1% formic acid in acetonitrile. The gradient used for separation was a linear ramp from 95% A to 5% A over 8 minutes, and an equilibration back to 95% A from 8.10 minutes to 12.10 minutes. A switching valve was employed to direct the first 5 minutes of eluent to waste. Based on the physicochemical properties of the added substituents within the paclitaxel analogues, the retention times shifted appropriately (Figure 2.2.5.1).

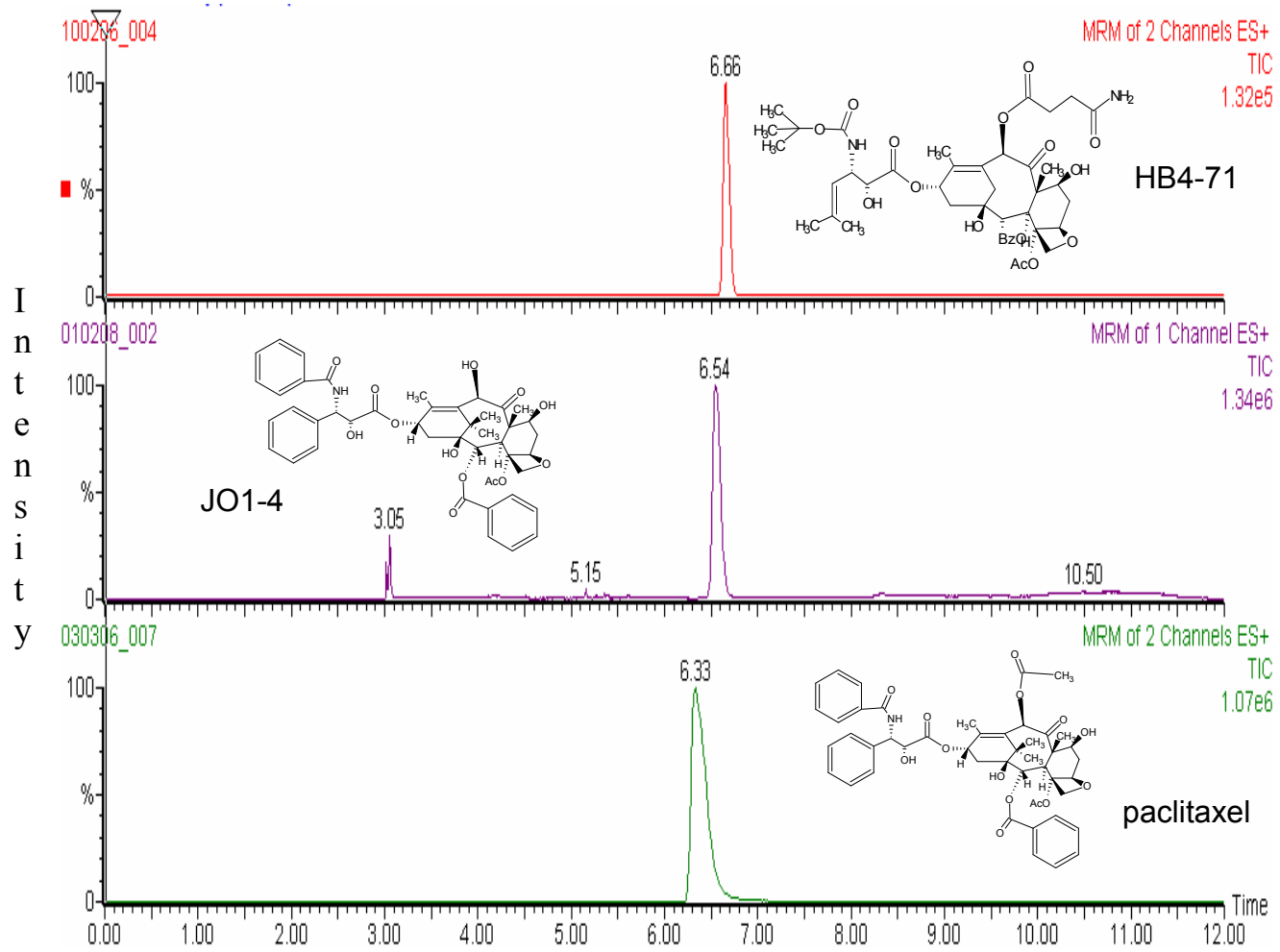

Figure 2.2.5.1 Representative MS chromatograms of paclitaxel and two derivatives, JO1-4 and HB4-71, demonstrating the slight shifts in retention time based on the structural modifications made. All chromatograms represent total ion current (TIC).

To select the optimal product-ions for analysis, solutions of paclitaxel and the paclitaxel analogues, made in 60% (v/v) acetonitrile with 0.1% (v/v) formic acid (25-50 µg/mL), were first infused into the mass spectrometer and fragmentation patterns were monitored and parameters were optimized. Paclitaxel and its derivatives were chromatographed and detected using multiple reaction monitoring. Fragmentation within the paclitaxel molecule occurred at the C13 side chain and the *m/z* 854 → *m/z* 569 transition was monitored (Figure 2.2.5.2). For the internal standard docetaxel, the *m/z* 808 → *m/z* 527 transition was monitored (Figure 2.2.5.3). Based on the modifications made within the paclitaxel molecule, the set masses and the daughter ion masses were shifted appropriately.

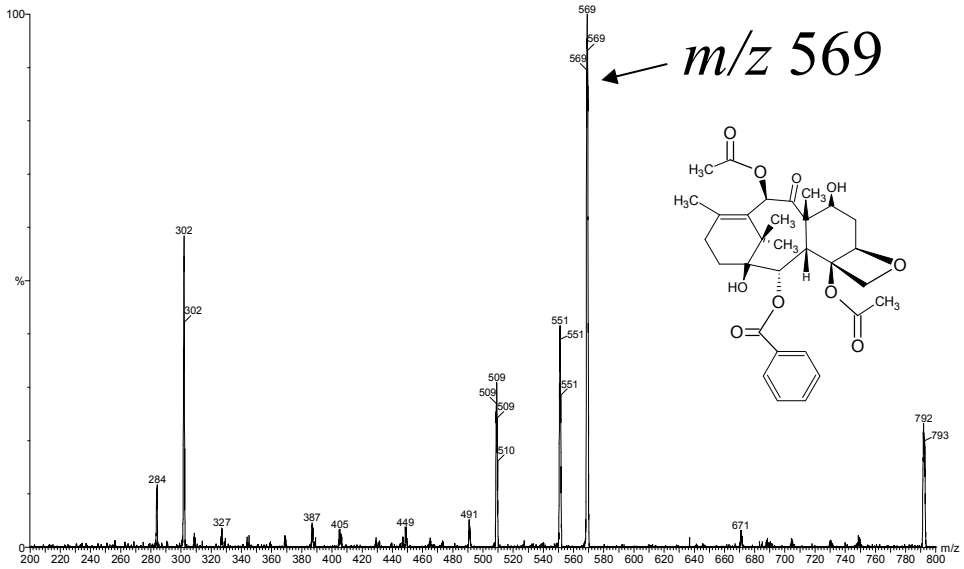

Figure 2.2.5.2 Electrospray ionization (ESI)-MS/MS (positive ion mode) product-ion spectra of paclitaxel (*m/z* 854)

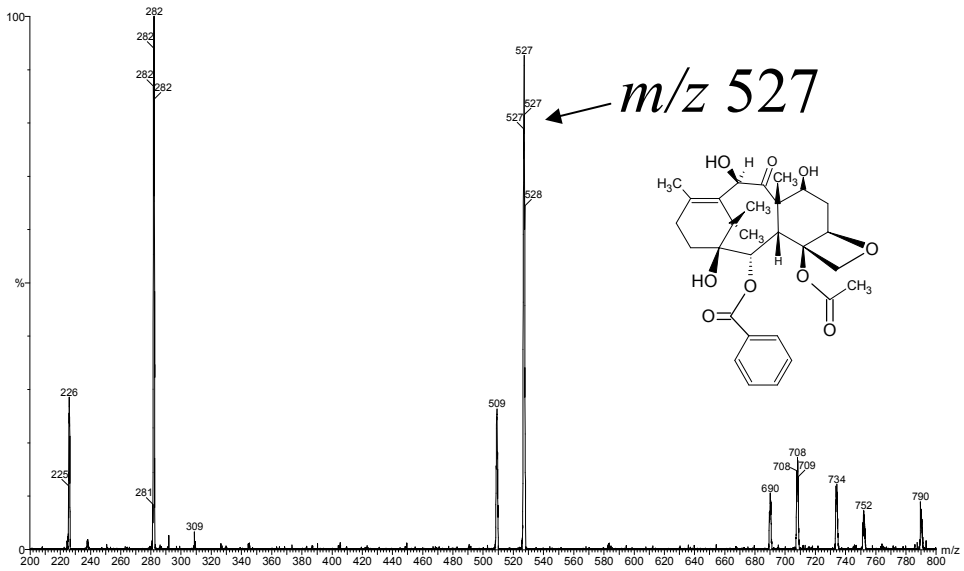

Figure 2.2.5.3 Electrospray ionization (ESI)-MS/MS (positive ion mode) product-ion spectra of docetaxel (*m/z* 808)

2.3 Results

2.3.1 Modifications at the C10 position: Effects of spatial rearrangement and oxidative state

Since the goal of this project was to structurally modify paclitaxel such that it retained its chemotherapeutic effect, but was no longer a substrate for P-gp, the site of modification was critical. Previous studies had shown that the C10 position was not necessary for binding to microtubules (Georg *et al*., 1995), which is how paclitaxel imparts its chemotherapeutic effect. Furthermore, the C10 position can be described as a "Type II recognition element" per the classification system created by Seelig (Seelig, 1998). Since Type II recognition elements appear in essentially all P-gp substrates, removal or alteration of this moiety was desired and this position was an ideal starting point for structural modification.

The paclitaxel molecule has an acetate ester in the β-configuration at the C10 position, indicating that the group sits above the baccatin ring structure. Modifications were made such that the acetate ester in the C10 position was changed to the α-configuration to determine the effects spatial arrangement has on P-gp recognition. Furthermore, we sought to investigate the effect of changes to the C10 oxidation state on the recognition by P-gp. Thus via ester hydrolysis the acetate ester was converted to a hydroxyl group, and we looked at the effects of a hydroxyl group in both the α- and β-configurations. This hypothesis that changes in the C10 oxidation state can alter recognition by P-gp is

supported by studies that show TXD-258, a novel taxoid, which has a C10- OME group in place of the acetate ester, can penetrate the blood brain barrier (Beckers and Mahboobi, 2003). Lastly, we looked at the effect a single carbon addition at C10 would have on P-gp recognition, so the acetate ester group was replaced with a propionate group in the α-configuration (Figure 2.3.1.1).

Results from the rhodamine 123 uptake assay performed in BBMECs confirm that paclitaxel, containing an acetate ester in the β-configuration at the C10 position, is a substrate for P-gp. This is indicated by the large increase in intracellular concentration of rhodamine 123 when incubated in the presence of paclitaxel as compared to the control. The paclitaxel derivative BJT2-57 however has an acetate ester in the α-configuration at the C10 position and the rhodamine 123 uptake results indicate a decrease in recognition by P-gp as compared to paclitaxel. This is indicated by the reduction in intracellular concentration of rhodamine 123 when incubated in the presence of this derivative (BJT2-57). (Figure 2.3.1.2). These data suggest that recognition by P-gp can be sensitive to changes as subtle as absolute configuration.

The paclitaxel derivatives BJT2-55 and JO1-4 have a hydroxyl group in the α- and β-configuration, respectively, at the C10 position. This change in C10 oxidation state compared to paclitaxel appears to decrease recognition by P-gp as indicated by a reduced intracellular concentration of rhodamine 123. (Figure 2.3.1.2). This reduction in recognition can be explained by the fact that the C10 position is no longer a Type II recognition element, but has been converted to a weaker Type I motif via hydrolysis.

The addition of a single carbon atom, yielding a propionate group at the C10 position (JTS6275) when in the α-configuration does not appear to result in any decreased recognition by P-gp relative to paclitaxel. (Figure 2.3.1.2)

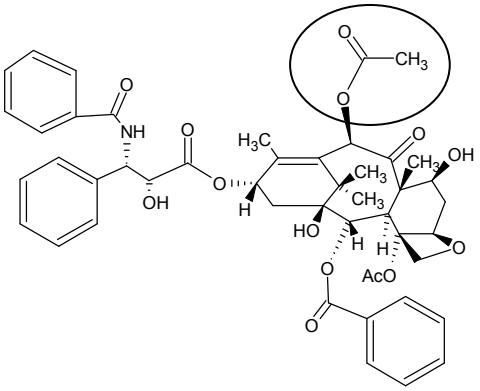

paclitaxel (β-acetate ester, C10 position)

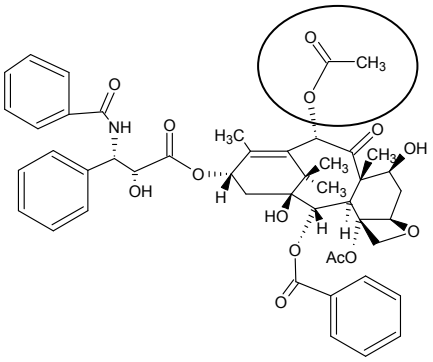

BJT2-57 (α-acetate ester, C10 position)

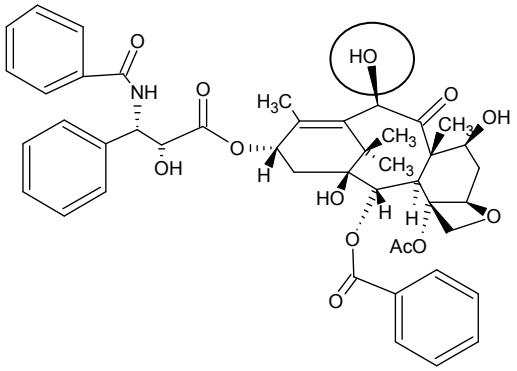

JO1-4 (β-hydroxy, C10 position)

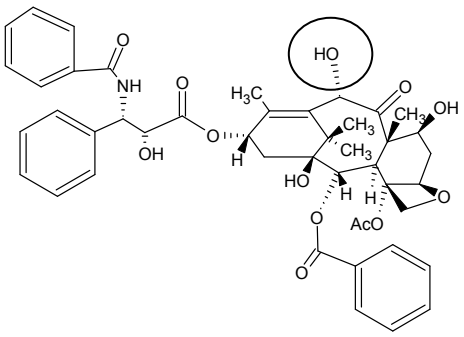

BJT2-55 (α-hydroxy, C10 position)

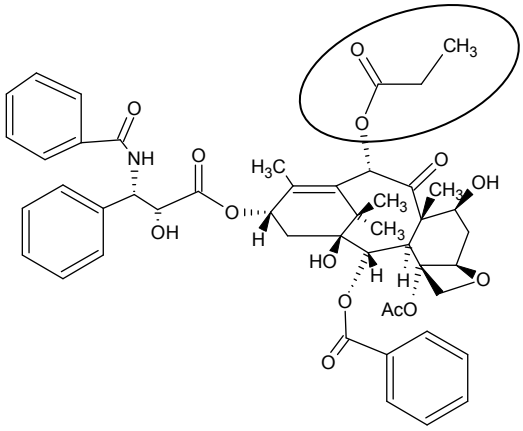

JTS6275 (α-propionate, C10 position)

Figure 2.3.1.1 Structural modifications of paclitaxel showing changes in absolute configuration and oxidation state at the C10 position

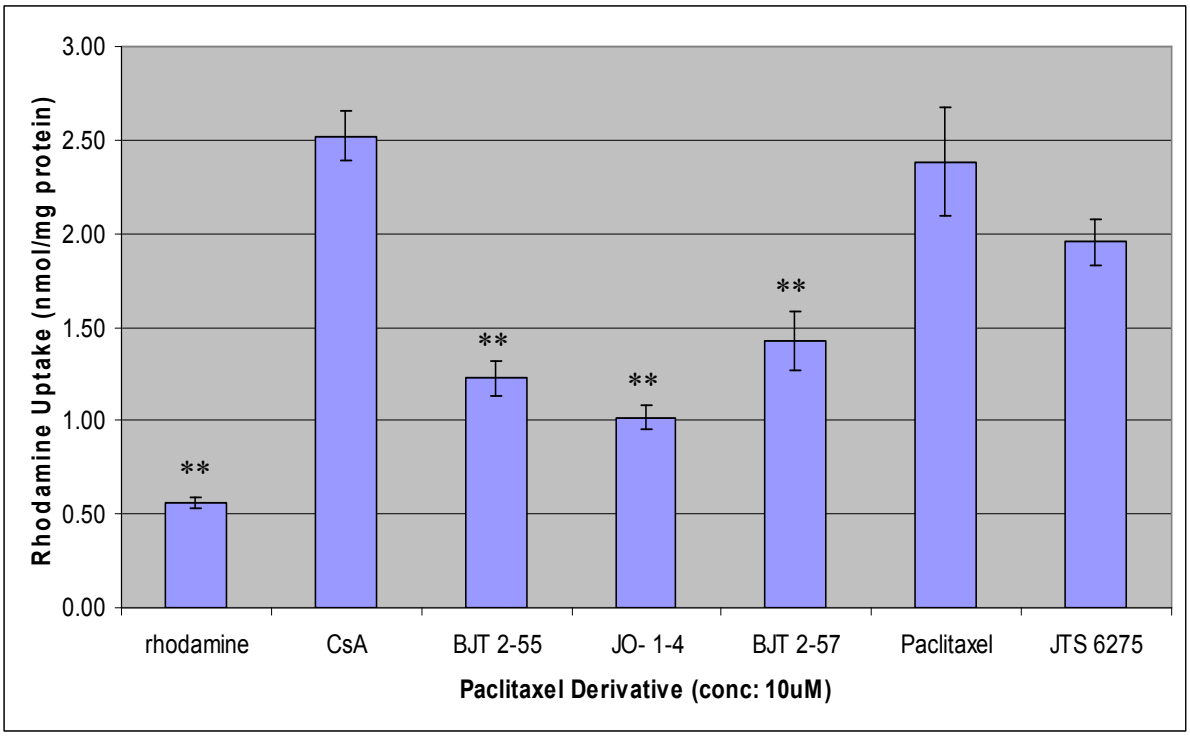

Figure 2.3.1.2 Rhodamine 123 uptake assay results indicate that derivatives BJT 2-55, JO1-4 and BJT2-57 exhibit reduced interaction with P-gp relative to paclitaxel. Cyclosporin A (CsA), a known substrate for P-gp, was used as a positive control. (** Denotes $p<0.01$ compared to paclitaxel as determined by ANOVA, Data ± SD, n=3). Structures found on page 48.

The same structural modifications were made on docetaxel to see if the trend held within a structurally similar series. (Structures found in Appendix 2, page 168). Docetaxel (Taxotere®) is a semi-synthetic analogue of paclitaxel and it differs in two positions. In the 3' position within the C13 sidechain, paclitaxel has a benzoyl group. This group has been converted to a t-butoxy carbonyl group within the docetaxel molecule. Also, in place of paclitaxel's β-acetate ester at the C10 position, there is an α-hydroxy group within docetaxel (Figure 2.3.1.3)

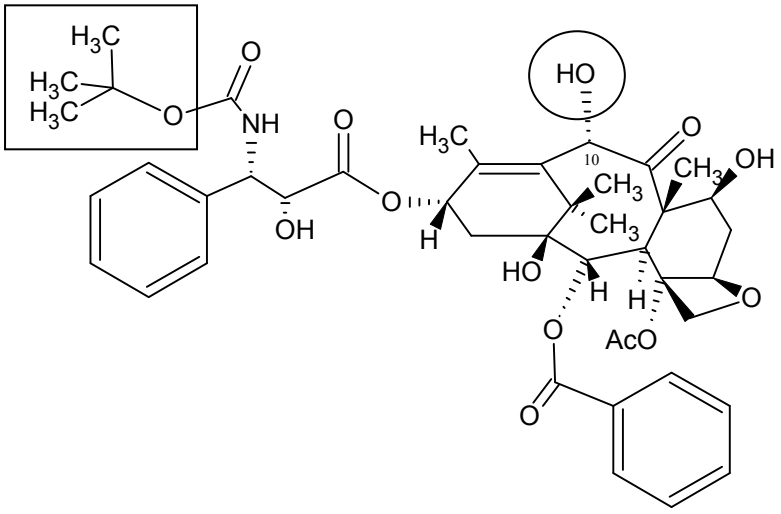

Figure 2.3.1.3 Structure of docetaxel, a semi-synthetic analogue of paclitaxel

Rhodamine 123 results indicate the same trend in recognition by P-gp is seen using the docetaxel backbone. Compound BJT 2-59 which has an acetate ester in the β-configuration at the C10 position interacts with P-gp; however, this interaction is decreased when that acetate ester is converted to the α-configuration (BJT1-109). Interaction with P-gp is also decreased when the C10 position is a hydroxyl group,

regardless of configuration (BJT1-97 and docetaxel) (Figure 2.3.1.4). No effect is seen with an α-configuration propionate group at C10 (SLA269). These data further confirm that recognition by P-gp can be affected by changes as subtle as absolute configuration and C10 oxidation state. Although the same trend was seen within this series, relative to paclitaxel, none of these derivatives exhibited a statistically significant reduction in interaction with P-gp. Therefore, they are not expected to have improved permeability compared to paclitaxel.

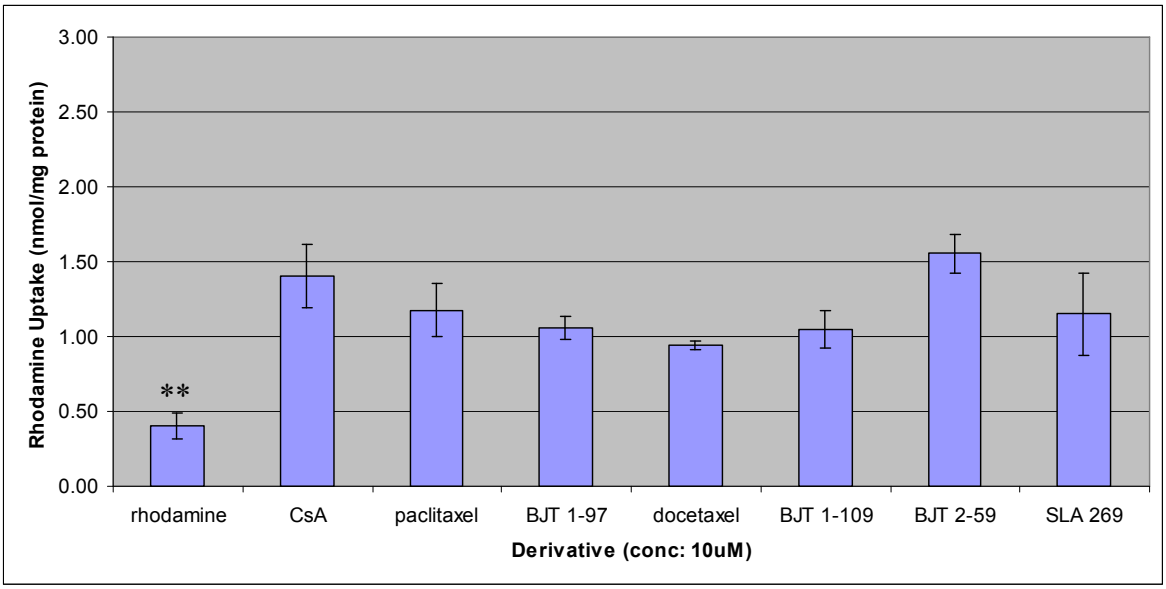

Figure 2.3.1.4 Rhodamine 123 uptake assay results indicate that conversion of the C10 acetate ester to the α-configuration (BJT 1-109) reduces P-gp interaction compared to BJT 2-59 containing an acetate ester in the β-configuration. Interaction can also be reduced when there is a hydroxyl group at the C10 position regardless of configuration (BJT 1-97 and docetaxel). (** Denotes $p<0.01$ compared to paclitaxel as determined by ANOVA, Data ± SD, n=3). Structures found in Appendix 2, page 168.

The same structural modifications were tested again using Taxol C as a backbone. (Structures found in Appendix 2, page 169). Paclitaxel is extracted from the Pacific yew tree (*Taxus brevifolia)*, and during this extraction process there are a variety of other taxanes present at trace levels, one of which is Taxol C. The only structural difference from paclitaxel occurs at the 3' position. The benzoyl group of paclitaxel is replaced with a 5 carbon chain on Taxol C (Figure 2.3.1.5)

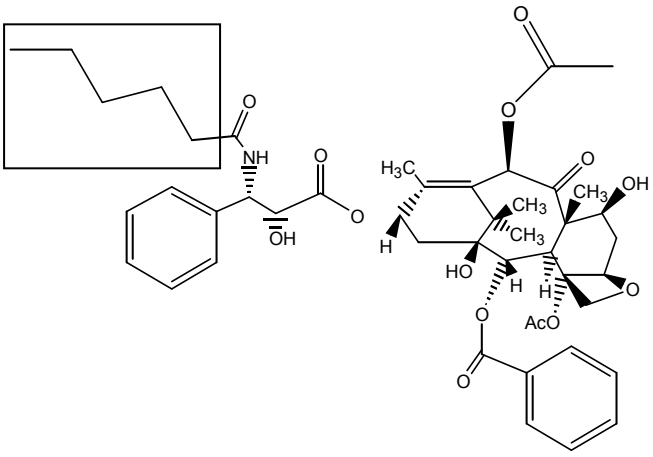

Figure 2.3.1.5 Structure of Taxol C, a trace taxane present during the extraction of paclitaxel.

Once again, the same trend was seen in which a β-acetate ester in the C10 position (Taxol C) exhibits interaction with P-gp and this interaction is reduced when there is an α-acetate ester in the C10 position (JTS1279). Furthermore, interaction with P-gp can also be reduced by having a hydroxyl group at the C10 position regardless of configuration

(JTS6209 and JTS6263). Lastly, no change in recognition is seen with a propionate group at the C10 position (JTS6221) (Figure 2.3.1.6).

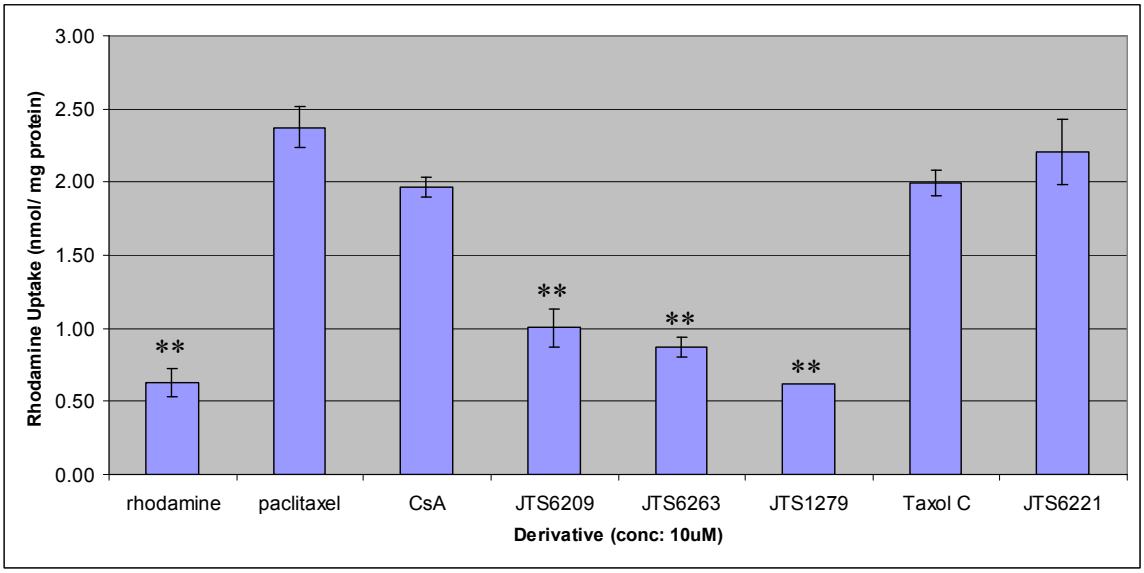

Figure 2.3.1.6 Rhodamine 123 uptake assay results indicate that conversion of the C10 acetate ester to the α-configuration (JTS1279) reduces P-gp interaction compared to Taxol C containing an acetate ester in the β-configuration. Interaction can also be reduced when there is a hydroxyl group at the C10 position regardless of configuration (JTS6209 and JTS6263). (** Denotes $p<0.01$ compared to paclitaxel as determined by ANOVA, Data ± SD, n=3). Structures found in Appendix 2, page 169.

Additional studies were performed in which JTS6209 and JTS6263 (derivatives containing a hydroxyl at the C10 position) were tested at a range of concentrations in the rhodamine 123 uptake assay. This was to determine if there were any concentration effects. Studies showed that although these compounds initially appeared not to be

substrates for P-gp, at greater concentrations their interaction with P-gp was revealed (Figure 2.3.1.7)

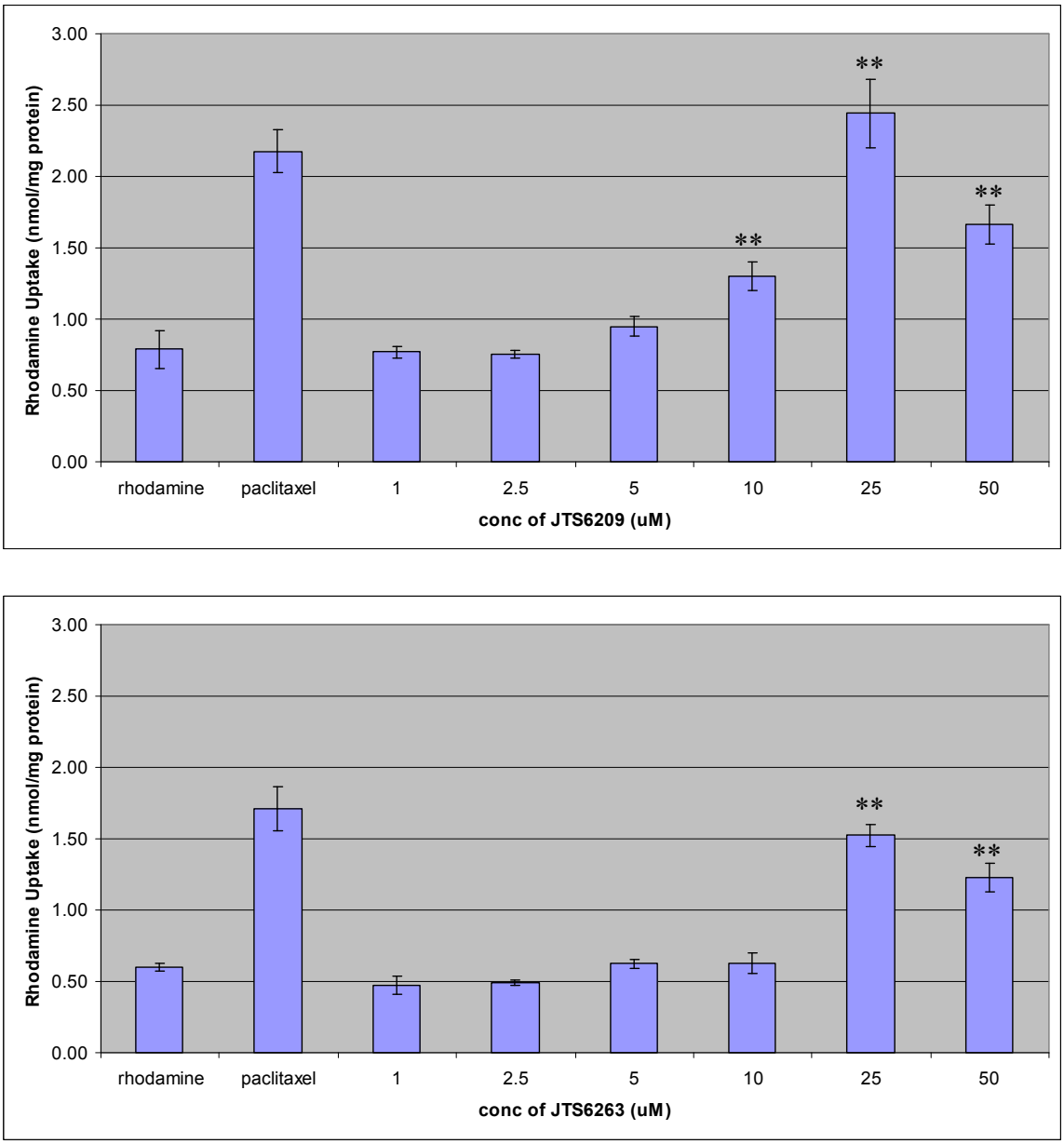

Figure 2.3.1.7 Rhodamine 123 uptake in the presence of increasing concentrations of JTS6209 and JTS6263. (** Denotes $p<0.01$ compared to negative control (rhodamine alone) as determined by ANOVA, Data ± SD, n=3). Structures found in Appendix 2 page 169.

2.3.2 Effect of nutrient-like groups at the C7 or C10 position

The second strategy utilized was one in which we attached nutrient-like groups at the C7 and C10 positions. Again, we focused on these positions because they are not essential for binding to microtubules and modifications at these sites should not result in dramatic changes in potency. The rationale behind attaching nutrient-like groups is that there are systems in place at the blood brain barrier responsible for the active uptake of nutrients. Such systems include the large neutral amino acid transporter (LAT1), monocarboxylate transporter (MCT1), glucose transporter (GLUT1)and various peptide transporters among others (Pardridge, 2003).

By attaching a nutrient-like group to the paclitaxel molecule there is the possibility of recognition by one of these uptake transporters and as a result increased permeability across the blood-brain barrier. First, the type of nutrient-like group to attach must be decided upon, and then the effects on P-gp recognition must be studied. Ideally, attachment of a nutrient-like group could decrease recognition by P-gp and at the same time target recognition by a nutrient uptake transporter expressed within the brain endothelial cells.

The first series of compounds had succinate derivatives attached at either the C7 or C10 position. Previous studies in our laboratory had shown that a succinate group attached at the C10 position of paclitaxel resulted in a molecule with greatly improved permeability across the blood-brain barrier (Rice *et al*., 2005). We sought to investigate whether the

acid moiety was essential to this reduction in P-gp interaction. The nutrient-like groups attached consisted of amide esters of succinate and methyl esters of succinate (Figure 2.3.2.1).

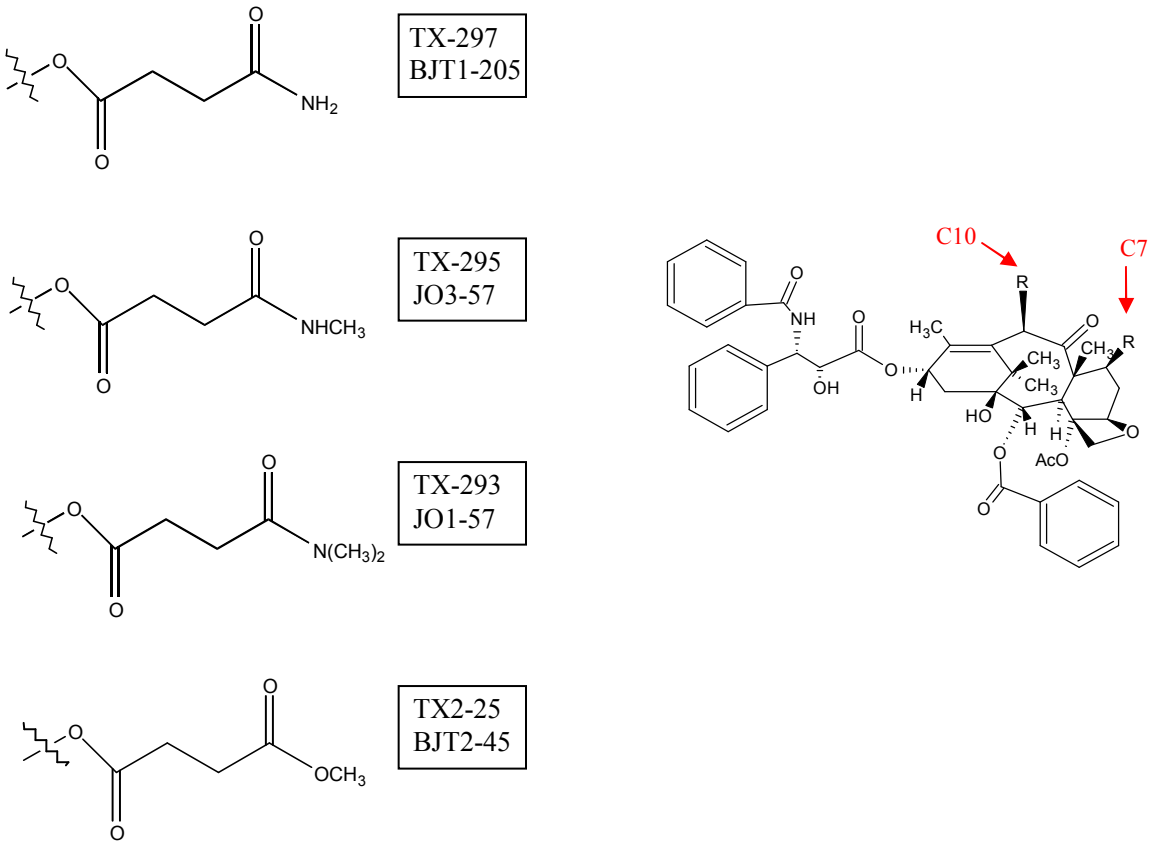

Figure 2.3.2.1 Paclitaxel derivatives containing succinate derivatives at either the C7 or C10 position. (C7 modifications: TX-297, TX-195, TX-293 and TX2-25, C10 modifications: BJT1-205, JO3-57, JO1-57 and BJT2-45)

Paclitaxel derivatives containing succinate-like groups were tested for interaction with P-gp using the rhodamine 123 uptake assay and results showed that nutrient group placement at the C7 position did not reduce interaction with P-gp and in some cases actually increased this interaction. However, when the same succinate-like modifications were made at the C10 position, the desired decrease in interaction with P-gp was observed. One exception was BJT 2-45, the methyl ester derivative, which exhibited interaction with P-gp similar to paclitaxel. These data again emphasized the importance of the C10 position for recognition of paclitaxel by P-gp. All compounds were tested at a range of concentrations (1, 2.5, 5, 10, 25 and 50 μM) while maintaining the same concentration of rhodamine 123 (5 μM) (Figures 2.3.2.2 and 2.3.2.3)

These studies suggest that placement of nutrient-like groups may be more effective at the C10 position, versus the C7 position, as they reduce interaction with P-gp. Furthermore, these data reiterate the importance of the C10 position in P-gp's recognition of the paclitaxel molecule.

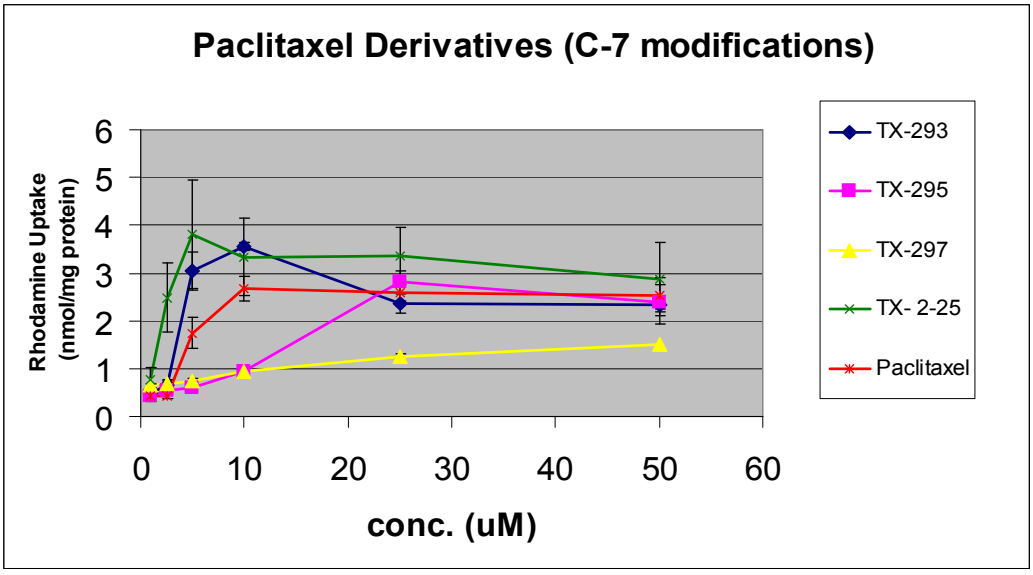

Figure 2.3.2.2 Paclitaxel derivatives containing succinate ester groups at the C7 position generally have interaction with P-gp equivalent to paclitaxel and in some cases have increased interaction. (Data ± SD, n=3). Structures found on page 56.

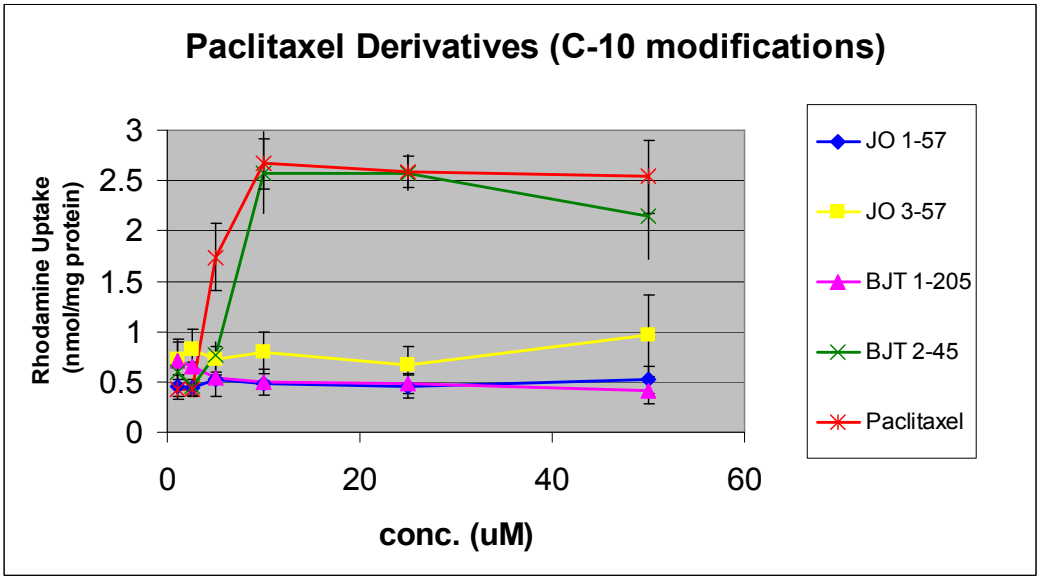

Figure 2.3.2.3 Paclitaxel derivatives containing succinate ester groups at the C10 position generally have reduced interaction with P-gp compared to paclitaxel, with the exception of BJT 2-45, the methyl ester derivative. (Data ± SD, n=3). Structures found on page 56.

The second series of compounds had biotin attached at either the C7 or C10 position. (Structures found in Apendix 2, pages 170-171). Spector *et al.* (Spector and Mock, 1987) have shown that a biotin transport system exists at the blood brain barrier. Furthermore, previous studies in our laboratory have confirmed the existence of a biotin transport system in BBMECs assuring us that ours is a good model to use for the testing of these compounds (Shi *et al*., 1993). Biotin was attached at either the C7 or C10 position and the effect of this modification on recognition by P-gp was first examined. Both compounds, JTS4169 (biotin attachment at C7) and JO2-38C (biotin attachment at C10) demonstrated a decreased interaction with P-gp in the rhodamine 123 uptake assay (Figure 2.3.2.4). Again, this strategy resulted in some paclitaxel analogues that show reduced interaction with P-gp that may also have improved permeability across the blood brain barrier.

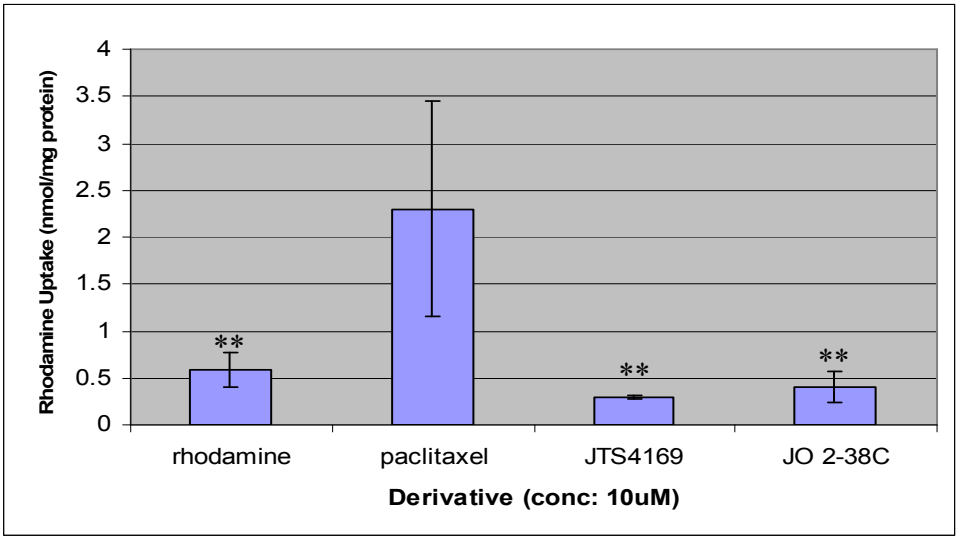

Figure 2.3.2.4 Paclitaxel derivatives containing a biotin group at the C7 or C10 position have reduced interaction with P-gp compared to paclitaxel. (** Denotes $p<0.01$ compared to paclitaxel as determined by ANOVA, Data ± SD, n=3). Structures found in Appendix 2, pages 170-171.

2.3.3 Modifications at the C13 position to enhance potency

The third chemical modification strategy included modifications at the C7 and C10 positions, as well as the C13 side chain. Ojima *et al.* have reported that docetaxel derivatives (t-butoxy carbonyl in place of the benzoyl in the 3' position) containing an isobutyl or isobutenyl group in place of the 3' phenyl group exhibited increased cytotoxicity against the drug-resistant human breast cancer cell line expressing the MDR phenotype (NCI/ADR-RES) (Ojima *et al*., 1996). Therefore, the goal of this strategy was to enhance the potency through modifications of the C13 side chain while still using the modifications at the C7 and C10 positions that had been shown previously in our lab to reduce interaction with P-gp. A large library of analogues containing this C13 modification was generated. Unfortunately, modification at the C13 residue appears to consistently result in a molecule displaying strong interaction with P-gp (Figure 2.3.3.1). The exceptions were three analogues, all of which had a nutrient-like group at the C10 position (Figure 2.3.3.2). (Structures found on page 70). HB4-63 and HB4-91 both contained a succinic acid group at the C10 position and HB4-91 contained an amide ester of succinate at the C10 position. The most surprising result was that HB4-99, which also contained a succinate ester at the C10 position, but had an isobutyl group at the 3' position, did not show a reduction in P-gp interaction. This result was not expected and to date cannot be explained.

Derivative	3' position	C7	C10	Interacts w/ P-gp
HB4-37	isobutenyl	β-hydroxy	β-hydroxy	yes
HB2-199	isobutenyl	β-hydroxy	α-hydroxy	yes
Taxol 273	isobutenyl	β-hydroxy	β-acetyl	yes
HB2-243	isobutenyl	β-hydroxy	α-acetyl	yes
HB4-79	isobutyl	β-hydroxy	β-hydroxy	yes
HB2-251	isobutyl	β-hydroxy	α-hydroxy	yes
Taxol 277	isobutyl	β-hydroxy	β-acetyl	yes
HB4-83	isobutyl	β-hydroxy	α-acetyl	yes
HB4-63	isobutenyl	β-hydroxy	β-succinic acid	no
HB4-71	isobutenyl	β-hydroxy	β-amide ester of succinate	no
HB4-153	isobutenyl	β-succinic acid	β-acetyl	yes
HB4-155	isobutenyl	β-amide ester of succinate	β-acetyl	yes
HB4-91	isobutyl	β-hydroxy	β-succinic acid	no
HB4-99	isobutyl	β-hydroxy	β-amide ester of succinate	yes
HB4-195	isobutyl	β-succinic acid	β-acetyl	yes
HB4-173	isobutyl	β-amide ester of succinate	β-acetyl	yes
HB4-203	isobutenyl	β-amide ester of succinate	β-propionate	yes
HB4-201	isobutenyl	β-succinic acid	β-propionate	yes
HB4-209	isobutyl	β-amide ester of succinate	β-propionate	yes
HB4-207	isobutyl	β-succinic acid	β-propionate	yes

Figure 2.3.3.1 Library of analogues containing C13 modifications to enhance potency as well as C7 and C10 modifications attempting to reduce interaction with P-gp. Structures of compounds showing reduced interaction with P-gp found on page 70.

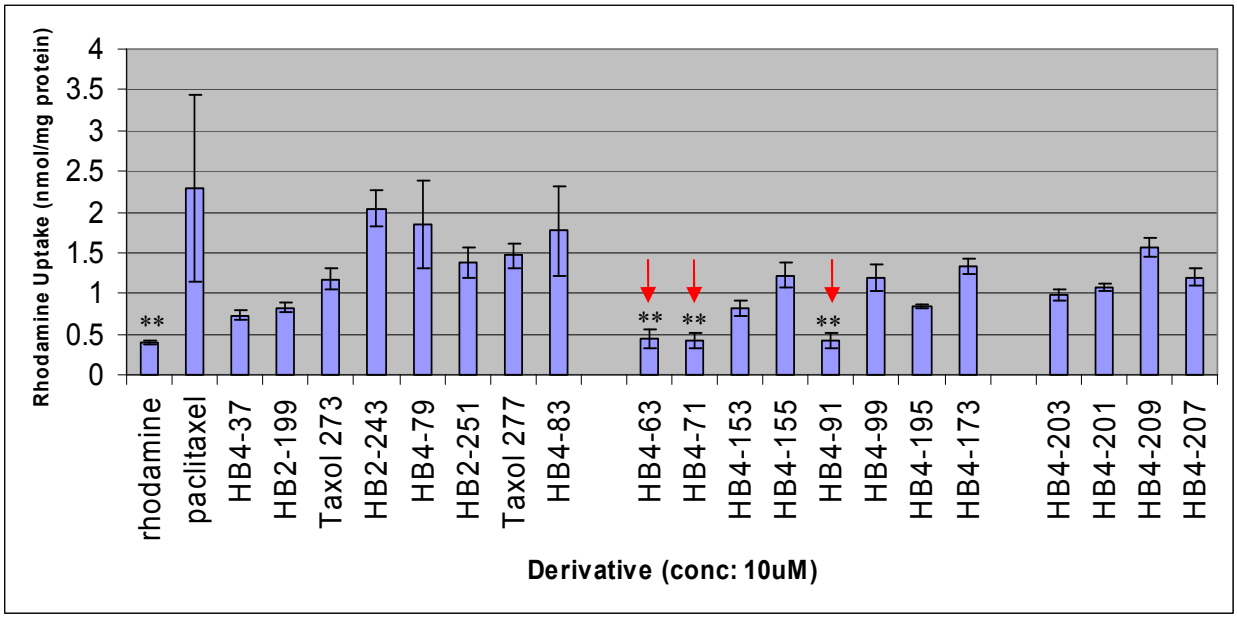

Figure 2.3.3.2 Rhodamine 123 uptake assay results for analogues containing C13 modifications to enhance potency as well as C7 and C10 modifications attempting to reduce interaction with P-gp. Only three analogues (HB4-63, HB4-71 and HB4-91) showed a decrease in interaction with P-gp. (** Denotes $p<0.01$ compared to paclitaxel as determined by ANOVA, Data ± SD, n=3). Structures found on page 70.

2.3.4 BBMEC permeability of derivatives showing reduced interaction with P-gp

For those analogues showing a reduction in interaction with P-gp, we wanted to investigate whether or not this translated into improved permeability. BBMECs mounted in Side-bi-Side™ chambers were used to test the permeability of the various analogues. The apparent permeability values of the derivatives were calculated using the following equation:

$P_{app} = (\Delta Q/\Delta t)/ A \times C_0$

where $\Delta Q/\Delta t$ is the linear appearance of the test compound in the receiver chamber, A is the cross sectional area of the cell monolayer (0.636 cm^2) and C_0 is the initial concentration of the test compound in the donor chamber at t = 0.

From the first strategy, three analogues showed a reduction in interaction with P-gp relative to paclitaxel. These analogues included BJT2-57, which possesses an α- acetate ester at the C10 position, as well as BJT2-55 and JO1-4 which both possess a C10 hydroxyl group in the α- and β-configurations respectively. Permeability studies performed with these analogues in BBMECs unfortunately showed no increase in permeability relative to paclitaxel and in fact had lower permeability (Figure 2.3.4.1)

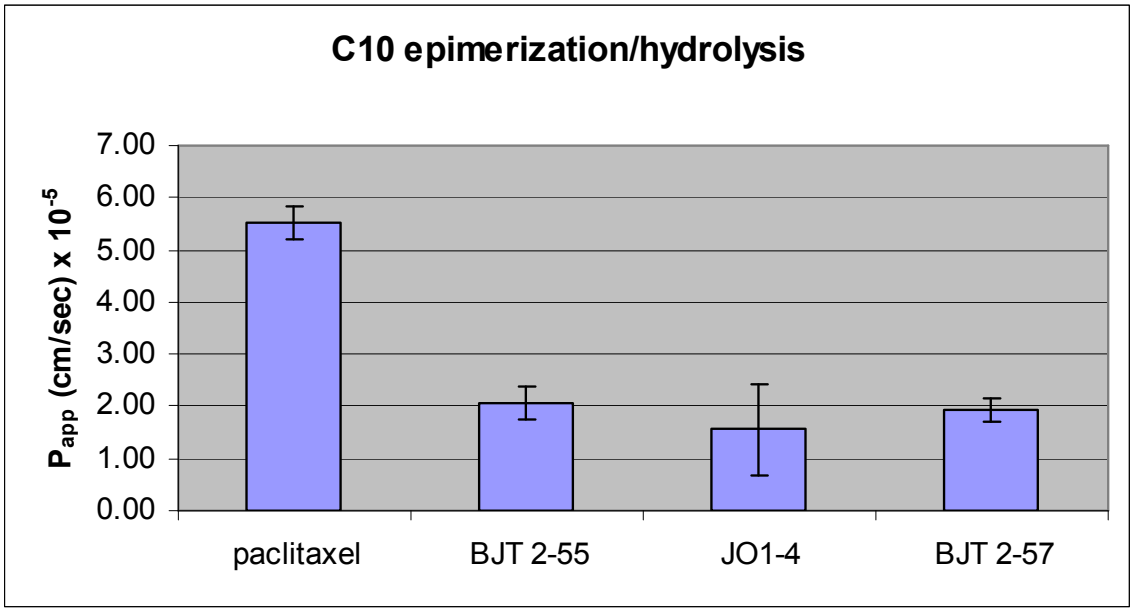

Figure 2.3.4.1 Permeability of analogues BJT2-55, JO1-4, and BJT2-57 across BBMEC monolayers. No improvement in permeability was seen relative to paclitaxel. (Data ± SD, n=4). Structures found on page 48.

From the second strategy, succinate-like groups attached to the C10 position generally reduced interaction with P-gp. Three analogues were expected to show improved permeability and included BJT1-205, an amide ester of succinate as well as JO1-57 and JO3-57 which were amide esters of succinate with increasing methylation. Unfortunately, once again, an improvement in permeability compared to paclitaxel was not seen. While BJT1-205 had equivalent permeability compared to paclitaxel, JO1-57 and JO3-57 had decreased permeability (Figure 2.3.4.2)

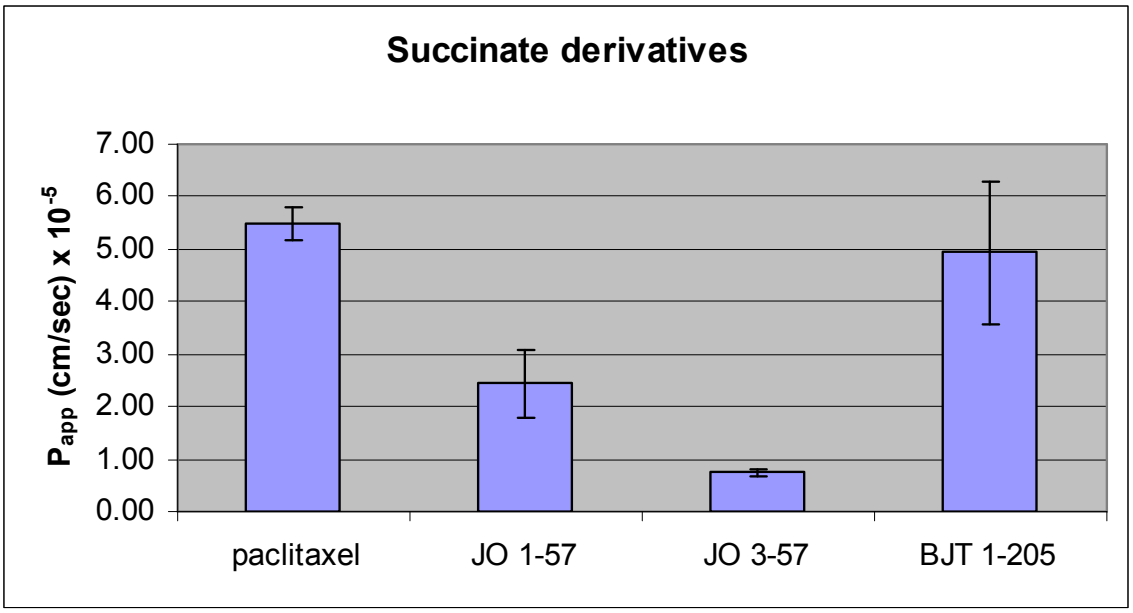

Figure 2.3.4.2 Permeability of analogues JO1-57, JO3-57 and BJT1-205 across BBMEC monolayers. No improvement in permeability was seen relative to paclitaxel. (Data ± SD, n=4). Structures found on page 56.

The other strategy in which nutrient-like groups were attached, included the two analogues which had biotin attached at either the C7 or C10 position. In both cases, a reduction in interaction with P-gp was observed; however, neither analogue showed an increase in permeability when tested using BBMECs (Figure 2.3.4.3).

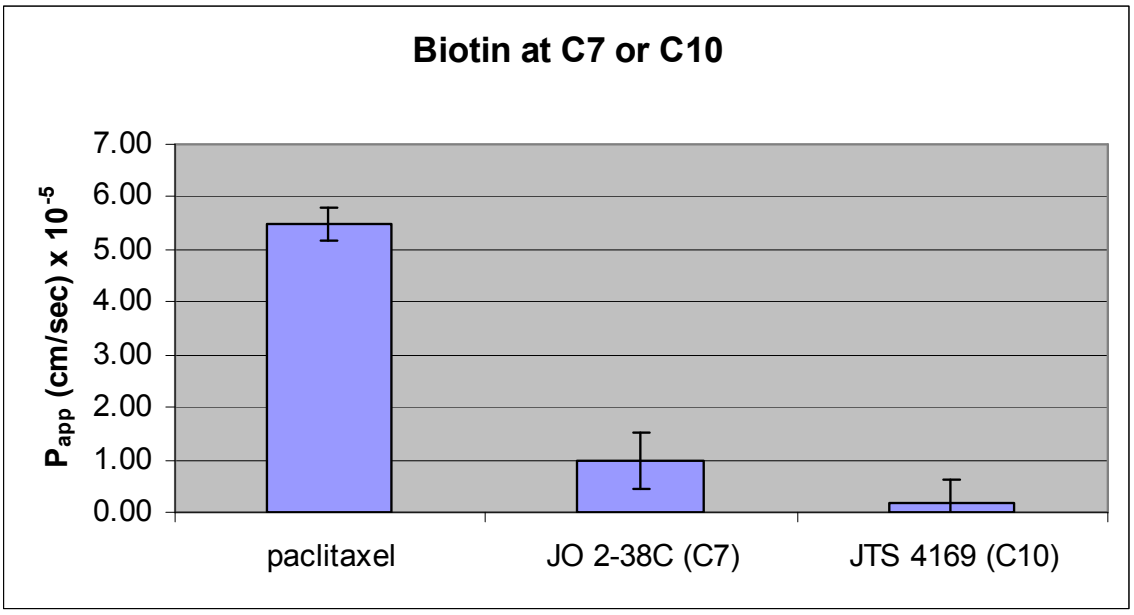

Figure 2.3.4.2 Permeability of analogues JO2-38C and JTS4169 across BBMEC monolayers. No improvement in permeability was seen relative to paclitaxel. (Data ± SD, n=4). Structures found in Appendix 2, pages 170-171.

The third and last strategy yielded three analogues that showed reduced interaction with P-gp. These analogues included HB4-63, which had an isobutenyl group in the 3' position and a succinic acid moiety at C10, HB4-91, which also had a succinic acid group at the C10 position, but an isobutyl group at the 3' position and HB4-71 which had an amide ester of succinate at the C10 position and an isobutenyl group at the 3' position. Once again, these analogues did not have improved permeability compared to paclitaxel as expected (Figure 2.3.4.3)

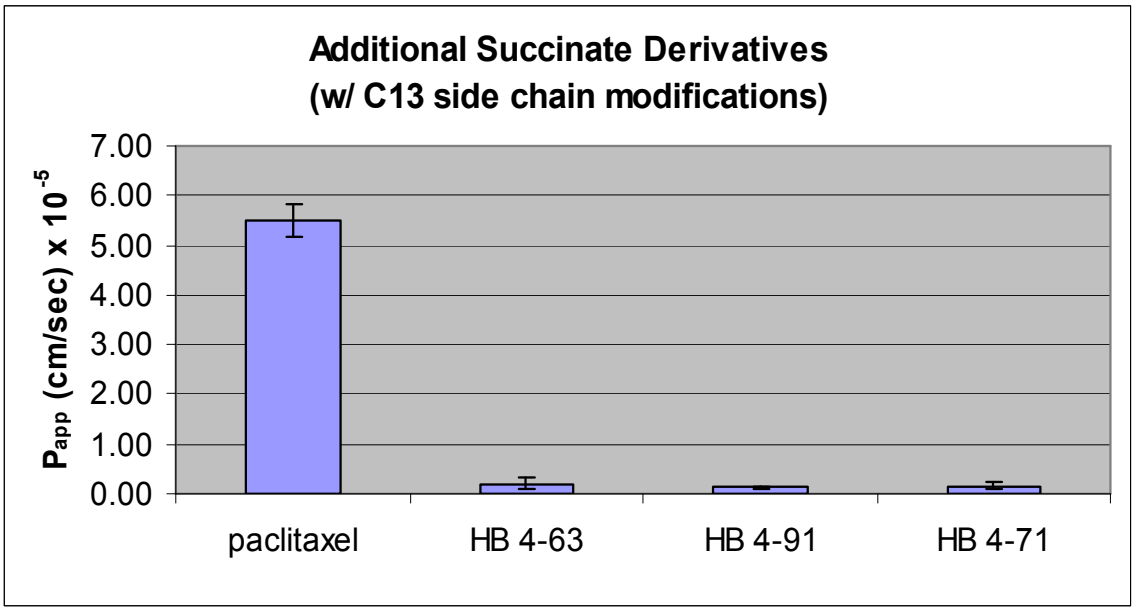

Figure 2.3.4.3 Permeability of analogues HB4-63, HB4-91 and HB4-71 across BBMEC monolayers. No improvement in permeability was seen relative to paclitaxel. (Data ± SD, n=3). Structures found on page 70.

2.3.5 Mass balance determination of select permeability studies

For permeability studies using paclitaxel analogues that contained nutrient-like groups, a mass balance calculation was performed. The donor chamber was sampled at time zero to obtain an initial concentration as well as at the end of the study to determine a final concentration. The cumulative concentration within the receiver chamber over time was also accounted for. Results showed some analogues to have a low mass balance compared to paclitaxel which has an average mass balance of approximately 94% (Figure 2.3.5.1). No trend could be seen among the compounds showing poor mass balance. It should also be noted that the cells were not examined for intracellular contents; therefore,

compound within the cells was not accounted for when calculating the mass balance. For structures of derivatives for which a mass balance was determined see Figure 2.3.5.2.

Derivative	% Mass Balance
paclitaxel	**93.4%**
JO1-57	**96.0%**
JO3-57	**64.1%**
BJT1-205	**59.3%**
JO2-38C	**55.6%**
JTS4169	**43.9%**
HB4-63	**62.7%**
HB4-91	**62.3%**
HB4-71	**94.9%**

Figure 2.3.5.1 Mass balance calculations for permeability studies of derivates containing nutrient-like groups. Structures found in Figure 2.3.5.2.

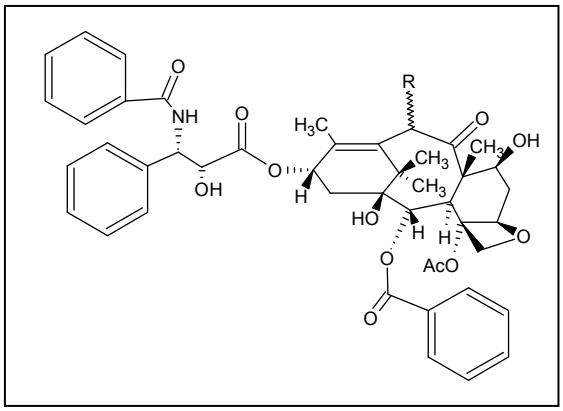

Modification (R)	Derivative name
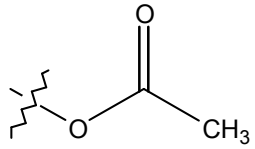	Paclitaxel
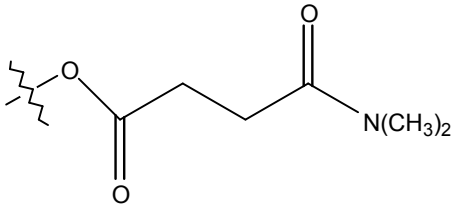	JO1-57
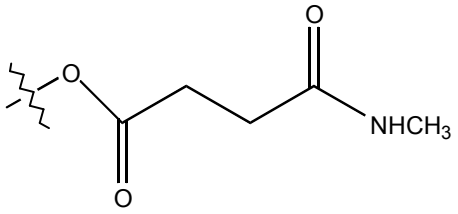	JO3-57
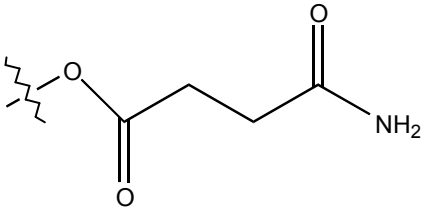	BJT1-205
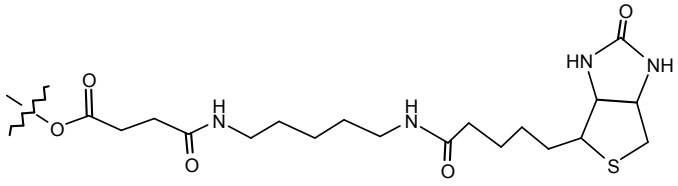	JO2-38C JTS4169 (see page 171)

Figure 2.3.5.2 Structures of derivatives for which a mass balance was determined

Derivative name

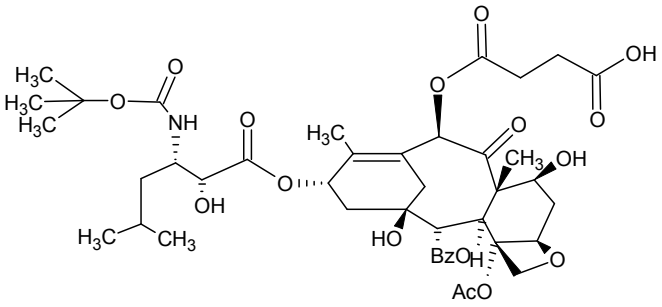

HB4-63

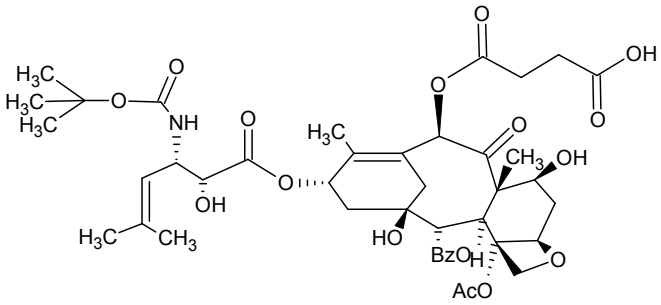

HB4-91

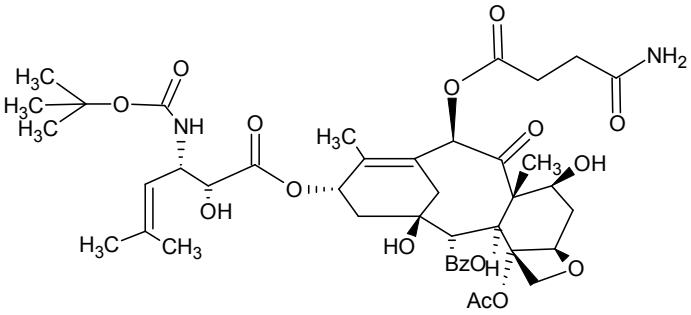

HB4-71

Figure 2.3.5.2 (cont.) Structures of derivatives for which a mass balance was determined

2.4 Discussion

Paclitaxel, a very successful chemotherapeutic agent, is unable to be used to treat cancers located within the CNS because it is a substrate for P-gp, one of the many efflux transporters located at the blood brain barrier that is responsible for keeping drugs out of the brain. One approach used to evade P-gp is modification of the structure of existing pharmacological agents such that they retain their pharmacological effect, but are no longer substrates for P-gp. This approach was taken by our laboratory in collaboration with Dr. Gunda Georg and structural analogues of paclitaxel were synthesized and their interactions with P-gp were evaluated. A variety of modification strategies were employed including 1) Spatial rearrangement at the C10 position via epimerization, 2) Addition of nutrient-like groups at the C7 and C10 position and 3) Modification of the C13 side chain to enhance potency combined with strategies one and two. For those analogues demonstrating reduced interaction with P-gp, the permeability of the analogue across monolayers of BBMECs was determined *in vitro* to predict if it would have improved permeability across the blood brain barrier.

Each of the modification strategies produced several compounds that demonstrated a reduction in P-gp interaction based on the results from the rhodamine 123 uptake assay. Although an increase in permeability was expected based on the rhodamine 123 results, an improvement in permeability relative to paclitaxel unfortunately was not seen. For those derivatives in which subtle changes in stereochemistry and the oxidation state of

the C10 carbon were made, the low permeability was surprising, as we had hoped to see an improvement in permeability once interaction with P-gp was minimized.

For those compounds which had a nutrient-like group attached, the low permeability results were not entirely surprising even though they were disappointing. Once the nutrient-like groups were attached (either succinate-like groups or biotin) the size of the molecule increased substantially. For example, the molecules containing biotin at the C7 and C10 positions had molecular weights of over 1000 Da. Studies have shown that compounds with substantially lower molecular weights (MW: 300-500 Da) have a better chance of success of crossing the blood brain barrier in a passive manner (Mahar Doan *et al*., 2002). Paclitaxel, which already has a very large molecular weight (MW: 853.92), is at an even greater disadvantage once these large nutrient-like groups are attached. If the uptake transporters that were being targeted had been able to recognize these paclitaxel molecules, then size would not have been an issue, however, it appears that recognition was not achieved.

The issue of poor mass balance in some of the permeability assays may be explained by the increase in size and lipophilicity of the molecules. There is the possibility that those compounds showing poor mass balance may be getting caught up in the lipid bilayer of the cell membrane and not permeating across to the receiver side. Additionally, since the solubility of every derivative was not calculated, there is the possibility of precipitation over the course of the permeability study. Since the intracellular contents of the BBMEC monolayer are not being analyzed, this could also account for the loss of mass.

Furthermore, there are a multitude of uptake transporters expressed at the blood brain barrier, and although many of these transporters may be expressed in the BBMECs, they have not been fully characterized. Additionally, the luminal versus abluminal expression patterns are not fully understood. Therefore, there is the possibility that these paclitaxel analogues containing nutrient-like groups are recognized by an uptake transporter at the luminal side, but there is no expression of that transporter at the abluminal side to facilitate the transport of the molecule out of the other side of the cell.

2.5 Conclusions

Structural analogues of paclitaxel were synthesized in the hopes of creating molecules that retained their pharmacological effect, but were no longer substrates for the efflux transporter P-gp. A variety of modification strategies were employed and results showed that P-gp recognition could in fact be altered with minor structural changes. Studies also reiterated the complex substrate specificity of P-gp. Changes as subtle as absolute configuration at one chiral center or the oxidation state at the C10 carbon were enough to alter recognition by P-gp. The importance of the C10 position to P-gp's recognition of paclitaxel was also highlighted. Although a reduction in interaction with P-gp did not translate to an improvement in permeability for this set of compounds, the data help improve our understanding of paclitaxel's recognition by P-gp and may direct chemistry efforts in the future.

Although paclitaxel and the structural analogues described herein would penetrate into the CNS at very low levels, recent research suggests there may be some utility of these microtubule stabilizing compounds as neuroprotective agents even at these concentrations (Michaelis *et al*., 2005). Studies have shown that taxanes, as well as other structurally diverse microtubule stabilizing compounds, may protect neurons against the β-amyloid induced neurodegeneration seen in Alzheimer's disease. A collaboration with The University of Kansas, Department of Pharmacology and Toxicology allowed us to test some of the paclitaxel analogues in a neuronal survival assay (data not shown). Additionally, this research prompted us to investigate other microtubule stabilizing compounds that possess improved physicochemical characteristics relative to paclitaxel and may more easily cross the blood brain barrier, in a passive manner.

2.6 References

Audus KL and Borchardt RT (1987) Bovine brain microvessel endothelial cell monolayers as a model system for the blood-brain barrier. *Ann N Y Acad Sci* **507**:9-18.

Beckers T and Mahboobi S (2003) Natural, semisynthetic and synthetic microtubule inhibitors for cancer therapy. *Drugs of the Future* **28**:767.

Dano K (1973) Active outward transport of daunomycin in resistant Ehrlich ascites tumor cells. *Biochim Biophys Acta* **323**:466-483.

Fellner S, Bauer B, Miller DS, Schaffrik M, Fankhanel M, Spruss T, Bernhardt G, Graeff C, Farber L, Gschaidmeier H, Buschauer A and Fricker G (2002) Transport of paclitaxel (Taxol) across the blood-brain barrier in vitro and in vivo. *J Clin Invest* **110**:1309-1318.

Georg G, Boge TC, Cheruvallath ZS, Clowers JS, Harriman GC, Hepperle M and Park H (1995) Taxol Science and Applications, in (Suffness M ed), CRC Press, Boca Raton, FL.

Jordan MA, Toso RJ, Thrower D and Wilson L (1993) Mechanism of mitotic block and inhibition of cell proliferation by taxol at low concentrations. *Proc Natl Acad Sci U S A* **90**:9552-9556.

Juliano RL and Ling V (1976) A surface glycoprotein modulating drug permeability in Chinese hamster ovary cell mutants. *Biochim Biophys Acta* **455**:152-162.

Mahar Doan KM, Humphreys JE, Webster LO, Wring SA, Shampine LJ, Serabjit-Singh CJ, Adkison KK and Polli JW (2002) Passive permeability and P-glycoprotein-

mediated efflux differentiate central nervous system (CNS) and non-CNS marketed drugs. *J Pharmacol Exp Ther* **303**:1029-1037.

Michaelis ML, Ansar S, Chen Y, Reiff ER, Seyb KI, Himes RH, Audus KL and Georg GI (2005) β-Amyloid-induced neurodegeneration and protection by structurally diverse microtubule-stabilizing agents. *J Pharmacol Exp Ther* **312**:659-668.

Ojima I, Slater JC, Michaud E, Kuduk SD, Bounaud PY, Vrignaud P, Bissery MC, Veith JM, Pera P and Bernacki RJ (1996) Syntheses and structure-activity relationships of the second-generation antitumor taxoids: exceptional activity against drug-resistant cancer cells. *J Med Chem* **39**:3889-3896.

Pardridge WM (2003) Blood-brain barrier drug targeting: the future of brain drug development. *Mol Interv* **3**:90-105, 151.

Rice A, Liu Y, Michaelis ML, Himes RH, Georg GI and Audus KL (2005) Chemical modification of paclitaxel (Taxol) reduces P-glycoprotein interactions and increases permeation across the blood-brain barrier in vitro and in situ. *J Med Chem* **48**:832-838.

Seelig A (1998) A general pattern for substrate recognition by P-glycoprotein. *Eur J Biochem* **251**:252-261.

Shi F, Bailey C, Malick AW and Audus KL (1993) Biotin uptake and transport across bovine brain microvessel endothelial cell monolayers. *Pharm Res* **10**:282-288.

Spector R and Mock D (1987) Biotin transport through the blood-brain barrier. *J Neurochem* **48**:400-404.

Spletstoser JT, Turunen BJ, Desino K, Rice A, Datta A, Dutta D, Huff JK, Himes RH, Audus KL, Seelig A and Georg GI (2006) Single-site chemical modification at

C10 of the baccatin III core of paclitaxel and Taxol C reduces P-glycoprotein interactions in bovine brain microvessel endothelial cells. *Bioorg Med Chem Lett* **16**:495-498.

van Asperen J, Mayer U, van Tellingen O and Beijnen JH (1997) The functional role of P-glycoprotein in the blood-brain barrier. *J Pharm Sci* **86**:881-884.

Chapter 3: TH-237A: A Novel Neuroprotective Agent Exhibiting Favorable Permeation Across the Blood Brain Barrier

Chapter 3: TH-237A: A Novel Neuroprotective Agent Exhibiting Favorable Permeation Across the Blood Brain Barrier

3.1 Introduction

Studies have shown that various paclitaxel analogues at nanomolar concentrations have the ability to protect neurons against β-amyloid (Aβ) induced neurotoxicity found in Alzheimer's (Michaelis *et al*., 2005). It is believed that the mechanism behind this effect is in part due to the microtubule stabilizing properties of the taxanes. Aβ deposition results in hyperphosphorylation of τ protein, a microtubule associated protein, which leads to neurofibrillary tangles that in turn leads to neuronal loss and cell death (Michaelis *et al*., 1998). Since taxanes, such as paclitaxel, promote microtubule stability (Jordan *et al*., 1993), they may help preserve the structure of the microtubule network from the destabilizing activity of Aβ. Although our laboratory has worked extensively with paclitaxel derivatives, we were prompted to investigate other microtubule stabilizing compounds that have inherently better physicochemical properties for blood brain barrier transport.

In 1997, Shintani *et al.* reported that GS-164, a small synthetic compound, stimulated microtubule assembly in a mechanism similar to that of paclitaxel (Taxol®) (Shintani *et al*., 1997). The R/R isomer was determined to be responsible for the microtubule stabilizing properties. A variety of stereoisomers of GS-164 have been synthesized in collaboration with Dr. Gunda Georg and the stereomerically pure *cis*-isomer, denoted TH-237A (Figure 3.1), showed excellent neuroprotective effects. Furthermore, this

compound showed excellent promise of permeation across the blood brain barrier based on its low molecular weight and improved solubility relative to paclitaxel.

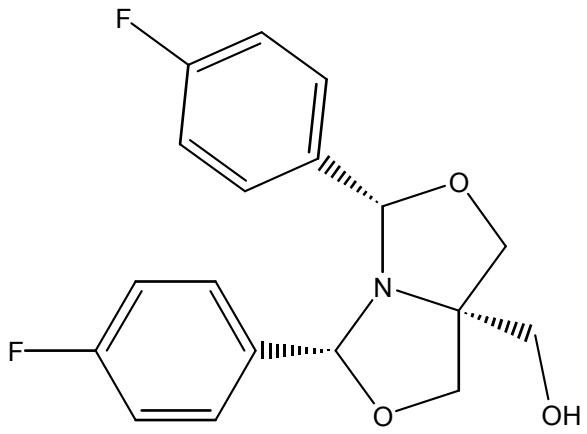

Figure 3.1 Structure of TH-237A.

The studies outlined herein demonstrate TH-237A's excellent neuroprotective properties as well as its potential to cross the blood brain barrier. A variety of *in vitro*, *in situ* and *in vivo* models were employed to predict TH-237A's brain penetration.

In collaboration with Dr. Mary Lou Michaelis' laboratory in the Department of Pharmacology and Toxicology at The University of Kansas, we investigated the neuroprotective properties of TH-237A in a neuronal culture after exposure to Aβ peptides. Primary neurons were isolated from embryonic Sprague-Dawley rats, grown in culture (Michaelis *et al*., 1994) and exposed to either $A\beta_{25-35}$ or $A\beta_{1-42}$ in the presence or absence of TH-237A at concentrations ranging from 0.5 to 60 nM. The neurons were treated with TH-237A for 2 hours prior to exposure to the Aβ peptides. Changes in

neuronal survival following treatment with TH-237A were evaluated using the Live/Dead assay (Michaelis *et al*., 1998; Michaelis *et al*., 2005). The EC_{50} for TH-237A (concentration that leads to a 50% increase in neuronal survival in the presence of the Aβ peptides) was 5 nM, demonstrating that it had excellent neuroprotective properties.

A neuroprotective agent's success as a pharmaceutical agent however depends on its ability to reach the site of action within the brain. There are a variety of barriers to brain penetration including anatomical barriers (i.e.: tight junctions, reduced pinocytosis, glycocalyx, etc.) (Reese and Karnovsky, 1967; Brightman and Reese, 1969), metabolic barriers (i.e.: peptidases, phase I and phase II enzymes, etc) (Spatz and Mrsula, 1982) and an electrostatic barrier due to sulfated glycoproteins at the cell surface. Another major barrier to brain penetration is the existence of efflux transporters expressed by the brain endothelial cells (Pardridge, 1998). If a drug is recognized as a substrate for one of these efflux transporters, the permeation across the blood brain barrier can be significantly compromised. Of the various efflux transporters, one of the most well known and most often studied is P-glycoprotein (P-gp). The rhodamine 123 uptake assay used in conjunction with bovine brain microvessel endothelial cells (BBMECs) is an efficient way to screen compounds *in vitro* for their recognition by P-gp (Fontaine *et al*., 1996). TH-237A was tested at a range of concentrations and showed no alteration in rhodamine 123 uptake, suggesting it was not a substrate for P-gp.

To test for the recognition of TH-237A by other efflux transporters as well as uptake transporters, directional permeability studies were performed *in vitro* using BBMECs. In

these studies, radiolabeled test compound ([^{3}H]-TH-237A) was added to either the luminal or abluminal side of the cells and permeability was monitored over time. A directional dependent difference in permeability is an indication that an active process is occurring. In studies with [^{3}H]-TH-237A, no directional permeability differences existed, indicating that the permeation of TH-237A was a passive process. This finding was confirmed with the use of temperature dependent permeability studies *in vitro* with BBMECs from which an Arrhenius plot was generated and an activation energy was calculated.

Since *in vitro* permeability studies with BBMECs suggested very favorable permeability across the blood brain barrier, TH-237A was tested using the *in situ* rat brain perfusion model. [^{3}H]-TH-237A infused directly into the carotid artery of anesthetized rats showed very good brain penetration after just 60 seconds of perfusion.

In collaboration with the Higuchi Biosciences Center, TH-237A was then tested *in vivo* in balb/C rats and complete pharmacokinetics parameters were determined. Blood was collected via cardiac puncture at multiple time points and brain tissue was harvested. After either intravenous injection into the tail vein or subcutaneous injection, significant amounts of TH-237A entered the brain, supporting the *in vitro* and *in situ* predictions that TH-237A would have very good brain penetration Furthermore, the high brain concentrations were achieved rapidly and drug loss from the brain was quite slow with a half-life on the order of hours.

3.2 Experimental

3.2.1 Synthesis of TH-237A

Sythesis of TH-237A was performed by the Georg laboratory at The University of Kansas. A suspension of *p*-fluorobenzaldehyde (27 g, 0.22 mol) and tris(hydroxymethyl)aminomethane (13 g, 0.11 mol) in toluene (350 ml) was heated at reflux temp with azeotropic removal of water for 12 hrs. The reaction mixture was concentrated, stirred at room temperature and the precipitated unreacted *p*-fluorobenzaldehyde was filtered off. The residue obtained after removal of solvent was subjected to flash chromatography on silica gel using hexane:ethylacetate (4:1 and 1:1). Crystallization of the respective fractions afforded pure compound in a yield of 66% based on equimolar product distribution ratio. The structure of the product was assigned by spectral data and the relative stereochemistry of TH-237A was assigned from single crystal X-ray diffraction data. For radiolabeled studies, the TH-237A was custom labeled with tritium [^{3}H] by Moravek Biochemicals, Inc. (Brea, CA).

3.2.2 Isolation and maintenance of BBMECs

Bovine brain microvessel endothelial cells (BBMECs) were isolated from the gray matter of bovine cerebral cortices by enzymatic digestion followed by centrifugation and then seeded as primary cultures following methods described by Audus *et al*. (Audus and Borchardt, 1987). Isolated BBMECs were seeded at a density of approximately 50,000 cells/cm^2 onto 24-well culture plates or 100 mm culture dishes (Corning Costar, Acton,

MA) containing Nucleopore® polycarbonate membranes (pore size 0.4 μm) (Whatman, Florham Park, NJ) pretreated with rat-tail collagen prepared in house and fibronectin (Sigma-Aldrich, St. Louis, MO). Culture medium was prepared and cells were maintained as described in the experimental section of Chapter 2.

3.2.3 Rhodamine 123 uptake assay

In this assay, rhodamine 123 is used as a surrogate P-glycoprotein (P-gp) substrate (Fontaine *et al*., 1996). The effect of the test compound on rhodamine123 is determined by monitoring intracellular fluorescence. If the test compound is a substrate for P-gp, then addition of the compound will increase rhodamine 123 uptake relative to the negative control. BBMECs were seeded onto 24-well plates coated with rat tail collagen and fibronectin at a density of approximately 50,000 cells/cm^2. Culture medium was replaced every other day until cells formed a confluent monolayer. At the start of the experiment, BBMECs were rinsed with warm PBSA (PBS containing $CaCl_2$, $MgSO_4$, glucose and L-ascorbic acid) and allowed to acclimate to the warm PBSA for 10 minutes. The PBSA was removed and solutions of TH-237A (conc.: 1-50μM) were added to the wells and allowed to incubate for 30 minutes at 37 degrees C in a hotbox. Rhodamine 123 was then added to all wells at a concentration of 5 μM and the plate was returned to the hotbox. Cells were incubated for an additional 2 hours. After the incubation, cells were quickly rinsed with ice cold PBS several times. Lysis buffer (0.5% v/v Triton X-100 in 0.2 N NaOH) was then added to all wells and allowed to solubilize cells for at least 30 minutes. 200 μL aliquots were taken from all wells to determine Rhodamine 123

concentration and 10 µL aliquots were taken from all wells to determine protein concentration. Rhodamine 123 concentrations were determined on a Biotek FL600 Microplate Fluorescence Reader (excitationλ: 485, emissionλ: 530). Protein determination was performed using a Pierce BCA Protein Assay Kit (Pierce, Rockford, IL) and samples were read on an EIA reader at 540 nm.

3.2.4 Permeation of TH-237A across BBMEC monolayers

3.2.4.1 Bi-directional permeation studies

BBMECs were grown on 0.4 µm Nucleopore® polycarbonate membranes in a 100 mm culture dish coated with rat tail collagen and fibronectin. Once cells had formed a confluent monolayer as determined by light microscopy, the membranes were transferred to Side-bi-Side™ diffusion chambers as previously described by Audus *et al.* (Audus *et al*., 1996; Audus *et al*., 1998). Briefly, each chamber was filled with 3 mL of PBSA and either the luminal or abluminal donor chambers contained 10 µM of unlabeled TH-237A and a trace amount of [^{3}H]-TH-237A. A temperature of 37 degrees C was maintained within the chamber with an external circulating water bath and chamber contents were stirred with Teflon coated magnetic stir bars driven by an external console. At the various time points (5, 15, 30, 45 and 90 minutes), 200 µL aliquots were removed from the receiver side and replaced with 200 µL of blank PBSA warmed to 37 degrees C. Samples of the donor solution were also taken for analysis. The integrity of the cell monolayer was tested post experiment by monitoring the permeability of [^{14}C]-sucrose, a

paracellular marker which should not readily cross the cell monolayer. All samples were analyzed for concentration by liquid scintillation counting.

3.2.4.2 Temperature dependent permeation studies

Again, BBMECs were grown on 0.4 μm Nucleopore® polycarbonate membranes then transferred to Side-bi-Side™ diffusion chambers. 10 μM TH-237A with trace amounts of [^{3}H]-TH-237A was added to the luminal chambers and 200μL samples were taken from the abluminal chamber at various time points (5, 15, 30, 45, and 90 minutes). Permeation of TH-237A was calculated at a range of temperatures (4, 8, 12, 16, 20, 26, 30 and 37 degrees C) in order to determine an activation energy. The integrity of the cell monolayer was tested post experiment by monitoring the permeability of [^{14}C]-sucrose and samples were analyzed by liquid scintillation counting.

3.2.4.3 Inhibition studies using [^{3}H]-TH-237A

BBMECs were grown in 24-well plates coated with rat tail collagen and fibronectin at a density of approximately 50,000 cells/cm^{2}. Upon confluency, cells were washed several times with warm PBSA and allowed to acclimate to the PBSA for approximately 10 minutes. [^{3}H]-TH-237A (1 nM) and non-radiolabeled TH-237A (0.5 nM, 1 nM, 10 nM, 10 0nM, 1 μM, 10 μM and 100 μM) were added (N=3) to the cells and allowed to incubate for 1 hour at 37 degrees C in a shaking hotbox. At the end of the incubation, cells were rinsed several times with ice cold PBS and lysis buffer (0.5% v/v Triton X-100

in 0.2 N NaOH) was then added to all wells and allowed to solubilize cells for at least 30 minutes. 200 μL aliquots of the lysed cells were then taken for analysis by liquid scintillation counting and 10 μL of lysed cells were taken for protein determination using a Pierce BCA Protein Assay Kit (Pierce, Rockford, IL). Inhibition of radiolabeled TH-237A uptake by increasing amounts of non-radiolabeled TH-237A was investigated.

3.2.5 In situ *rat brain perfusion*

Adult male Sprague-Dawley rats, weighing approximately 250-350 g were purchased from Charles River and the *in situ* rat brain perfusion described by Smith and Allen (Smith and Allen, 2003) was used. Rats were administered, by subcutaneous injection, a complete anesthetic cocktail including 0.37 mg/mL acepromazine, 1.9 mg/mL xylazine and 37.5 mg/mL ketamine in sterile saline at a dose of 1.5 mg/kg. To maintain the anesthetic plane throughout the experiment an incomplete anesthetic cocktail was used containing 0.37 mg/mL acepromazine and 37.5 mg/mL ketamine at 1/3 of the initial dose every hour. Once anesthetized, the rat was placed on a warming pad to maintain a body temperature of 37 degrees C. Briefly, an incision was made at the neck of the animal and the salivary gland, sternohyodious and sternomastoideus muscles were moved to expose the carotid artery. The external carotid artery and occipital artery were tied off with a suture while the internal carotid artery was clamped. Once the internal carotid artery was cannulated, the clamp was removed and perfusion buffer containing 10 μM TH-237A and trace amounts of [^{3}H]-TH-237A was perfused for 60 seconds with a 30 second pre-perfusion and 10 second post-perfusion of blank saline. Following perfusion, the animal

was decapitated by guillotine and the brain was removed and placed on ice. The brain was then dissolved in Solvable® for approximately 24 hours before analysis by liquid scintillation counting. Animals were used and housed in accordance with The University of Kansas Institutional Animal Care and Use Committee's policies. The blood brain barrier transfer coefficient for unidirectional uptake of TH-237A into the brain from the perfusion buffer was calculated using the following equation:

$$K_{in} = (Q_{br}/C_{pf})/t$$

where Q_{br} is the total amount of drug in the brain, C_{pf} is the concentration of drug in the perfusion buffer and t is the perfusion time. K_{in} can then be converted into the cerebrovascular permeability-surface area product (PA) by using the Crone-Renkin model of capillary transfer (Crone and Levitt, 1984):

$$PA = -F \ln (1 - K_{in}/F)$$

Where F is the regional cerebral blood flow which was previously determined by using the flow limited diffusion marker [^{3}H]-diazepam and A is the rat brain capillary surface area of 130 cm^2/g as previously reported (Crone and Levitt, 1984). P is the apparent permeability coefficient of the blood brain barrier for the test compound.

3.3 Results

3.3.1 Effects of TH-237A on rhodamine 123 uptake

TH-237A was tested in the rhodamine 123 uptake assay using BBMECs grown in a 24-well plate. The uptake of rhodamine 123 was monitored in the presence of TH-237A at concentrations ranging from 1 to 50 µM (Figure 3.3.1). No significant increase in rhodamine 123 was observed, except for in the presence of the positive control, cyclosporine A (CsA), a known substrate for P-gp. These data suggest TH-237A is not recognized as a substrate for the efflux transporter P-glycoprotein, which is expressed at the brain endothelium, and can present a barrier to brain penetration.

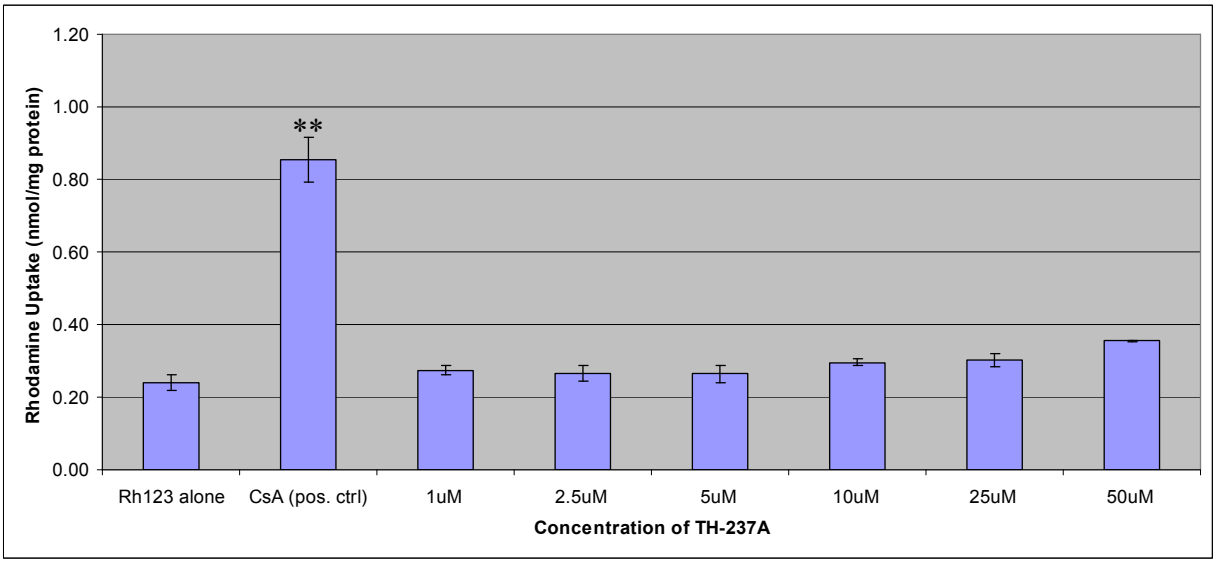

Figure 3.3.1. TH-237A tested at a range of concentrations in the rhodamine 123 uptake assay, a surrogate measure of P-gp interaction. (** Denotes $p<0.01$ compared to the control (rhodamine alone) as determined by ANOVA, Data ± SD, n=3)

3.3.2 Bi-directional permeation of TH-237A across BBMEC monolayers

TH-237A (10 μM) was added to the luminal (blood) or abluminal (brain) side of the BBMEC monolayer and permeation was monitored for 1.5 hours. During this time, permeation across the monolayer was linear (R^2= 0.99) and all experiments were carried out N=4. The apparent permeability value of TH-237A was calculated using the following equation:

$$P_{app} = (\Delta Q/\Delta t)/ A \times C_0$$

where $\Delta Q/\Delta t$ is the linear appearance of TH-237A in the receiver chamber, A is the cross sectional area of the cell monolayer (0.636 cm^2) and C_0 is the initial concentration of TH-237A in the donor chamber at t = 0. In the luminal to abluminal direction, the P_{app} = 2.86 x 10^{-4} cm/sec and in the abluminal to luminal direction, the P_{app} = 2.44 x 10^{-4} producing no statistically significant difference in permeability as a result of direction (Figure 3.3.2).

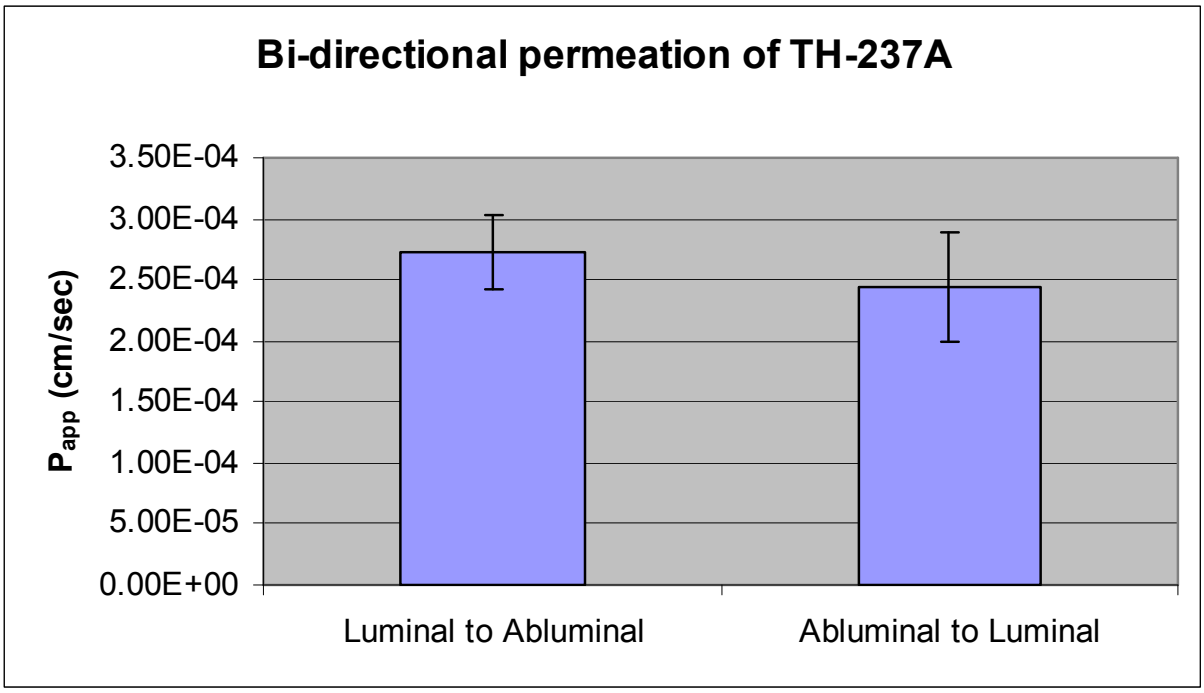

Figure 3.3.2. Bi-directional permeability data for TH-237A in BBMECs. No statistical difference was observed. (Data ± SD, n=8)

3.3.3 Temperature-dependent permeation of TH-237A across BBMEC monolayers

Permeation of TH-237A was investigated at a range of temperatures in order to generate an Arrhenius plot. The permeability of TH-237A was calculated in the luminal to abluminal direction at temperatures of 4, 8, 12, 16, 20, 26, 30 and 37 degrees C. The activation energy calculated from the slope of the Arrhenius plot is 26.3 kJ/mol, suggestive of a passive process (Figure 3.3.3).

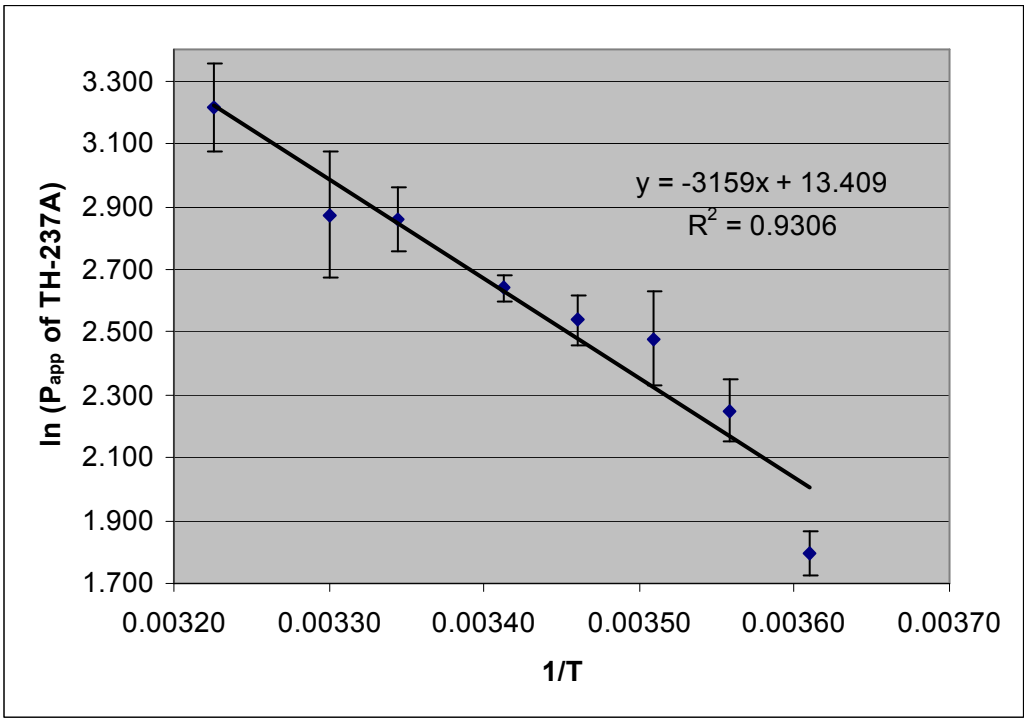

Figure 3.3.3. Arrhenius plot generated by the temperature dependent permeability of TH-237A in BBMECs. Permeability values were calculated at a variety of temperatures ranging from 4 degrees C to 37 degrees C. (Data ± SD, n=4)

3.3.4 Inhibition studies using [^{3}H]-TH-237A

The uptake of [^{3}H]-TH-237A into BBMECs was measured in the presence of varying amounts of unlabeled TH-237A. There was no significant difference in [^{3}H]-TH-237A uptake in the presence of small amounts, equal amounts nor excess amounts of unlabeled TH-237A, further suggesting that the uptake of the compound into the cells was passive diffusion (Figure 3.3.4).

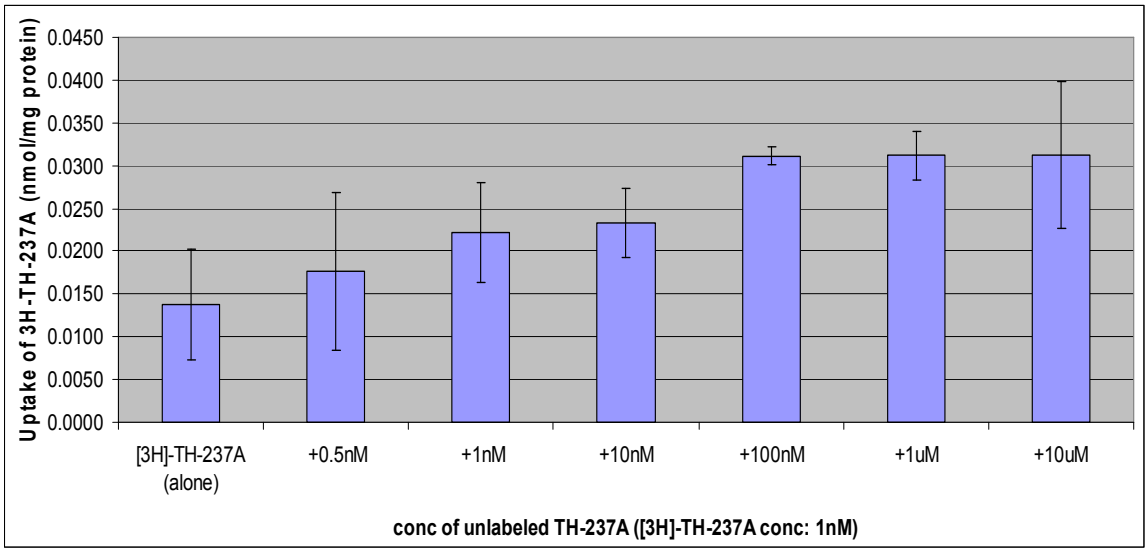

Figure 3.3.4. The intracellular uptake of [^{3}H]-TH-237A in the presence of increasing concentrations of unlabeled TH-237A. (no statistical difference from control, Data ± SD, n=3)

3.3.5 In situ *rat brain perfusion*

Brain penetration of TH-237A was investigated using the *in situ* rat brain perfusion modeled described by Smith and Allen (Smith and Allen, 2003). A solution of 10 µM TH-237A containing trace amounts of [^{3}H]-TH-237A was infused into the carotid artery of cannulated rats for 60 seconds. A pre-wash infusion of saline was performed for 30 seconds and a post-wash infusion was performed for 10 seconds before harvesting the brain. Solubilized brain tissue was then analyzed by liquid scintillation counting. The blood brain barrier transfer coefficient (K_{in}) for unidirectional uptake of TH-237A was determined to be 3.87 x 10^{-3} mL/s/g where Q_{br} =2.32 nmol/g, C_{pf} = 10.01 nmol/mL and

t= 60 sec. The K_{in} was converted to the cerebrovascular permeability-surface area product (PA) using a regional cerebral flow of 0.0253 mL/s/g and an area = 130 cm^2 to give an apparent permeability coefficient of the blood brain barrier for TH-237A = 3.23 x 10^{-5} cm/sec (Figure 3.3.5). For comparison purposes, the permeability of sucrose, a low permeability, paracellular marker, was determined as well as that of paclitaxel which is a pharmaceutical agent known to have very minimal brain penetration. Sucrose and paclitaxel had apparent permeability coefficients of 7.43 x 10^{-6} cm/sec and 1.70 x 10^{-7} cm/sec respectively.

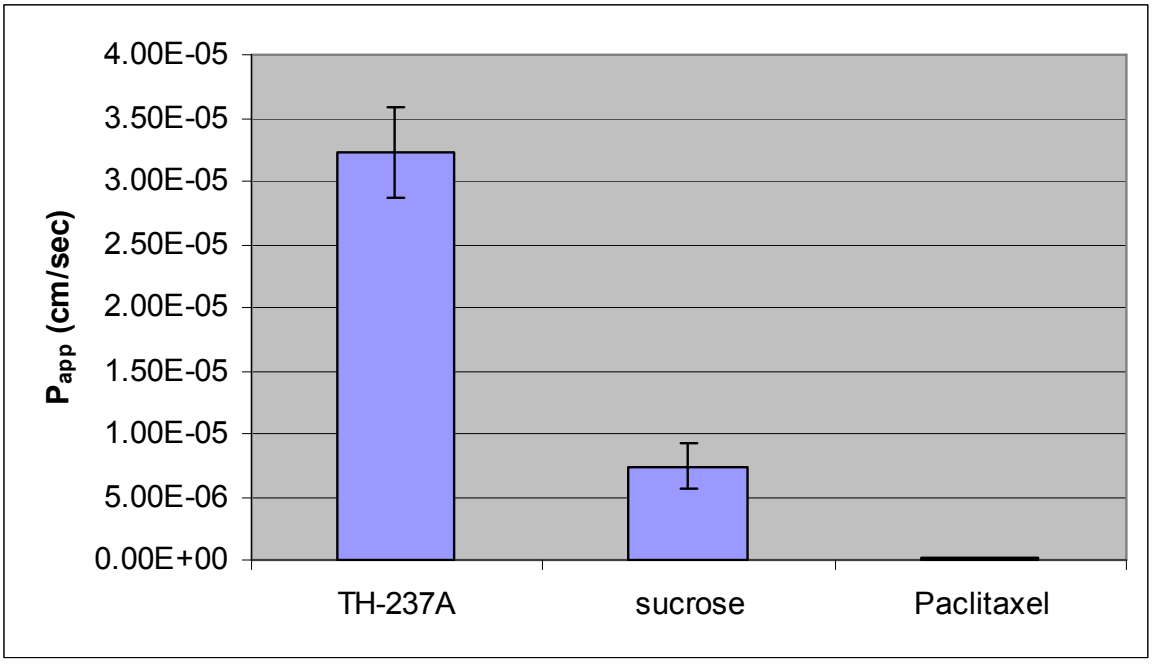

Figure 3.3.5. Apparent permeability coefficients of TH-237A, sucrose and paclitaxel as determined using the *in situ* rat brain perfusion model. (Data ± SD, n=3).

3.4 Discussion

Like paclitaxel, GS-164 is a microtubule stabilizing compound that has been shown to be both chemotherapeutic and neuroprotective. A variety of isomers of GS-164 were synthesized and TH-237A, the *cis*-isomer of GS-164, has been shown to have excellent neuroprotective properties, but is only mildly chemotherapeutic (data not shown). Since TH-237A must be able to cross the blood brain barrier to exert its neuroprotective effects, the potential for TH-237A to penetrate the blood brain barrier was thoroughly investigated *in vitro, in situ* and *in vivo*. *In vitro* studies performed using BBMECs as a model of the blood brain barrier indicated that TH-237A had excellent potential for brain penetration and this was confirmed with *in situ* and *in vivo* studies. Although TH-237A is a microtubule stabilizing agent like paclitaxel, it is structurally very different. The physicochemical properties of TH-237A make it a much better candidate for use as a CNS drug. Compared to paclitaxel, TH-237A has a much lower molecular weight (MW: 333.3), possesses halogen groups that improve passive diffusion and is not a substrate for any of the efflux transporters expressed at the brain endothelium. All of these features are very important in determining whether a drug will be able to cross the blood brain barrier and reach a site of action within the brain (Birnbaum, 1985; Mahar Doan *et al*., 2002; Raub, 2006).

3.5 Conclusion

Studies suggesting that microtubule stabilizing compounds can be neuroprotective against the effects of Aβ induced neurodegeneration prompted our collaborators in the Department of Pharmacology and Toxicology to examine the effect of various taxane molecules as well as structurally diverse microtubule stabilizing compounds in an *in vitro* neuronal survival assay. Since neuroprotection was observed with paclitaxel and several of its derivatives (Michaelis *et al*., 2005), we investigated GS-164, a small molecule purported to bind microtubules in a similar fashion as paclitaxel. In addition to GS-164, pure stereoisomers of GS-164 were also tested. The *cis*-isomer, TH-237A, was seen to have excellent neuroprotective properties as well as excellent penetration across the blood brain barrier, making it an excellent candidate for a neuroprotective agent. *In vitro* studies indicated that TH-237A crosses the blood brain barrier in a passive fashion and *in vivo* studies demonstrated that brain uptake was rapid and the drug remained in the brain for a prolonged time, with a half-life on the order of hours.

3.6 References

Audus KL and Borchardt RT (1987) Bovine brain microvessel endothelial cell monolayers as a model system for the blood-brain barrier. *Ann N Y Acad Sci* **507**:9-18.

Audus KL, Ng L, Wang W and Borchardt RT (1996) Brain microvessel endothelial cell culture systems, in *Model Systems for Biopharmaceutical Assessment of Drug Absorption and Metabolism* (Borchardt RT, Smith, P.L., Wilson, G. ed) pp 239-258, Plenum, New York.

Audus KL, Rose JM, Wang W and Borchardt RT (1998) Brain microvessel endothelial cell culture systems, in *An Introduction to the Blood-Brain Barrier: Methodology and Biology* (Pardridge W ed) pp 86-93, Cambridge University, Cambridge.

Birnbaum LS (1985) The role of structure in the disposition of halogenated aromatic xenobiotics. *Environ Health Perspect* **61**:11-20.

Brightman MW and Reese TS (1969) Junctions between intimately apposed cell membranes in the vertebrate brain. *J Cell Biol* **40**:648-677.

Crone C and Levitt DG (1984) Capillary permeability to small solutes, in (Renkin EM and Michel CC eds) pp 411-466, American Physiological Society, Bethesda.

Fontaine M, Elmquist WF and Miller DW (1996) Use of rhodamine 123 to examine the functional activity of P-glycoprotein in primary cultured brain microvessel endothelial cell monolayers. *Life Sci* **59**:1521-1531.

Jordan MA, Toso RJ, Thrower D and Wilson L (1993) Mechanism of mitotic block and inhibition of cell proliferation by taxol at low concentrations. *Proc Natl Acad Sci U S A* **90**:9552-9556.

Mahar Doan KM, Humphreys JE, Webster LO, Wring SA, Shampine LJ, Serabjit-Singh CJ, Adkison KK and Polli JW (2002) Passive permeability and P-glycoprotein-mediated efflux differentiate central nervous system (CNS) and non-CNS marketed drugs. *J Pharmacol Exp Ther* **303**:1029-1037.

Michaelis ML, Ansar S, Chen Y, Reiff ER, Seyb KI, Himes RH, Audus KL and Georg GI (2005) β-Amyloid-induced neurodegeneration and protection by structurally diverse microtubule-stabilizing agents. *J Pharmacol Exp Ther* **312**:659-668.

Michaelis ML, Ranciat N, Chen Y, Bechtel M, Ragan R, Hepperle M, Liu Y and Georg G (1998) Protection against beta-amyloid toxicity in primary neurons by paclitaxel (Taxol). *J Neurochem* **70**:1623-1627.

Michaelis ML, Walsh JL, Pal R, Hurlbert M, Hoel G, Bland K, Foye J and Kwong WH (1994) Immunologic localization and kinetic characterization of a Na^{+}/Ca^{2+} exchanger in neuronal and non-neuronal cells. *Brain Res* **661**:104-116.

Pardridge WM (1998) CNS drug design based on principles of blood-brain barrier transport. *J Neurochem* **70**:1781-1792.

Raub TJ (2006) P-glycoprotein recognition of substrates and circumvention through rational drug design. *Mol Pharm* **3**:3-25.

Reese TS and Karnovsky MJ (1967) Fine structural localization of a blood-brain barrier to exogenous peroxidase. *J Cell Biol* **34**:207-217.

Shintani Y, Tanaka T and Nozaki Y (1997) GS-164, a small synthetic compound, stimulates tubulin polymerization by a similar mechanism to that of Taxol. *Cancer Chemother Pharmacol* **40**:513-520.

Smith QR and Allen DD (2003) In situ brain perfusion technique. *Methods Mol Med* **89**:209-218.

Spatz M and Mrsula B (1982) Progress in cerebral microvascular studies related to the function of the blood-brain barrier. *Adv Cell Neurobiol* **3**:311–337.

Chapter 4: TCP-FA4: A Derivative of Tranylcypromine Showing Improved Blood Brain Barrier Permeability

Chapter 4: TCP-FA4: A Derivative of Tranylcypromine Exhibiting Improved Blood Brain Barrier Permeability

4.1 Introduction

Delivery of pharmaceutical agents to the brain is one of the most challenging areas of drug delivery. The biological makeup of the blood brain barrier creates a very formidable barrier. Tight junctions, minimized surface area, electrostatics and increased metabolism as well as efflux systems all work together to create this barrier (Reese and Karnovsky, 1967; Brightman and Reese, 1969; Hegmann *et al*., 1992; Huai-Yun *et al*., 1998). A variety of approaches have been taken to improve the brain penetration of pharmaceutical agents, some of which have been outlined in previous chapters of this dissertation. The objective of this specific study was to investigate the effect of the attachment of lipoamino acids and fatty acid chains on the blood brain barrier permeability of a model compound, tranylcypromine. This project was in collaboration with colleagues at the Dipartimento de Scienze Farmaceutiche at Univerità degli Studi di Catania in Catania, Italy.

The rationale behind this study was that by increasing the membrane-like character of a compound, one can improve it's interaction with the lipid bilayer within cell membranes, and as a result improve permeability. The proof of concept was attempted using the irreversible monoamine oxidase inhibitor (MAOI) tranylcypromine (TCP) (Figure 4.1). Various derivatives of TCP were synthesized by our collaborators at the Univerità degli

Studi di Catania in which fatty acid chains or lipoamino acids of various lengths were attached (Pignatello et al., 2005) (Figure 4.2).

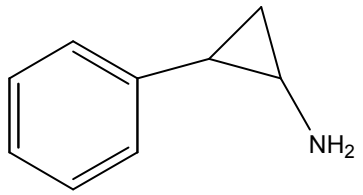

Figure 4.1 Tranylcypromine an irreversible MAO inhibitor

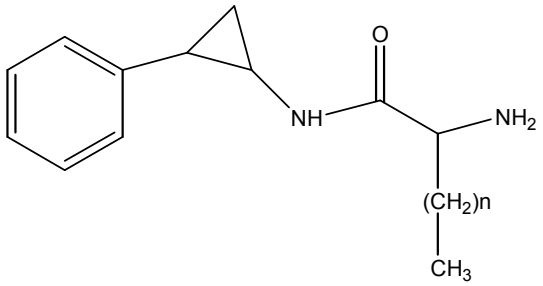

Compound	**n**
TCP-LAA6	3
TCP-LAA10	7
TCP-LAA12	9

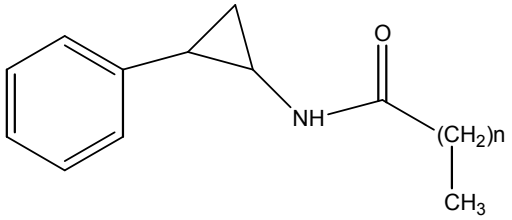

Compound	**n**
TCP-FA4	2
TCP-FA12	10

Figure 4.2 Tranylcypromine derivatives of lipoamino acids (LAA) or fatty acids (FA) of varying length.

Although the addition of fatty acid chains increases lipophilicity, the addition of lipoamino acids has the added advantage of incorporating amphipathic character into the drug molecules which in turn can facilitate their interaction with cell membranes. This approach to improving permeability across biological barriers, including the blood brain barrier, has been taken before and has shown some success (Jolliet-Riant and Tillement, 1999; Bodor and Buchwald, 2002; Waterhouse, 2003). Various approaches both computational and experimental were taken by our Italian collaborators to predict the TCP derivatives' interaction with membranes (Pignatello *et al*., 2005; Pignatello *et al*., 2006) (data not included). These TCP derivatives were then tested in our laboratory using an *in vitro* model of the blood brain barrier in which we use bovine brain microvessel endothelial cells (BBMECs). Studies showed that although TCP derivatives containing lipoamino acids were predicted to have better permeability than their fatty acid counterparts, TCP-FA4, one of the derivatives containing a four carbon fatty acid chain showed the greatest improvement in permeability. The transport properties of this derivative were thoroughly characterized and are described herein.

Furthermore, we briefly investigated the neuroprotective properties of TCP-FA4. Although this compound was originally synthesized as a model compound to demonstrate a proof of concept, literature suggested that tranylcypromine could have neuroprotective properties (Sowa *et al*., 2004). Since TCP-FA4 is predicted to have such excellent blood brain barrier permeability, it could prove to be an important discovery if it is neuroprotective. TCP (and potentially its derivatives) could be neuroprotective as a result of their ability to induce synthesis of brain derived neurotrophic factor (BDNF)

(Sowa *et al*., 2004). BDNF is a 27 kDa protein found within the brain and periphery that supports the survival of existing neurons as well as aids in the growth and differentiation of new neurons (Pezet and Malcangio, 2004). In recent years, BDNF has become a drug target for many CNS disorders including Alzheimer's, Parkinson's, epilepsy, (Pezet and Malcangio, 2004) as well as cerebral ischemia (Sowa *et al*., 2004). Since neurotrophins possess less than optimal pharmacological properties including poor stability and minimal blood brain barrier permeation, the discovery of small molecules that can regulate BDNF expression could prove beneficial (Longo and Massa, 2005).

4.2 Experimental

4.2.1 Isolation and maintenance of BBMECs

Bovine brain microvessel endothelial cells (BBMECs) were isolated from the gray matter of bovine cerebral cortices by enzymatic digestion followed by centrifugation and then seeded as primary cultures following methods described by Audus *et al*. (Audus and Borchardt, 1987). Isolated BBMECs were seeded at a density of approximately 50,000 cells/cm^2 onto 24-well culture plates or 100 mm culture dishes (Corning Costar, Acton, MA) containing Nucleopore® polycarbonate membranes (pore size 0.4 μm) (Whatman, Florham Park, NJ) pretreated with rat-tail collagen prepared in house and fibronectin (Sigma-Aldrich, St. Louis, MO). Culture medium was prepared and cells were maintained as described in the experimental section of Chapter 2.

4.2.2 Maintenance of HUVECs

Human umbilical vein endothelial cells (HUVECs) were obtained from American Type Culture Collection (ATCC) (Manassas, VA) and cultured in Dulbecco's modified eagle's media containing 10% fetal bovine serum, 100 units/mL of penicillin G sodium, 100 μg/mL of streptomycin sulfate, 2.0 g/L $NaHCO_3$, 1.42 g/L HEPES-Na, 1% glutamine, and 1% nonessential amino acids. Cell culture medium was replaced every other day after seeding until cells had grown to confluency. Cells were grown at 37 degrees C under 5% CO_2 and 95% relative humidity.

4.2.3 Rhodamine 123 uptake assay

Although tranylcypromine is not known to be a substrate for any efflux transporters expressed at the brain endothelium, the TCP derivatives were tested for potential interaction with P-glycoprotein (P-gp), one of the most prevalent of the efflux transporters that is most responsible for limiting drug entry into the brain (van Asperen *et al*., 1997). Since these molecules had increased lipophilicity, there was a chance they could become substrates since P-gp substrates are often lipophilic in nature (Stouch and Gudmundsson, 2002). The rhodamine 123 assay is a rather facile and reliable way to predict potential P-gp interaction (Fontaine *et al*., 1996). The effect of the test compound on rhodamine123 is determined by monitoring intracellular fluorescence. If the test compound is a substrate for P-gp, then addition of the compound will increase rhodamine 123 uptake relative to the negative control. BBMECs were seeded onto

24-well plates coated with rat tail collagen and fibronectin at a density of approximately 50,000 cells/cm^2. Culture medium was replaced every other day until cells formed a confluent monolayer. At the start of the experiment, BBMECs were rinsed with warm PBSA (PBS containing $CaCl_2$, $MgSO_4$, glucose and L-ascorbic acid) and allowed to acclimate to the warm PBSA for 10 minutes. The PBSA was removed and solutions of TCP derivatives (conc.: 10 μM) were added to the wells and allowed to incubate for 30 minutes at 37 degrees C in a hotbox. Rhodamine 123 was then added to all wells at a concentration of 5 μM and the plate was returned to the hotbox. Cells were incubated for an additional 2 hours. After the incubation, cells were quickly rinsed with ice cold PBS several times. Lysis buffer (0.5% v/v Triton X-100 in 0.2N NaOH) was then added to all wells and allowed to solubilize cells for at least 30 minutes. 200 μL aliquots were taken from all wells to determine Rhodamine 123 concentration and 10 μL aliquots were taken from all wells to determine protein concentration. Rhodamine 123 concentrations were determined on a Biotek FL600 Microplate Fluorescence Reader (excitationλ: 485, emissionλ: 530). Protein determination was performed using a Pierce BCA Protein Assay Kit (Pierce, Rockford, IL) and samples were read on an EIA reader at 540 nm.

4.2.4 Characterization of TCP derivative transport using BBMEC monolayers

4.2.4.1 Permeability studies

BBMECs were grown on 0.4 μm Nucleopore® polycarbonate membranes in a 100 mm culture dish coated with rat tail collagen and fibronectin. Once cells had formed a confluent monolayer as determined by light microscopy, the membranes were transferred to Side-bi-Side™ diffusion chambers as previously described by Audus *et al.* (Audus *et al*., 1996; Audus *et al*., 1998). Briefly, each chamber was filled with 3mL of PBSA and the luminal donor chamber contained 10 μM of the TCP derivative. A temperature of 37 degrees C was maintained within the chamber with an external circulating water bath and chamber contents were stirred with Teflon coated magnetic stir bars driven by an external console. At the various time points (5, 15, 30, 45 and 90 minutes), 200 μL aliquots were removed from the receiver side and replaced with 200 μL of blank PBSA warmed to 37 degrees C. For the derivative TCP-FA4, permeability was extremely rapid, so in order to monitor permeability within a linear range, earlier timepoints had to be taken. For all studies with TCP-FA4, timepoints were instead taken at 2, 5, 10, 15, 20 and 30 minutes. Samples of the donor solution were also taken for analysis. All samples were analyzed for concentration using LC/MS/MS analysis (see section 4.2.4.5 for details). The integrity of the cell monolayer was tested post experiment by monitoring the permeability of [^{14}C]-sucrose, a paracellular marker which should not readily cross the cell monolayer. All sucrose samples were analyzed for concentration by liquid scintillation counting.

Additionally, this same experimental setup was used to investigate whether there were any directional differences in transport due to membrane transporters. In these bi-directional permeability studies, compound was added to the abluminal side and the luminal side was monitored over time.

4.2.4.2 TCP-FA4: Temperature dependent permeation studies

Again, BBMECs were grown on 0.4 μm Nucleopore® polycarbonate membranes then transferred to Side-bi-Side™ diffusion chambers. 10 μM of TCP-FA4 was added to the luminal chambers and 200 μL samples were taken from the abluminal chamber at various time points (2, 5, 10, 15, 20 and 30 minutes) and analyzed by LC/MS/MS. Permeation of TCP-FA4 was calculated at a range of temperatures (4, 8, 16, 23, 30 and 37 degrees C) in order to determine an activation energy. The integrity of the cell monolayer was tested post experiment by monitoring the permeability of [^{14}C]-sucrose and samples were analyzed by liquid scintillation counting.

4.2.4.3 TCP-FA4: Inhibition studies

Inhibition studies were performed to determine if permeation of TCP-FA4 was an active process. Inhibitors used included 4,4'-diisothiocyanostilbene-2,2'-disulfonic acid (DIDS) an anion-exchange inhibitor, ouabain, a sodium pump blocker (Na-K-ATPase), sodium azide, a metabolic inhibitor capable of depleting ATP and carbonyl cyanide *p*-(trifluoromethoxy)phenylhydrazone (FCCP), an ionophore inhibitor. Inhibitor

concentrations and treatment conditions were decided upon based on prior studies performed in the laboratory (Utoguchi *et al*., 1999). BBMECs were grown on 0.4 μm Nucleopore® polycarbonate membranes in a 100 mm culture dish coated with rat tail collagen and fibronectin at a density of approximately 50,000 cells/cm^2. Upon confluency, cells were washed several times with warm PBSA and allowed to acclimate. Cells were then mounted in Side-bi-Side™ chambers and TCP-FA4 permeability was monitored in the presence of the various inhibitors. Aliquots were taken from the receiver chamber at 2, 5, 10, 15, 20 and 30 minutes.

4.2.4.4 Measurement of BDNF with enzyme-linked immunosorbent assay (ELISA)

To determine if TCP-FA4 can increase the production of brain derived neurotropic factor (BDNF), analysis of cell culture media post treatment with TCP-FA4 was performed. Initially, BBMECs were used for these studies; however, there was no existing literature confirming that BBMECs grown in culture synthesize or secrete BDNF. Our studies showed that in fact BBMECs do not secrete detectable levels of BDNF (detection limit: 15.6 pg/mL). Therefore, another cell culture system had to be used and, based on studies by Nakahashi *et al.,* it was seen that human umbilical vein endothelial cells (HUVECs) synthesize and secrete BDNF (Nakahashi *et al*., 2000). HUVECs were grown to confluency in a 6-well tissue culture plate (approximately 5 days) then washed three times with phosphate buffered saline warmed to 37 degrees C. Solutions of 5 μM TCP and 5 μM TCP-FA4 were prepared in culture media and added to the wells (N=2). The remaining two wells contained blank media and served as a control. Aliquots of 200 μL

were taken from the wells at 0, 24, 31 and 48 hours and stored at – 20 degrees C until analysis. Prior to analysis samples were centrifuged at 4 degrees C at 1500 x *g* to remove any particulates. Concentrations of BDNF were measured using a commercial ELISA kit (Promega, Madison, WI). For optimal results, all samples were diluted 1:1 with the provided Block & Sample Buffer. A standard curve was created and linearity ($R^2 = 0.99$) was observed from 7 to 250 pg/mL (Figure 4.2.4.4.1). According to the manufacturer's brochure, the assay provides specific detection of BDNF with typically less than 3% cross reactivity with other related neurotrophic factors and provides a lower detection limit of 15.6 pg/mL.

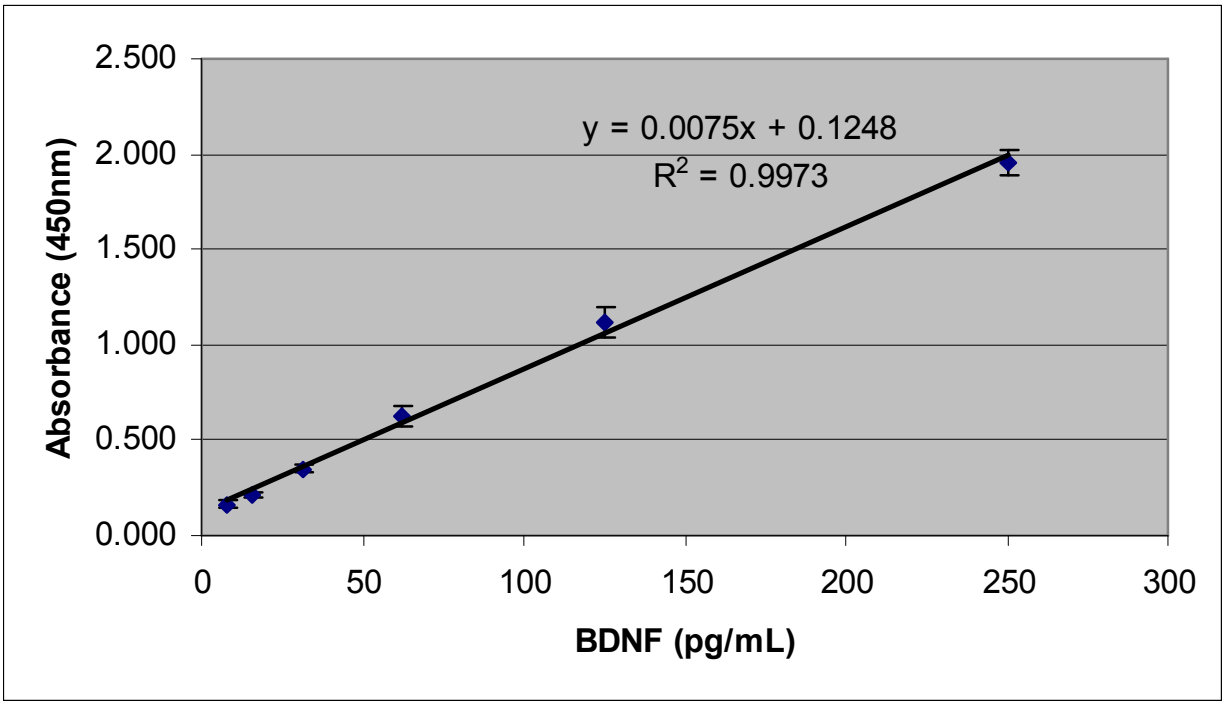

Figure 4.2.4.4.1 Representative calibration curve for the BDNF immunoassay showing linearity over a range of 7 – 250 pg/mL. (Data ± SD, n=4)

4.2.4.5 Sample analysis of TCP and derivatives by LC/MS/MS

Samples generated by the permeability studies using BBMECs were analyzed by LC/MS/MS. The chromatography system consisted of a Waters 2690 system and a Phenomenex Onyx monolithic C18 column (50 x 4.6 mm). After chromatographic separation, samples were directed into the mass spectrometer (Micromass™ triple quadrupole) and detected by tandem mass spectrometry in positive ion mode using electrospray ionization.

A method was adapted from Kirchher *et al.* (Kirchherr and Kuhn-Velten, 2005) that included an isocratic HPLC method using a mobile phase of acetonitrile/5mM acetic acid, pH 3.9 with ammonia. The ratio of aqueous to organic was modified slightly based on the lipophilicity of the derivative and ranged from 10:90 (v/v) acetonitrile: 5 mM acetic acid to 50:50 (v/v) acetonitrile: 5 mM acetic acid. A diversion of the HPLC eluent between 0 and 2 minutes reduced the exposure of the mass spectrometer to possible salts and cellular contaminates in the sample. Based on the mobile phase ratios and the lipophilicity of the derivatives, the retention times shifted appropriately (Figure 4.2.4.5.1).

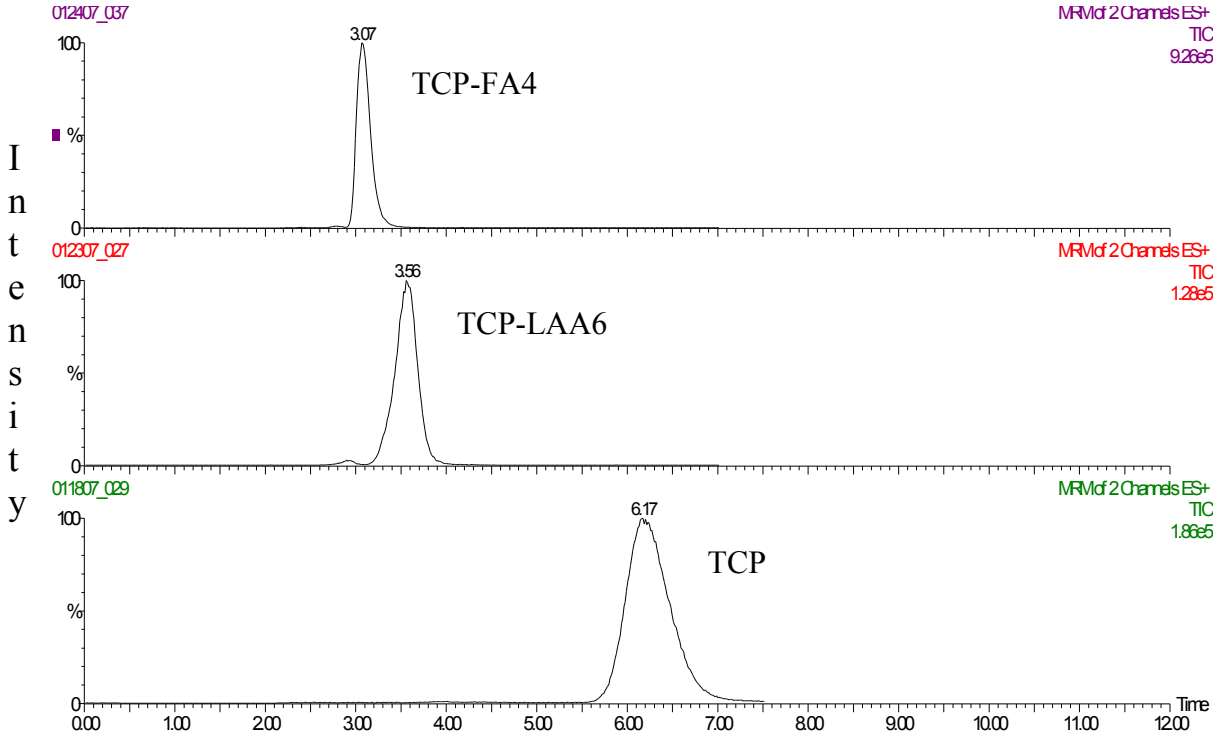

Figure 4.2.4.5.1 Representative MS chromatograms of tranylcypromine and two derivatives, TCP-FA4 and TCP-LAA6, demonstrating the slight shifts in retention time based on isocratic method and the changes in lipophilicity. All chromatograms represent total ion current (TIC). Structures found on page 103.

To select the optimal product-ions for analysis, solutions of tranylcypromine and the various derivatives, made in acetonitrile/5 mM acetic acid, pH 3.9 with ammonia (10:90, v/v), were first infused into the mass spectrometer and fragmentation patterns were monitored and parameters were optimized. Tranylcypromine and its derivatives were chromatographed and detected using multiple reaction monitoring. For tranylcypromine the *m/z* 134 → *m/z* 117 transition was monitored (Figure 4.2.4.5.2). The derivatives

fragmented such that there was cleavage at the added fatty acid or lipoamino acid groups giving tranylcypromine as a daughter ion as well as the *m/z* 117 daughter ion (Figure 4.2.4.5.3).

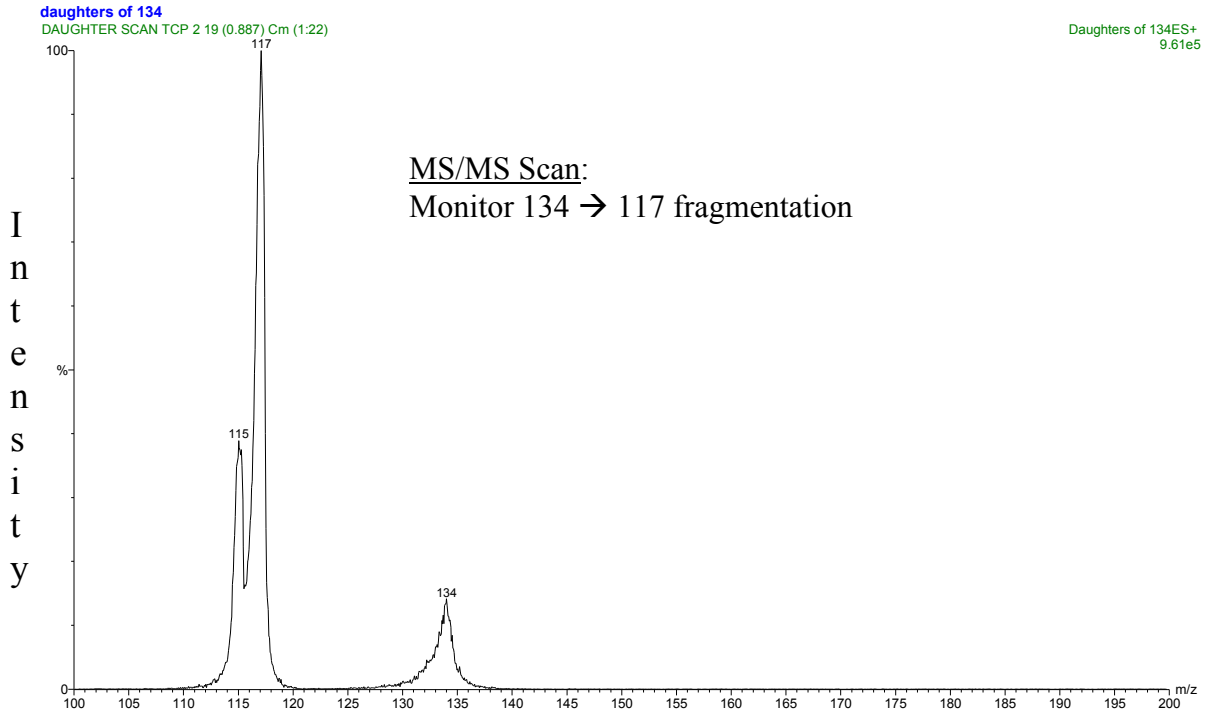

Figure 4.2.4.5.2 Electrospray ionization (ESI)-MS/MS (positive ion mode) product-ion spectra of tranylcypromine (*m/z* 134)

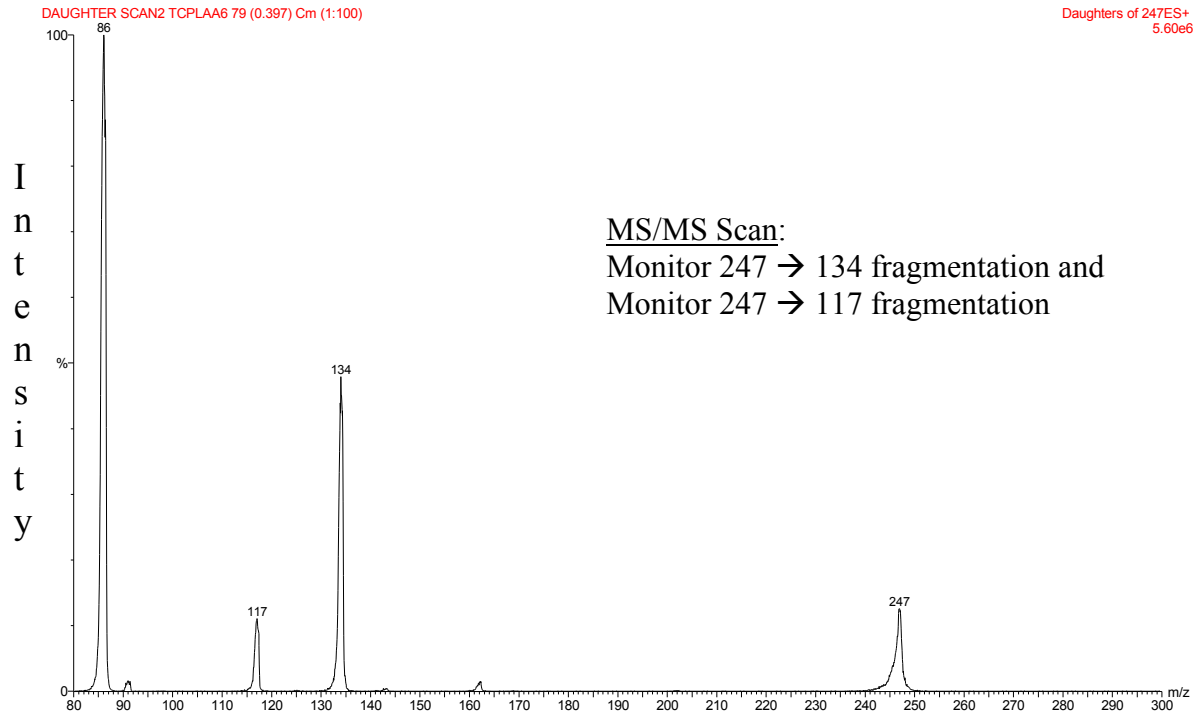

Figure 4.2.4.5.3 Electrospray ionization (ESI)-MS/MS (positive ion mode) product-ion spectra of a representative derivative of tranylcypromine, TCP-LAA6 (*m/z* 247). Structure found on page 103.

Standards generated showed good linearity over a calibration range of 10-1000 ng/mL and this was consistent for the various derivatives as well. Standard curves for TCP-FA4 were extended to include concentrations up to 5000 ng/mL, and good linearity was still maintained. Figure 4.2.4.5.4 is a calibration curve for tranylcypromine and Figure 4.2.4.5.5 is a representative calibration curve of one of the tranylcypromine derivatives (TCP-FA4), showing linearity was achieved for the derivatives as well.

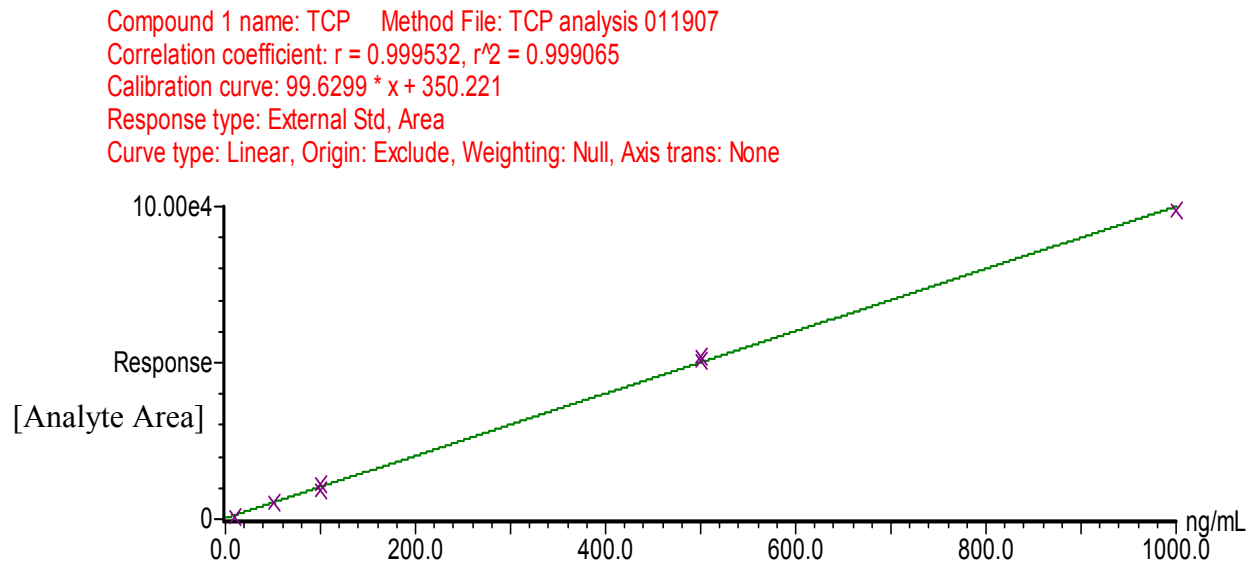

Figure 4.2.4.5.4 Calibration curve of tranylcypromine. Linearity was seen from 5 – 1000 ng/mL.

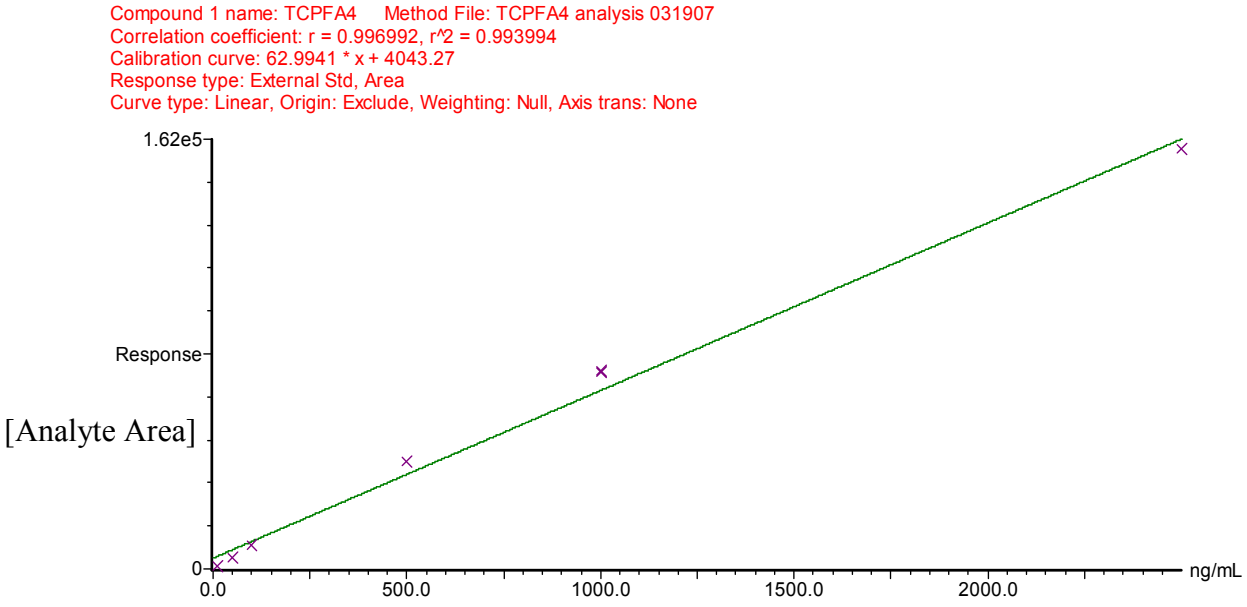

Figure 4.2.4.5.5 Representative calibration curve of a tranylcypromine derivative (TCP-FA4). Linearity was seen from 5 – 5000 ng/mL.

4.3 Results

4.3.1 Rhodamine 123 uptake assay

Tranylcypromine is not a known substrate for any of the efflux transporters expressed at the blood brain barrier, but once lipophilicity is increased, the likelihood that the compounds could become substrates increases. Therefore, we tested the various derivatives for potential P-gp interaction which is one of the most prevalent of the efflux transporters. Results from the rhodamine 123 uptake assay suggest that none of the derivates were interacting with P-gp (Figure 4.3.1.1). All compounds were tested at a concentration of 10 μM and only the positive control showed any effect on intracellular rhodamine 123 uptake.

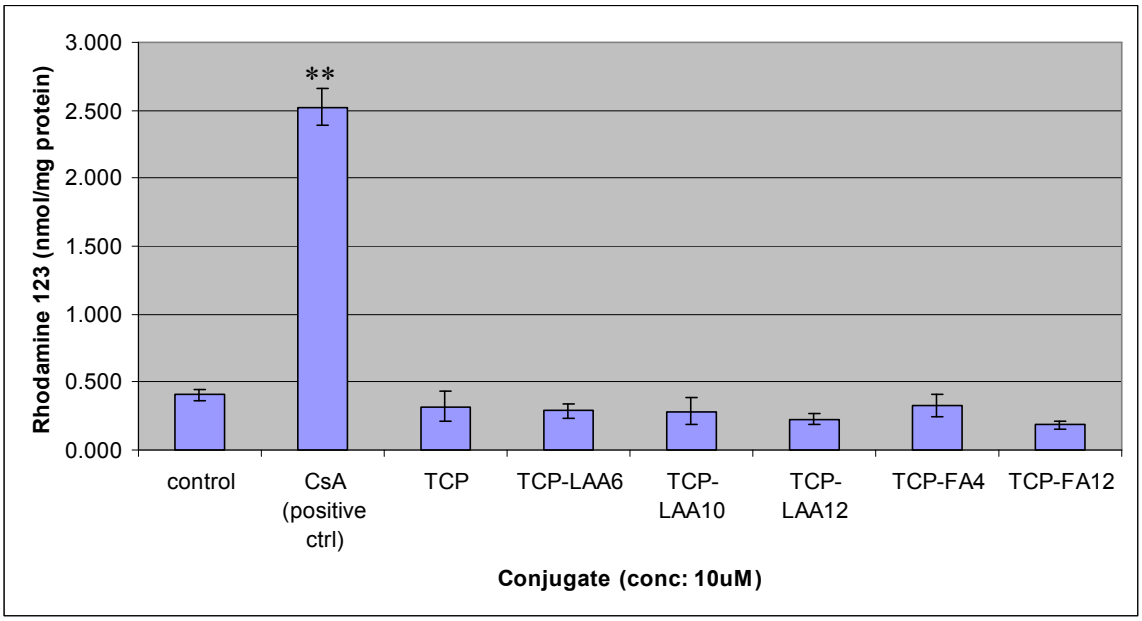

Figure 4.3.1.1 Rhodamine 123 uptake assay results suggest that the TCP derivatives do not interact with the efflux protein, P-gp. (** Denotes $p<0.01$ compared to control (rhodamine alone) as determined by ANOVA, Data ± SD, n=3). Structures found on page 103.

4.3.2 Permeability studies in BBMECs

The permeability of tranylcypromine and its derivatives was calculated using BBMEC monolayers mounted in Side-bi-Side™ chambers. The apparent permeability values were calculated using the following equation:

$P_{app} = (\Delta Q/\Delta t)/ A \times C_0$

where $\Delta Q/\Delta t$ is the linear appearance of the test compound in the receiver chamber, A is the cross sectional area of the cell monolayer (0.636 cm^2) and C_0 is the initial concentration of the test compound in the donor chamber at t = 0. Tranylcypromine had a permeability of approximately 2.9 x 10^{-4} cm/sec and TCP-FA4, a derivative containing a fatty acid side chain, showed an improved permeability of 3.8 x 10^{-4} cm/sec. The derivatives containing the lipoamino acid groups did not show an improvement in permeability relative to tranylcypromine and those derivatives with the longest fatty acid and lipoamino acid groups (TCP-FA12 and TCP-LAA12) were below the limit of detection (Figure 4.3.2.1). Sucrose values for these studies ranged from 2.0 x 10^{-5} cm/sec to 7 x 10^{-5} cm/sec.

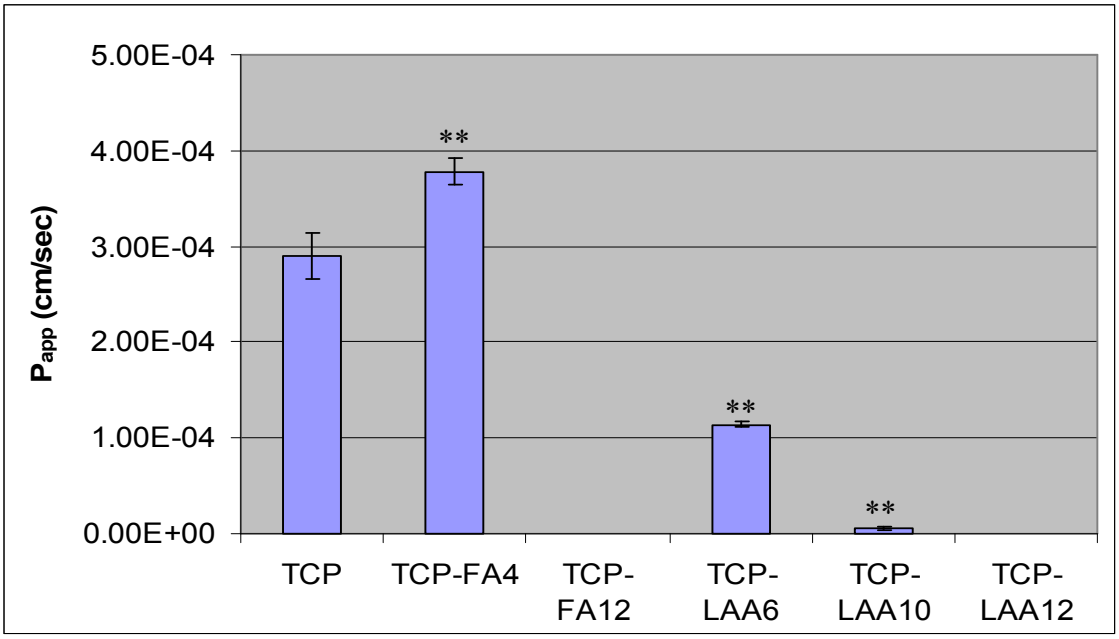

Figure 4.3.2.1 Permeability of tranylcypromine and its derivatives in BBMECs. TCP-FA12 and TCP-LAA12 were below the limit of detection. (** Denotes $p<0.01$ compared to TCP as determined by ANOVA, Data ± SD, TCP and TCP-FA4 n=8, TCP-LAA6 and TCP LAA10 n=4). Structures found on page 103.

4.3.3 Bi-directional permeability study of TCP-FA4

To determine if TCP-FA4's improved permeability was due to an uptake transporter, the percentage of TCP-FA4 transported over time across a BBMEC monolayer was monitored in both the luminal to abluminal and abluminal to luminal directions. Studies indicated that there was a slight decrease in permeability going from the abluminal to luminal side (Figure 4.3.3.1). The apparent permeability of TCP-FA4 in the luminal to abluminal direction had an average P_{app} = 5.47 x 10^{-4} cm/sec (std dev: 2.4 x 10^{-5} cm/sec) and in the abluminal to luminal direction a P_{app} = 4.38 x 10^{-4} cm/sec (std dev: 1.4 x 10^{-5} cm/sec). To determine if this difference was in fact due to some sort of uptake or facilitative process, additional temperature dependent and inhibition studies were performed.

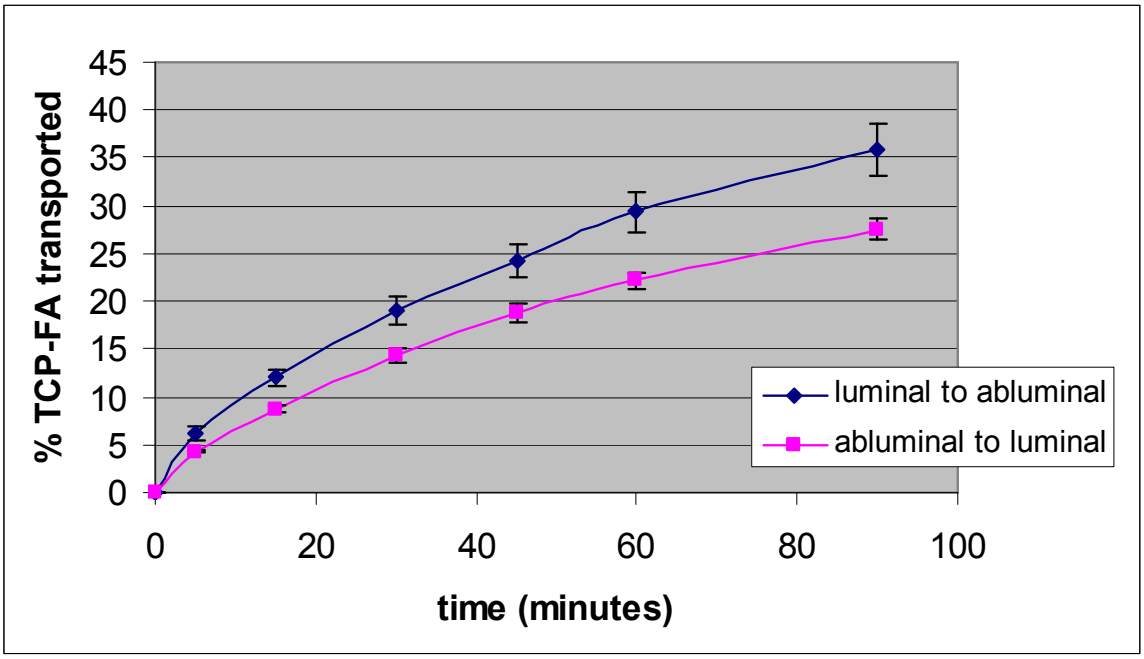

Figure 4.3.3.1 Percentage of TCP-FA4 transported over time in the luminal to abluminal and abluminal to luminal directions. (Data ± SD, n=8)

4.3.4 Temperature dependent permeability studies of TCP-FA4

The permeability of TCP-FA4 was monitored at a range of temperatures such that an activation energy of transport could be calculated. Studies were performed using BBMEC monolayers mounted in Side-bi-Side™ chambers. An Arrhenius plot was generated by plotting 1/ T versus the natural log of the apparent permeability values and the activation energy of transport was determined to be 28.0 kJ/mol (Figure 4.3.4.1).

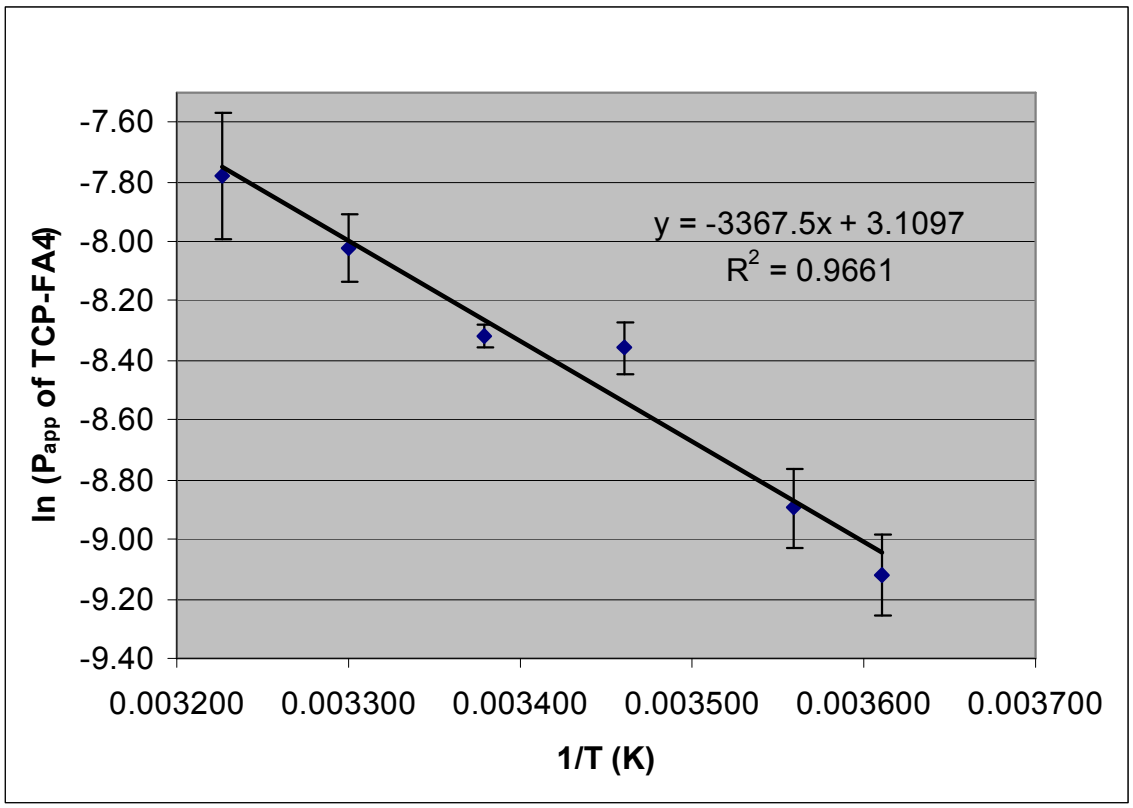

Figure 4.3.4.1 Arrhenius plot generated by the temperature dependent permeability of TCP-FA4 in BBMECs. Permeability values were calculated at a variety of temperatures ranging from 4 degrees C to 37 degrees C. (Data ± SD, n=4, except 4 and 37 degrees C, n=8)

4.3.5 TCP-FA4: Inhibition studies

The effect of various inhibitors on the permeability of TCP-FA4 was investigated (Figure 4.3.5.1). For all inhibition studies, BBMECs were pretreated with agents for 15 minutes prior to performing the permeability study. Ouabain octahydrate, a sodium pump blocker, was used to determine if the permeability of TCP-FA4 was a sodium coupled process. Permeability of TCP-FA4 was monitored in the presence of 100 μM ouabain, but no significant changes in permeability were noted. Sodium azide, a respiratory chain inhibitor, was used as a metabolic inhibitor to investigate if the transport of TCP-FA4 was via a process that required cell-dependent energy expenditure. However, the permeability of TCP-FA4 did not decrease in the presence of 10 mM sodium azide. FCCP, a protonophore, was used to determine if the permeability of TCP-FA4 would be altered upon disruption of the proton gradient, but at a final concentration of 50 μM FCCP no changes in TCP-FA4 permeability were noted. Furthermore, in the presence of 50 μM DIDS, an anion-exchange inhibitor, no changes in TCP-FA4 permeability were observed. These studies suggested that the permeation of TCP-FA4 was most likely a passive process and was neither an active nor facilitative process.

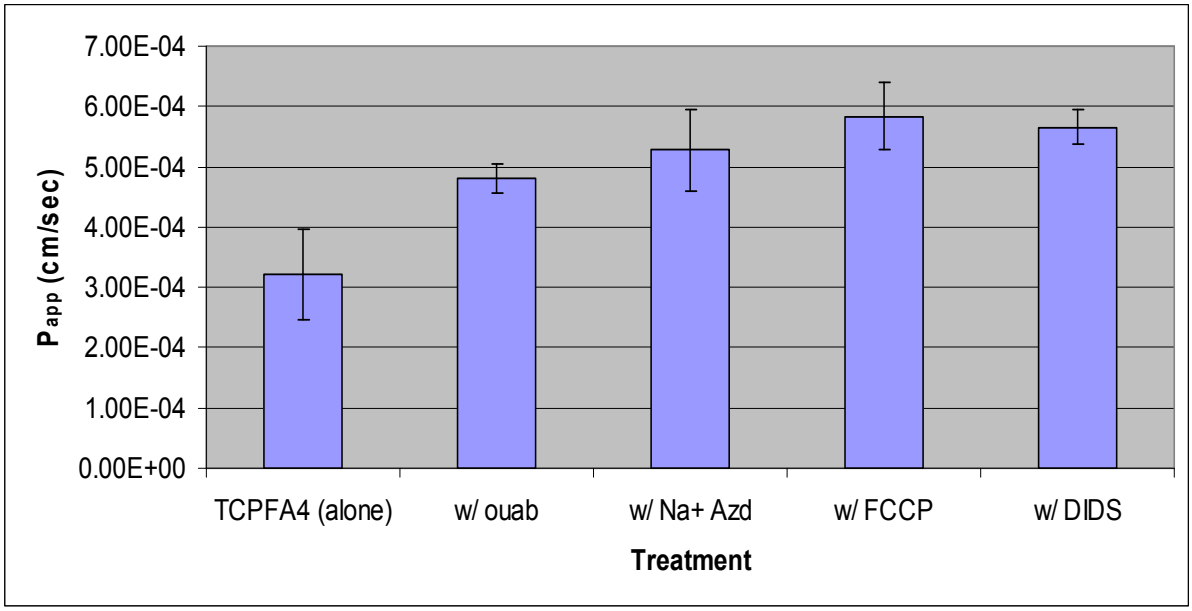

Figure 4.3.5.1 Effects of various inhibitors on the transport of TCP-FA4 in BBMECs. (Data ± SD, n=4)

4.3.6 BDNF production by HUVECs in the presence of TCP-FA4

The effect of TCP-FA4 on the production of BDNF in HUVECs was investigated. HUVECs were treated with 5 μM TCP-FA4 to determine if the derivative was capable of increasing production of BDNF relative to tranylcypromine. Results showed an increase in BDNF production relative to the control (blank media) as well as tranylcypromine. Levels of secreted BDNF increased over time and were highest when treated with TCP-FA4. At 48 hours post treatment with TCP-FA4, BDNF was detected at 122.6 ± 1.9 pg/mL, compared to 101.8 ± 4.6 and 92.3 ± 2.1 pg/mL for TCP and blank media respectively (n = 4) (Figure 4.3.6.1)

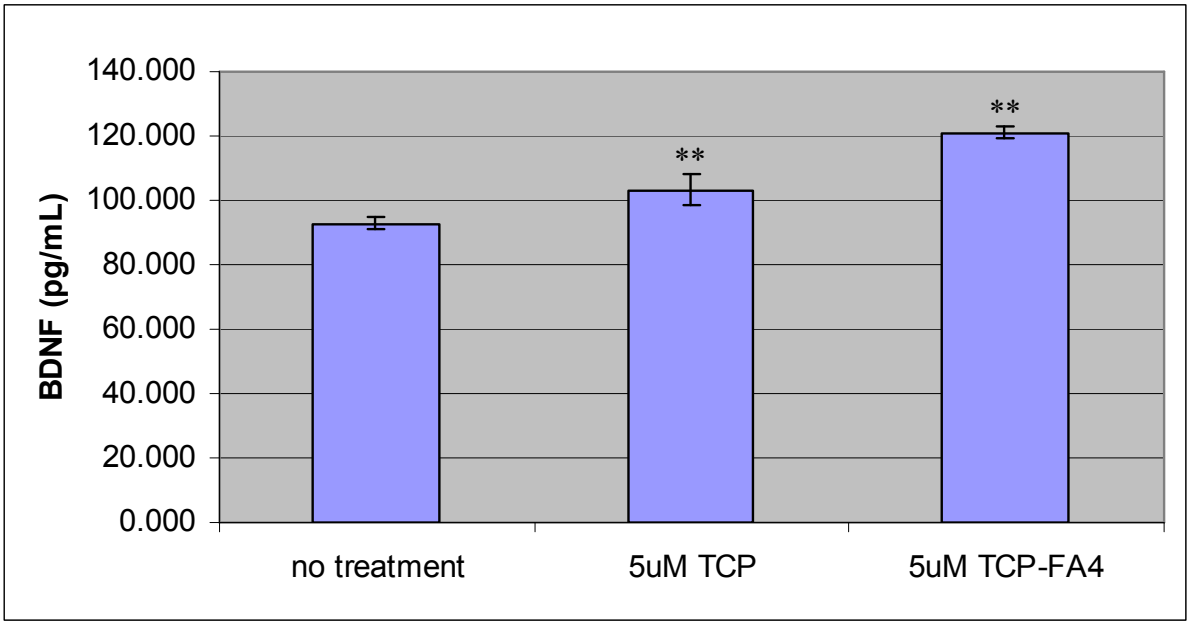

Figure 4.3.6.1 BDNF secretion by cultured HUVECs in the presence of TCP and TCP-FA4. (** Denotes $p<0.01$ compared to control as determined by ANOVA, Data ± SD, n=4)

4.4 Discussion

Derivatives of tranylcypromine containing fatty acid and lipoamino acid chains of varying length were synthesized in an attempt to improve the blood brain barrier permeability by increasing the lipophilicity as well as amphiphatic character of the molecule. Our collaborators investigated the altered lipophilicity of these derivatives by calculating the log P as well as the partition coefficient between the blood and brain (log BB) using the software programs ACD log *P* 5.15, Pallas 3.0, Osiris Property Explorer and KOWIN 1.57. Results suggested that lipoamino acid promoieties containing medium

to long side alkyl chains would be most useful in improving the permeability and membrane interaction of these compounds (Pignatello *et al*., 2006). Additionally, studies using multilamellar vesicles and dimyristoylphosphatidylcholine (DMPC) monolayers as biomembranes models confirmed these results (Pignatello *et al*., 2006). However, when using BBMECs as a model for the blood brain barrier, the fatty acid derivative TCP-FA4 showed the greatest improvement in permeability. This derivative contained a four carbon fatty acid chain and had an approximate 2 fold increase in lipophilicity over the parent compound (Pignatello *et al*., 2005). The permeability results for this compound indicated that TCP-FA4 had good passive permeability and was not a substrate for any active transport systems expressed in the BBMECs. Furthermore, the utility as a pharmaceutical agent of a tranylcypromine derivative possessing improved permeability was investigated. Our collaborators investigated the activity of this derivative as an MAO inhibitor. Although it was found that TCP-FA4 does exhibit inhibitory activity against MAO enzymes, its affinity was reduced compared to the parent compound, tranylcypromine (data not yet published). However, our studies indicate that TCP-FA4 may possess neuroprotective properties. In a β-amyloid induced neurodegeneration assay, neurons exposed to β-amyloid in the presence of 200 nM TCP-FA4 showed a 20% improvement in survival rate (data not shown). Additionally, using HUVECs grown in culture, increased levels of the neurotrophic factor BDNF were observed in the presence of TCP-FA4. Since BDNF is instrumental in the survival and differentiation of neurons and BDNF expression is altered in many brain disorders, the discovery of small molecules capable of regulating BDNF may be beneficial.

4.5 Conclusion

TCP-FA4, is a derivative of the MAO inhibitor tranylcypromine containing a fatty acid chain to enhance lipophilicity, which is predicted to have improved blood brain barrier permeability based on *in vitro* studies using BBMECs. This molecule has also been shown to be a potential neuroprotective agent. In addition to its favorable physicochemical properties, it has been shown to be slightly neuroprotective in a β-amyloid induced neurodegeneration assay and may also be capable of upregulating the neurotrophic factor BDNF as indicated by cell culture assays using HUVECs. Since decreased levels of BDNF are observed in many CNS disorders, and direct injection of BDNF is not a viable option due to its poor permeability across the blood brain barrier, small molecules capable of regulating BDNF that also cross the blood brain barrier may be a treatment option (Longo and Massa, 2005).

4.6 References

Audus KL and Borchardt RT (1987) Bovine brain microvessel endothelial cell monolayers as a model system for the blood-brain barrier. *Ann N Y Acad Sci* **507**:9-18.

Audus KL, Ng L, Wang W and Borchardt RT (1996) Brain microvessel endothelial cell culture systems, in *Model Systems for Biopharmaceutical Assessment of Drug Absorption and Metabolism* (Borchardt RT, Smith, P.L., Wilson, G. ed) pp 239-258, Plenum, New York.

Audus KL, Rose JM, Wang W and Borchardt RT (1998) Brain microvessel endothelial cell culture systems, in *An Introduction to the Blood-Brain Barrier: Methodology and Biology* (Pardridge W ed) pp 86-93, Cambridge University, Cambridge.

Bodor N and Buchwald P (2002) Barriers to remember: brain-targeting chemical delivery systems and Alzheimer's disease. *Drug Discov Today* **7**:766-774.

Brightman MW and Reese TS (1969) Junctions between intimately apposed cell membranes in the vertebrate brain. *J Cell Biol* **40**:648-677.

Fontaine M, Elmquist WF and Miller DW (1996) Use of rhodamine 123 to examine the functional activity of P-glycoprotein in primary cultured brain microvessel endothelial cell monolayers. *Life Sci* **59**:1521-1531.

Hegmann EJ, Bauer HC and Kerbel RS (1992) Expression and functional activity of P-glycoprotein in cultured cerebral capillary endothelial cells. *Cancer Res* **52**:6969-6975.

Huai-Yun H, Secrest DT, Mark KS, Carney D, Brandquist C, Elmquist WF and Miller DW (1998) Expression of multidrug resistance-associated protein (MRP) in brain microvessel endothelial cells. *Biochem Biophys Res Commun* **243**:816-820.

Jolliet-Riant P and Tillement JP (1999) Drug transfer across the blood-brain barrier and improvement of brain delivery. *Fundam Clin Pharmacol* **13**:16-26.

Kirchherr H and Kuhn-Velten W (2005) A simple and sensitive method for the determination of tranylcypromine in plasma with LC-MS/MS. *Pharmacopsychiatry* **38**.

Longo FM and Massa SM (2005) Neurotrophin receptor-based strategies for Alzheimer's disease. *Curr Alzheimer Res* **2**:167-169.

Nakahashi T, Fujimura H, Altar CA, Li J, Kambayashi J, Tandon NN and Sun B (2000) Vascular endothelial cells synthesize and secrete brain-derived neurotrophic factor. *FEBS Lett* **470**:113-117.

Pezet S and Malcangio M (2004) Brain-derived neurotrophic factor as a drug target for CNS disorders. *Expert Opin Ther Targets* **8**:391-399.

Pignatello R, Guccione S, Castelli F, Sarpietro MG, Giurato L, Lombardo M, Puglisi G and Toth I (2006) Enhancement of drug affinity for cell membranes by conjugation with lipoamino acids II. Experimental and computational evidence using biomembrane models. *Int J Pharm* **310**:53-63.

Pignatello R, Puleo A, Guccione S, Raciti G, Acquaviva R, Campisi A, Ventura CA and Puglisi G (2005) Enhancement of drug affinity for cell membranes by conjugation with lipoamino acids. I. Synthesis and biological evaluation of lipophilic conjugates of tranylcypromine. *Eur J Med Chem* **40**:1074-1079.

Reese TS and Karnovsky MJ (1967) Fine structural localization of a blood-brain barrier to exogenous peroxidase. *J Cell Biol* **34**:207-217.

Sowa BN, Holt A, Todd KG and Baker GB (2004) Monoamine oxidase inhibitors, their structural analogues, and neuroprotection. *Indian J Exp Biol* **42**:851-857.

Stouch TR and Gudmundsson O (2002) Progress in understanding the structure-activity relationships of P-glycoprotein. *Adv Drug Deliv Rev* **54**:315-328.

Utoguchi N, Magnusson M and Audus KL (1999) Carrier-mediated transport of monocarboxylic acids in BeWo cell monolayers as a model of the human trophoblast. *J Pharm Sci* **88**:1288-1292.

van Asperen J, Mayer U, van Tellingen O and Beijnen JH (1997) The functional role of P-glycoprotein in the blood-brain barrier. *J Pharm Sci* **86**:881-884.

Waterhouse RN (2003) Determination of lipophilicity and its use as a predictor of blood-brain barrier penetration of molecular imaging agents. *Mol Imaging Biol* **5**:376-389.

Chapter 5: Summary and Future Direction

Chapter 5: Summary and Future Direction

Drug delivery to the brain is often challenging and with an aging population brain disorders are becoming a major problem (Riggs, 1998). Alzheimer's, Parkinson's and conditions such as cerebral ischemia in stroke are all prevalent diseases in an aging population, which currently have no cure. Investigating therapeutics which address these unmet medical needs is very important. In order for CNS therapeutics to be effective, they must be able to penetrate the blood brain barrier and reach their site of action. Therefore, understanding ways to improve a molecule's blood brain barrier permeability becomes essential in developing more effective CNS drugs. There are a variety of approaches to improving blood brain barrier permeability, a select few which have been discussed within this dissertation.

Paclitaxel is a chemotherapeutic compound that has been successfully used for a variety of cancers, but cannot be used to treat brain cancer because it does not cross the blood brain barrier (Fellner *et al*., 2002). In the case of paclitaxel, the drug is a substrate for an efflux transporter expressed at the brain endothelium. To improve the blood brain barrier permeability in a case in which drug efflux is a problem, one approach is to structurally modify the drug such that is retains its chemotherapeutic effect but is no longer a substrate for the efflux transporter. GS-164 is a molecule that has been shown to be both chemotherapeutic and neuroprotective. To optimize this compound's success as a chemotherapeutic or neuroprotective agent, a variety of stereoisomers were synthesized and the *cis*-isomer TH-237A was shown to have excellent neuroprotective properties.

This is an example of taking a molecule that has inherently good physicochemical properties that make it a good candidate for a CNS drug and evaluating slight structural changes to make it the most effective as a neuroprotective agent. Another approach to improve the blood brain barrier penetration is to modify a compound so that it has enhanced lipophilicity and improve its interaction with the cell membrane. This was successful in the example with tranylcypromine in which the fatty acid derivative TCP-FA4 showed an improvement in permeability in BBMECs over the parent compound.

An interesting feature that is common to the molecules discussed within this dissertation is that they are chemotherapeutic as well as neuroprotective to varying degrees. The exception being the tranylcypromine derivatives which only hold promise as being potential neuroprotective agents. Derivatives of paclitaxel and GS-164 have been seen to have anti-proliferative effects *in vitro* when tested in cancer cell lines (Shintani *et al*., 1997; Spletstoser *et al*., 2006). Furthermore, at low concentrations they have shown to be neuroprotective *in vitro* against the β-amyloid induced neurodegeneration seen in Alzheimer's disease (Michaelis *et al*., 2005). These two groups of molecules are classified as microtubule stabilizing agents. Although their binding interactions with microtubules seem to vary, it may be via this interaction that they are able to provide neuroprotection. The molecule A4, a small molecule novobiocin analogue, which is discussed within Appendix 1 also has the unique characteristic of being both chemotherapeutic and neuroprotective. However, this molecule cannot be classified as a microtubule stabilizing compound, but rather an Hsp90 inhibitor. Lastly, TCP-FA4,

showed possible neuroprotective properties with yet another possible mechanism of action. Cell culture studies showed that TCP-FA4 is capable of increasing the expression of the neurotrophin BDNF. BDNF has been implicated in the survival and maintenance of neurons *in vivo*.

Future work on improving the blood brain barrier permeation of paclitaxel should focus on those structural changes that showed the greatest reduction in P-gp interaction such as the addition of nutrient-like groups at the C10 position and changes to the oxidation state of the C10 position. Since many of our studies showed the importance of the C10 position to P-gp's recognition of the paclitaxel derivatives, chemistry efforts should focus on modification of this position. Furthermore, the lack of improvement in permeability for those molecules showing a reduction in interaction in P-gp must be investigated. Since the substrate specificity of many of the efflux transporters overlap, it is possible that these newly synthesized derivatives are now substrates for efflux transporters other than P-gp. Development of assays that allow researchers to tease out the contribution of individual transporters would be very beneficial.

Studies further investigating the utility of TH-237A as a neuroprotective agent are ongoing. Future studies include the *in vivo* effects of TH-237A in *tau* mutant mice. End points for these studies will include progression of disease state as well as the levels of abnormal *tau* protein.

Furthermore, additional work could be done investigating the role of TCP-FA4 as a neuroprotective agent. Preliminary studies suggest that TCP-FA4 increases levels of secreted BDNF in HUVECs. Additional studies could be done to determine if this effect is dose dependent. Moreover, it would be interesting to see if this increase in BDNF translates into a protective effect on the cells. Cell culture studies performed in a hypoxic environment could mimic the stress conditions in an *in vivo* situation such as cerebral ischemia.

5. 1 References

Audus KL and Borchardt RT (1986) Characteristics of the large neutral amino acid transport system of bovine brain microvessel endothelial cell monolayers. *J Neurochem* **47**:484-488.

Audus KL and Borchardt RT (1987) Bovine brain microvessel endothelial cell monolayers as a model system for the blood-brain barrier. *Ann N Y Acad Sci* **507**:9-18.

Audus KL, Ng L, Wang W and Borchardt RT (1996) Brain microvessel endothelial cell culture systems, in *Model Systems for Biopharmaceutical Assessment of Drug Absorption and Metabolism* (Borchardt RT, Smith, P.L., Wilson, G. ed) pp 239-258, Plenum, New York.

Audus KL, Rose JM, Wang W and Borchardt RT (1998) Brain microvessel endothelial cell culture systems, in *An Introduction to the Blood-Brain Barrier: Methodology and Biology* (Pardridge W ed) pp 86-93, Cambridge University, Cambridge.

Bartus R, Elliott P, Hayward N, Dean R, McEwan E and Fisher S (1996) Permeability of the blood brain barrier by the bradykinin agonist RMP-7: Evidence for a sensitive, auto-regulated, receptor mediated system. *Immunopharmacology* **33**:270-278.

Beckers T and Mahboobi S (2003) Natural, semisynthetic and synthetic microtubule inhibitors for cancer therapy. *Drugs of the Future* **28**:767.

Birnbaum LS (1985) The role of structure in the disposition of halogenated aromatic xenobiotics. *Environ Health Perspect* **61**:11-20.

Bodor N and Buchwald P (2002) Barriers to remember: brain-targeting chemical delivery systems and Alzheimer's disease. *Drug Discov Today* **7**:766-774.

Brightman MW and Reese TS (1969) Junctions between intimately apposed cell membranes in the vertebrate brain. *J Cell Biol* **40**:648-677.

Crone C and Levitt DG (1984) Capillary permeability to small solutes, in (Renkin EM and Michel CC eds) pp 411-466, American Physiological Society, Bethesda.

Croteau D, Walbridge S, Morrison PF, Butman JA, Vortmeyer AO, Johnson D, Oldfield EH and Lonser RR (2005) Real-time in vivo imaging of the convective distribution of a low-molecular-weight tracer. *J Neurosurg* **102**:90-97.

Dano K (1973) Active outward transport of daunomycin in resistant Ehrlich ascites tumor cells. *Biochim Biophys Acta* **323**:466-483.

de Vrueh RL, Smith PL and Lee CP (1998) Transport of L-valine-acyclovir via the oligopeptide transporter in the human intestinal cell line, Caco-2. *J Pharmacol Exp Ther* **286**:1166-1170.

Degen JW, Walbridge S, Vortmeyer AO, Oldfield EH and Lonser RR (2003) Safety and efficacy of convection-enhanced delivery of gemcitabine or carboplatin in a malignant glioma model in rats. *J Neurosurg* **99**:893-898.

Fellner S, Bauer B, Miller DS, Schaffrik M, Fankhanel M, Spruss T, Bernhardt G, Graeff C, Farber L, Gschaidmeier H, Buschauer A and Fricker G (2002) Transport of paclitaxel (Taxol) across the blood-brain barrier in vitro and in vivo. *J Clin Invest* **110**:1309-1318.

Fontaine M, Elmquist WF and Miller DW (1996) Use of rhodamine 123 to examine the functional activity of P-glycoprotein in primary cultured brain microvessel endothelial cell monolayers. *Life Sci* **59**:1521-1531.

Georg G, Boge TC, Cheruvallath ZS, Clowers JS, Harriman GC, Hepperle M and Park H (1995) Taxol Science and Applications, in (Suffness M ed), CRC Press, Boca Raton, FL.

Groothuis DR (2000) The blood-brain and blood-tumor barriers: a review of strategies for increasing drug delivery. *Neuro Oncol* **2**:45-59.

Hegmann EJ, Bauer HC and Kerbel RS (1992) Expression and functional activity of P-glycoprotein in cultured cerebral capillary endothelial cells. *Cancer Res* **52**:6969-6975.

Ho N, Raub T, Burton P, Barsuhn C, Adson A, Audus K and Borchardt R (1999) *Transport Processes in Pharmaceutical Systems*. Marcel Dekker, New York.

Huai-Yun H, Secrest DT, Mark KS, Carney D, Brandquist C, Elmquist WF and Miller DW (1998) Expression of multidrug resistance-associated protein (MRP) in brain microvessel endothelial cells. *Biochem Biophys Res Commun* **243**:816-820.

Jolliet-Riant P and Tillement JP (1999) Drug transfer across the blood-brain barrier and improvement of brain delivery. *Fundam Clin Pharmacol* **13**:16-26.

Jordan MA, Toso RJ, Thrower D and Wilson L (1993) Mechanism of mitotic block and inhibition of cell proliferation by taxol at low concentrations. *Proc Natl Acad Sci U S A* **90**:9552-9556.

Juliano RL and Ling V (1976) A surface glycoprotein modulating drug permeability in Chinese hamster ovary cell mutants. *Biochim Biophys Acta* **455**:152-162.

Kaiser MG, Parsa AT, Fine RL, Hall JS, Chakrabarti I and Bruce JN (2000) Tissue distribution and antitumor activity of topotecan delivered by intracerebral clysis in a rat glioma model. *Neurosurgery* **47**:1391-1398; discussion 1398-1399.

Kirchherr H and Kuhn-Velten W (2005) A Simple and Sensitive Method for the Determination of Tranylcypromine in Plasma with LC-MS/MS. *Pharmacopsychiatry* **38**.

Longo FM and Massa SM (2005) Neurotrophin receptor-based strategies for Alzheimer's disease. *Curr Alzheimer Res* **2**:167-169.

Mahar Doan KM, Humphreys JE, Webster LO, Wring SA, Shampine LJ, Serabjit-Singh CJ, Adkison KK and Polli JW (2002) Passive permeability and P-glycoprotein-mediated efflux differentiate central nervous system (CNS) and non-CNS marketed drugs. *J Pharmacol Exp Ther* **303**:1029-1037.

Michaelis ML, Ansar S, Chen Y, Reiff ER, Seyb KI, Himes RH, Audus KL and Georg GI (2005) {beta}-Amyloid-induced neurodegeneration and protection by structurally diverse microtubule-stabilizing agents. *J Pharmacol Exp Ther* **312**:659-668.

Michaelis ML, Ranciat N, Chen Y, Bechtel M, Ragan R, Hepperle M, Liu Y and Georg G (1998) Protection against beta-amyloid toxicity in primary neurons by paclitaxel (Taxol). *J Neurochem* **70**:1623-1627.

Michaelis ML, Walsh JL, Pal R, Hurlbert M, Hoel G, Bland K, Foye J and Kwong WH (1994) Immunologic localization and kinetic characterization of a Na+/Ca2+ exchanger in neuronal and non-neuronal cells. *Brain Res* **661**:104-116.

Morrison PF, Chen MY, Chadwick RS, Lonser RR and Oldfield EH (1999) Focal delivery during direct infusion to brain: role of flow rate, catheter diameter, and tissue mechanics. *Am J Physiol* **277**:R1218-1229.

Nakahashi T, Fujimura H, Altar CA, Li J, Kambayashi J, Tandon NN and Sun B (2000) Vascular endothelial cells synthesize and secrete brain-derived neurotrophic factor. *FEBS Lett* **470**:113-117.

Nobili S, Landini I, Giglioni B and Mini E (2006) Pharmacological strategies for overcoming multidrug resistance. *Curr Drug Targets* **7**:861-879.

O'Connor R (2007) The pharmacology of cancer resistance. *Anticancer Res* **27**:1267-1272.

Ojima I, Slater JC, Michaud E, Kuduk SD, Bounaud PY, Vrignaud P, Bissery MC, Veith JM, Pera P and Bernacki RJ (1996) Syntheses and structure-activity relationships of the second-generation antitumor taxoids: exceptional activity against drug-resistant cancer cells. *J Med Chem* **39**:3889-3896.

Pardridge WM (1986) Receptor-mediated peptide transport through the blood-brain barrier. *Endocr Rev* **7**:314-330.

Pardridge WM (1998) CNS drug design based on principles of blood-brain barrier transport. *J Neurochem* **70**:1781-1792.

Pardridge WM (2003) Blood-brain barrier drug targeting: the future of brain drug development. *Mol Interv* **3**:90-105, 151.

Pardridge WM and Oldendorf WH (1977) Transport of metabolic substrates through the blood-brain barrier. *J Neurochem* **28**:5-12.

Pezet S and Malcangio M (2004) Brain-derived neurotrophic factor as a drug target for CNS disorders. *Expert Opin Ther Targets* **8**:391-399.

Pignatello R, Guccione S, Castelli F, Sarpietro MG, Giurato L, Lombardo M, Puglisi G and Toth I (2006) Enhancement of drug affinity for cell membranes by

conjugation with lipoamino acids II. Experimental and computational evidence using biomembrane models. *Int J Pharm* **310**:53-63.

Pignatello R, Puleo A, Guccione S, Raciti G, Acquaviva R, Campisi A, Ventura CA and Puglisi G (2005) Enhancement of drug affinity for cell membranes by conjugation with lipoamino acids. I. Synthesis and biological evaluation of lipophilic conjugates of tranylcypromine. *Eur J Med Chem* **40**:1074-1079.

Rapoport SJ and Thompson HK (1973) Osmotic opening of the blood-brain barrier in the monkey without associated neurological deficits. *Science* **180**:971.

Raub TJ (2006) P-glycoprotein recognition of substrates and circumvention through rational drug design. *Mol Pharm* **3**:3-25.

Reese TS and Karnovsky MJ (1967) Fine structural localization of a blood-brain barrier to exogenous peroxidase. *J Cell Biol* **34**:207-217.

Rice A, Liu Y, Michaelis ML, Himes RH, Georg GI and Audus KL (2005) Chemical modification of paclitaxel (Taxol) reduces P-glycoprotein interactions and increases permeation across the blood-brain barrier in vitro and in situ. *J Med Chem* **48**:832-838.

Rice AH (2002) Taxanes: Identification of Structures that Elude P-glycoprotein Efflux at the Blood Brain Barrier, in *Department of Pharmaceutical Chemistry* p 133, The University of Kansas, Lawrence.

Riggs JE (1998) THE AGING POPULATION Implications for the Burden of Neurologic Disease. *Neurologic Clinics* **16**:555-560.

Sakaeda T, Siahaan TJ, Audus KL and Stella VJ (2000) Enhancement of transport of D-melphalan analogue by conjugation with L-glutamate across bovine brain microvessel endothelial cell monolayers. *J Drug Target* **8**:195-204.

Seelig A (1998) A general pattern for substrate recognition by P-glycoprotein. *Eur J Biochem* **251**:252-261.

Shi F, Bailey C, Malick AW and Audus KL (1993) Biotin uptake and transport across bovine brain microvessel endothelial cell monolayers. *Pharm Res* **10**:282-288.

Shintani Y, Tanaka T and Nozaki Y (1997) GS-164, a small synthetic compound, stimulates tubulin polymerization by a similar mechanism to that of Taxol. *Cancer Chemother Pharmacol* **40**:513-520.

Sikic B, Fisher GA, Lum BL, Halsey J, Beketic-Oreskovic L and Chen G (1997) Modulation and prevention of multidrug resistance by inhibitors of P-glycoprotein. *Cancer Chemother Pharmacol* **40 (suppl)**:S13-S19.

Smith QR (1996) Brain perfusion systems for studies of drug uptake and metabolism in the central nervous system. *Pharm Biotechnol* **8**:285-307.

Smith QR and Allen DD (2003) In situ brain perfusion technique. *Methods Mol Med* **89**:209-218.

Sowa BN, Holt A, Todd KG and Baker GB (2004) Monoamine oxidase inhibitors, their structural analogues, and neuroprotection. *Indian J Exp Biol* **42**:851-857.

Spatz M and Mrsula B (1982) Progress in cerebral microvascular studies related to the function of the blood-brain barrier. *Adv Cell Neurobiol* **3**:311–337.

Spector R and Mock D (1987) Biotin transport through the blood-brain barrier. *J Neurochem* **48**:400-404.

Spletstoser JT, Turunen BJ, Desino K, Rice A, Datta A, Dutta D, Huff JK, Himes RH, Audus KL, Seelig A and Georg GI (2006) Single-site chemical modification at C10 of the baccatin III core of paclitaxel and Taxol C reduces P-glycoprotein interactions in bovine brain microvessel endothelial cells. *Bioorg Med Chem Lett* **16**:495-498.

Stouch TR and Gudmundsson O (2002) Progress in understanding the structure-activity relationships of P-glycoprotein. *Adv Drug Deliv Rev* **54**:315-328.

Tatsuta T, Naito M, Oh-hara T, Sugawara I and Tsuruo T (1992) Functional involvement of P-glycoprotein in blood-brain barrier. *J Biol Chem* **267**:20383-20391.

Utoguchi N, Magnusson M and Audus KL (1999) Carrier-mediated transport of monocarboxylic acids in BeWo cell monolayers as a model of the human trophoblast. *J Pharm Sci* **88**:1288-1292.

van Asperen J, Mayer U, van Tellingen O and Beijnen JH (1997) The functional role of P-glycoprotein in the blood-brain barrier. *J Pharm Sci* **86**:881-884.

Walker I, Nicholls D, Irwin WJ and Freeman S (1994) Drug delivery via active transport at the blood–brain barrier: affinity of a prodrug of phosphonoformate for the large amino acid transporter. *International Journal of Pharmaceutics* **104**:157-167.

Waterhouse RN (2003) Determination of lipophilicity and its use as a predictor of blood-brain barrier penetration of molecular imaging agents. *Mol Imaging Biol* **5**:376-389.

Yazdanian M and Bormann BJ (2000) Immortalized brain endothelial cells, in, Boehringer Ingelheim Pharmaceuticals, Inc., United States.

Appendix 1: A Non-toxic Hsp90 Inhibitor Protects Neurons from Aβ-induced Toxicity

Appendix 1: A Non-toxic Hsp90 Inhibitor Protects Neurons from Aβ-induced Toxicity

Sabah Ansar, Joseph A. Burlison, M. Kyle Hadden, Xiao Ming Yu, **Kelly E. Desino**, Jennifer Bean, Len Neckers, Ken A. Audus, Jeffrey Holzbeierlein, Mary L. Michaelis, and Brian S. J. Blagg

Abstract

The molecular chaperones have been implicated in numerous neurodegenerative disorders in which a defining pathology is misfolded proteins and the accumulation of protein aggregates. In Alzheimer's Disease, hyperphosphorylation of tau protein results in its dissociation from microtubules and the formation of pathogenic aggregates. An inverse relationship was demonstrated between Hsp90/Hsp70 levels and aggregated tau, suggesting that Hsp90 inhibitors that upregulate these chaperones could provide neuroprotection. We recently identified a small molecule novobiocin analogue, **A4** that induces Hsp90 overexpression at low nanomolar concentrations and sought to test its neuroprotective properties. **A4** protected neurons against Aβ-induced toxicity at low nanomolar concentrations that paralleled its ability to upregulate Hsp70 expression. **A4** exhibited no cytotoxicity in neuronal cells at the highest concentration tested, 10 μM, thus providing a large therapeutic window for neuroprotection. In addition, **A4** was transported across BBMECs *in vitro*, suggesting the compound has the ability to permeate the blood brain barrier *in vivo*. Taken together, these data establish **A4**, a C-terminal inhibitor of Hsp90, as a potent lead for the development of a novel class of compounds to treat Alzheimer's Disease.

Introduction

The accumulation of aggregated, fibrillar proteins is a unifying characteristic of chronic, late-onset neurodegenerative diseases, leading to intense research on the protein quality control systems within cells. The accumulation of protein aggregates within or outside neurons is a characteristic of the two most common age-related neurodegenerative diseases, Alzheimer's (AD) and Parkinson's Disease (PD). AD is characterized by two distinct cytopathologies: β-amyloid (Aβ) plaques and neurofibrillary tangles (NFTs) (1). Normally, the microtubule-associated protein tau is expressed in the neuronal cytoplasm where it serves to stabilize the microtubule network in axons. In AD, however, tau becomes hyperphosphorylated and results in misfolded proteins that dissociate from microtubules and form filamentous aggregates that polymerize into NFTs (2). PD is characterized by the accumulation of Lewy bodies composed primarily of fibrillar α-synuclein (3). Other neurodegenerative diseases such as Huntington's disease, amyotrophic lateral sclerosis, prion diseases, and the taupathies are also characterized by similar protein aggregates.

Molecular chaperones are responsible for the conformational maturation of nascent polypeptides, refolding denatured and aggregated proteins, and directing the ubiquitination and degradation of proteins that cannot be repaired. One family of molecular chaperones, the heat shock proteins (Hsps), has a profound effect on critical cellular processes such as cell cycle regulation and apoptosis due to its diverse biological activities (4,5). The major Hsp, Hsp90, exerts its effects through a wide-array of co-chaperones, partner proteins, and immunophilins, forming the major chaperone system

responsible for protecting cells against toxicity resulting form the accumulation of protein aggregates. Based on these properties, it was proposed that increased chaperone activity may refold aggregating proteins and have therapeutic applications for the treatment of neurodegenerative diseases. Recently, Greengard and coworkers demonstrated that increased Hsp70 and Hsp90 levels resulted in decreased tau aggregates and provided neuroprotection in cells expressing mutant tau that becomes hyperphosphorylated as in AD brain (6). Consequently, regulation of Hsp70 and Hsp90 expression levels has been pursued as a novel approach toward the treatment of diseases caused by protein aggregates.

Cellular stresses such as elevated temperature, abnormal pH, oxidative stress, and malignancy result in the denaturation of native proteins as well as the overexpression of molecular chaperones to refold these structures or target them for degradation via the ubiquitin-proteasome pathway (7-9). Upon exposure to these stresses, Hsp90 and Hsp70 levels are increased to assist in the rematuration process. The expression of these heat shock proteins is tightly regulated by the transcription factor heat shock factor 1 (HSF1). Under normal conditions, Hsp90 forms a stable complex with HSF1 and prevents the transcriptional activation of the heat shock response (10). Cellular stressors result in destabilization of Hsp90/HSF1, the subsequent trimerization and phosphorylation of HSF1, and its translocation to the nucleus, where it induces Hsp expression (11,12). Another key protein in the Hsp90 heteroprotein complex is the co-chaperone CHIP (carboxyl terminus of the Hsc70-interacting protein) (13). CHIP binds Hsp70 through its tetratricopeptide repeat (TPR) domain and also possesses intrinsic ubiquitin ligase activity, suggesting a direct link between the chaperone and the ubiquitin-proteasome

pathway which may modulate the cellular equilibrium of protein folding and degradation (14).

Previously identified inhibitors of Hsp90 include geldanamycin (GA, Fig. 1) and its derivatives, which bind to the N-terminal ATP binding pocket. These N-terminal inhibitors manifest their activity by competitive inhibition of ATP, which serves as the requisite source of energy for the Hsp90-mediated protein folding process. The concentration of N-terminal inhibitors required to induce degradation of Hsp90-dependent client proteins is approximately equal to that needed to increase Hsp70 and Hsp90 levels. Unfortunately, there is a small therapeutic window for the treatment of neurodegenerative diseases with these molecules because cytotoxicity generally occurs at these concentrations. To circumvent these issues, the further development of Hsp90 inhibitors for the treatment of neurodegenerative diseases requires the identification of non-toxic inhibitors that provide a large therapeutic window, but stimulate the dissociation of HSF1 from Hsp90 at low concentrations and penetrate the blood-brain barrier (BBB). A compound with such attributes could potentially regulate the refolding of protein aggregates, including tau, or initiate their degradation through the ubiquitin-proteasome pathway and provide an alternative approach toward the development of drugs for these diseases.

Recently, an additional ATP-binding site on the C-terminus of Hsp90 was elucidated and novobiocin (Fig. 1) was identified as a competitive inhibitor of ATP with low affinity (~ 700 μM) (15). Elucidation of this new inhibitor and nucleotide-binding domain provided a novel opportunity to regulate the Hsp90-mediated protein folding machinery with small molecules. In an effort to prepare more efficacious inhibitors, a

small library of novobiocin analogues was prepared and evaluated (16). **A4** induced Hsp90 expression at concentrations significantly lower than those needed for client protein degradation. Because of this finding, we proposed that **A4** possessed unique properties that could prove useful for the treatment of neurodegenerative diseases. In this communication, we detail the neuroprotective effects of **A4** and describe its potential promise as a therapeutic lead compound for the treatment of Alzheimer's Disease.

Results

Synthesis of A4. In order to prepare sufficient quantities of **A4** for biological testing, it was necessary to devise an efficient synthetic route. As shown in Scheme 1, the coumarin ring (**2**) was constructed by the condensation of commercially available benzaldehyde **1** with glycine in the presence of acetic anhydride (17). After selective deprotection, the free phenol was coupled with the trichloroacetimidate of noviose carbonate (**4**) (18) in the presence of catalytic boron trifluoride etherate (19). **A4** was furnished in excellent yield by treatment of the cyclic carbonate (**5**) with triethylamine in methanol, resulting in solvolysis of the carbonate to afford the desired product.

Neuroprotective effects of A4. Treatment of embryonic primary neurons and neuronal cell cultures with $A\beta_{25-35}$ produces distinct morphological changes and eventual cell death (20). Pretreatment with neuroprotective agents can reduce or abolish these effects. The neuroprotective effects of **A4** were determined in primary neurons derived from embryonic rat brain exposed to Aβ (10 μM) in the presence or absence of drug for 48 h.

In the majority of experiments, the toxic $A\beta_{25-35}$ was used to induce cell death. However, a smaller number of cultures were treated with the $A\beta_{1-42}$ formed in excess in AD. In all cases we found that $A\beta_{1-42}$ produced effects virtually identical to those of $A\beta_{25-35,}$ and the toxicity of both was dramatically inhibited in the presence of the drug. The percentage of surviving neurons was determined by labeling with the fluorescent dyes calcein-AM and propidium iodide as previously described (21,22). The numbers of calcein-labeled live cells and propidium iodide-labeled dead neurons in several fields were visualized via fluorescence microscopy and counted as described. In our studies, treatment of primary cortical neurons with Aβ alone (10 μM) represented the basal level for neuronal survival. Pretreatment of neuronal cells with **A4** prevented Aβ–induced toxicity in a dose-dependent fashion, with an EC_{50} value of ~6 nM (Fig. 2). While there were minor neuroprotective effects associated with **A4** concentrations as low as 0.5 nM, significant protection was not demostrated until 5 nM. Treatment of neuronal cells with **A4** alone at 20X the EC_{50} value (100 nM) did not result in any observed neurotoxicity.

A4 up-regulates Hsp70 in neuronal cells. Inhibition of Hsp90 induces overexpression of both Hsp90 and Hsp70 through dissociation of Hsp90-HSF1 complexes and subsequent translocation of HSF1 to the nucleus (23). Induction of both Hsp90 and Hsp70 by GA in cultured cells was reported to result in decreased levels of aggregated tau and increased levels of soluble tau, indicating that Hsp90 inhibitors can reduce toxic tau aggregates (6). In our neuronal cultures, **A4** significantly increased Hsp70 levels at the concentration of 0.2 μM (Figs. 3a and b). However, concentrations of **A4** as low as 1nM also led to increases in Hsp70 levels, compared to DMSO controls, after 48 h

incubation. Hsp70 induction at 0.2 μM was comparable to that seen upon treatment with GA at the same concentration, suggesting **A4** could potentially attenuate tau aggregation in a manner similar to that reported for GA. In addition, incubation with higher concentrations of **A4** (1 and 10 μM) did not significantly increase Hsp70 levels, suggesting that the maximal neuroprotective effects of **A4** can be elicited at concentrations significantly lower than any potential cytotoxic effects.

A4 up-regulation of Hsps does not mirror client protein degradation. To determine whether **A4** exhibited its neuroprotective effects via Hsp90 inhibition, **A4** was incubated with the well-studied mutated androgen receptor (AR)-dependent prostate cancer cell line, LNCaP. As reported previously, **A4** induced Hsp90 at the lowest concentrations tested (10nM). In contrast, degradation of the Hsp90 client proteins AR and AKT did not occur until 1 μM, providing a therapeutic window of ≥ 200 fold, suggesting increased levels of Hsps do not correlate directly with client protein degradation for inhibitors of the C-terminal ATP-binding pocket (16).

Anti-proliferative effects of A4. For most Hsp90 inhibitors, efficacy in degrading client proteins, such as Her2 and Akt, in two distinct cancer cell lines, SkBr3 and MCF-7, correlates well with their anti-proliferative effects (24). The anti-proliferative effect of GA treatment in these cell lines is well established, and we confirmed almost complete cytotoxicity with GA at 1 μM. GA elicited dose-dependent anti-proliferation in both cell lines, and the IC_{50} values were comparable to those reported previously (18 and 133 nM, respectively). In contrast, **A4** demonstrated no anti-proliferative effects in either cell line

up to 100 μM (Fig. 4a and b), a concentration well above that necessary for complete neuroprotection, suggesting that C-terminal inhibitors possess a mechanism of action distinct from GA and other inhibitors of the N-terminus. When the effects of GA and **A4** alone were examined in neuronal cells, GA induced significant cytotoxicity at 10 μM after 24 h (Fig. 4c). Lower concentrations of GA led to substantial cytotoxicity after 72 h of incubation (data not shown). In contrast, 10 μM of A4 caused no toxic effects even after incubation for 72 h, clearly indicating a novel utility for C-terminal inhibitors.

Transport of A4 across the blood-brain barrier. The BBB expresses high levels of P-glycoprotein (P-gp), an efflux pump responsible for the extrusion of numerous drugs and other xenobiotics from cells (25). The rhodamine 123 assay is often used to predict whether a compound is a potential substrate for P-gp. In this assay, rhodamine 123 is used as a surrogate P-gp substrate. If **A4** is a substrate for P-gp, then its addition will increase rhodamine 123 uptake relative to the negative control determined by monitoring intracellular fluorescence. Taxol, a microtubule stabilizing agent that exhibits neuroprotective effects both *in vitro* and *in vivo*, is hampered as a CNS therapeutic because it is a known P-gp substrate (26). Used as a positive control, Taxol significantly increased rhodamine 123 uptake in bovine brain microvessel endothelial cells (BBMECs), while addition of **A4** had no effect on uptake even up to 50 μM, suggesting **A4** is not likely a substrate for P-gp (Fig. 5a).

The ability to partition across the blood-brain barrier is an essential property of drugs that are designed to produce beneficial effects on neuronal cells of the central nervous system (CNS). Transport across primary cultures of BBMECs *in vitro* often

correlates well with the BBB permeability of a compound *in vivo* (27). In the side-by-side diffusion chamber, **A4** exhibited time-dependent linear transport across BBMECs for up to 90 min in the receiving chamber (Fig.5b). The concentration of **A4** at 90 min in the receiving chamber (1.2 μM) was 200-fold greater than the concentration necessary (5 nM) for 50% neuroprotection from Aβ-induced toxicity. These data offer preliminary indication that pharmacologically active amounts of **A4** might penetrate the BBB and result in the presence of drug in brain tissue.

Discussion

Intracellular protein aggregation is a defining pathology of numerous neurodegenerative disorders, including Huntington's disease, PD, and AD (1). In AD, tau aggregation results from its hyperphosphorylation and subsequent disassociation from microtubules to form filamentous aggregates that polymerize into NFTs. It has been proposed that increased Aβ levels lead to alterations in intracellular kinase and phosphatase activity, which ultimately results in pathogenic hyperphosphorylation. Therapeutic strategies directed at numerous individual pharmacological targets in this pathway have been tested as potential treatments for AD. Strategies designed to reduce the levels of Aβ peptides in the brain include inhibition of proteolytic enzymes that form Aβ, prevention of Aβ oligomerization through metal chelators, and upregulation of proteases that normally degrade Aβ (28). Previous attempts to prevent tau aggregation have generally focused on the identification and inhibition of specific kinases involved in its abnormal phosphorylation. Microtubule-stabilizing agents such as Taxol may prevent

loss of the microtubule-stabilizing activity of tau and such agents have also exhibited neuroprotective activity against a variety of toxic insults (21).

The inducible nature of Hsps makes Hsp90 inhibition a unique and exciting strategy for the treatment of AD and other neurodegerative disorders in which protein aggregation is a major pathology. The direct mechanism responsible for the neuroprotective effects of Hsp90 inhibitors appears to be the upregulation of chaperones that can resolubilize these toxic aggregates. Dou et al suggest that Hsps can directly associate with tau proteins and prevent their misfolding and subsequent aggregation (6). The independent identification of a series of Hsp90 inhibitors that lower intracellular tau levels through induction of Hsps supports this hypothesis (29). Recently, tau was identified as a substrate for CHIP, and it was suggested that increased levels of Hsp70 can shift the equilibrium towards formation of the CHIP/Hsp70/tau complex, resulting in rapid clearance of tau aggregates via the ubiquitin-proteasome pathway (30). Therefore, induction of Hsp70 appears to play a major role in the removal of tau aggregates. More recently, a high-throughput assay designed to identify compounds that block JNK-dependent apoptosis identified AEG3482 as an Hsp90 inhbitor with potential neuroprotective properties (31). The data suggest that JNK inhibition is a downstream result of Hsp90 inhibition and subsequent Hsp70 induction. Hsp70 is known to bind JNK and disrupt substrate interactions, thereby, inhibiting its kinase activity. Taken together, this evidence strongly suggests that increased Hsp70 levels are a key factor in the neuroprotective effects of **A4** and other Hsp90 inhibitors.

The development of Hsp90 inhibitors as chemotherapeutics has focused almost entirely on their use as anticancer agents. Numerous Hsp90 client proteins are essential

for the growth and proliferation of cancer cells, resulting in cytotoxic effects. This detrimental property has been a key reason behind their lack of development as neuroprotective agents. In contrast to GA and other N-terminal inhibitors, **A4** is the first compound reported that induces Hsp70 and provides complete protection against Aβ-induced toxicity at non-cytotoxic concentrations. In fact, no toxicity was observed in our assays even at 20,000 X the EC_{50} (100 μM) in non-neuronal cells, a concentration at which GA is severely toxic. In addition, **A4** increases Hsp90 levels at concentrations ~ 200-fold less than those required for client protein degradation. This provides a large therapeutic window for treatment of several disorders in which chaperones provide a protective effect. These attributes make **A4** an ideal lead compound for development as a novel chemotherapeutic that might slow progression of neurodegeneration in AD. Current studies are underway to evaluate this new lead compound in animal models as well as in cells transfected with mutant tau to elicit the effects of p-tau aggregation.

A major obstacle for any drug whose site of action is within the CNS is the ability to penetrate the BBB. In general, only small molecules with high lipid solublility and relatively low molecular weight (~400-500 Da) are able to cross the BBB (32). To date, few brain disorders have responded to small molecule therapies and many, including AD, PD, and Huntington's disease have not been successfully targeted (33,34). The time-dependent linear transport of **A4** across BBMECs *in vitro* suggests that significant concentrations of the drug will be available to the CNS *in vivo*. Within 15 min, the concentration of **A4** present in the abluminal chamber was enough to provide full neuroprotective effects as demonstrated *in vitro*, suggesting that *in vivo* neuroprotection could be fast-acting.

In summary, we have further characterized a novel C-terminal Hsp90 inhibitor, **A4,** as a potent neuroprotective agent for the treatment of AD. The protection against Aβ-induced toxicity exhibited by **A4** at concentrations that are non-cytotoxic provides a large therapeutic window and establishes it as the first Hsp90 inhibitor to manifest this unique property. In addition, the biological activities of **A4** suggest that C-terminal inhibitors of Hsp90 work through a different mechanism than the known N-terminal inhibitors and may exhibit other unique pharmacological profiles that will be useful for the treatment of other neurodegenerative disorders.

Uncited References

Refs. 35-40

Acknowledgments

This work was supported by NIH Grants R01CA120458 and U01CA39610 (B.S.J.B) and ISOA AG027419 and AG12993 (M.L.M).

References

1. Muchowski, P.J. (2002) *Neuron* **35,** 9-12.

2. Lee, V.M., Goedert, M., Trojanowski, J.Q. (2001) *Annu. Rev. Neurosci.* **24,** 1121-1159.

3. Goedert, M. (2001) *Nat. Rev. Neurosci.* **2,** 492-501.

4. Burrows, F., Zhang, H., Kamal, A. (2004) *Cell Cycle* **3,** 1530-1536.

5. Sreedhar, A.S., Kalmar, E., Csermely, P., Shen, Y.F. (2004) *FEBS Lett.* **562,** 11-15.

6. Dou, F., Netzer, W.J., Tanemura, K., Li, F., Hartl, U., Takashima, A., Gouras, G.K., Greengard, P., & Xu, H. (2002) *Proc. Natl. Acad. Sci.* **100,** 721-726.

7. Lindquist, S., Craig, E.A. (1988) *Annu. Rev. Genet.* **22,** 631-677.

8. Watson, K. (1990) *Adv. Micro. Physiol.* **31,** 183-223.

9. Lathigra, R.B., Butcher, P.D., Garbe, T.R., Young, D.B. (1991) *Curr. Top. Microbiol. Immunol.* **167,** 125-143.

10. Shi, Y., Mosser, D.D., Morimoto, R.I. (1998) *Genes Dev.* **12,** 654-666.

11. Rabindran, S.K., Wisniewski, J., Li, L., Li, G.C., Wu, C. (1994) *Mol. Cell. Biol.* **14,** 6552-6560.

12. Zuo, J., Rungger, D., Voellmy, R. (1995) *Mol. Cell. Biol.* **15,** 4319-4330.

13. Ballinger, C.A., Connell, P., Wu, Y., Hu, Z., Thompson, L.J., Yin, L-Y., Patterson, C. (1999) *Mol. Cell. Biol.* **19,** 4535-4545.

14. Dai, Q., Zhang, C., Wu, Y., McDonough, H., Whaley, R.A., Godfrey, V., Li, H-H., Madamanchi, N., Xu, W., Neckers, L. et al. (2003) *EMBO J.* **22,** 5446-5458.

15. Marcu, M.G., Chadli, A., Bouhouche, I., Catelli, M., Neckers, L.M. (2000) *J. Biol. Chem.* **275,** 37181-37186.

16. Yu, X.M., Shen, G., Neckers, L., Blake, H., Holzbeierlein, J., Cronk, B., & Blagg, B.S.J. (2005) *J. Am. Chem. Soc.* **127,** 12778-12779.

17. Madhavan, G.R., Balraju, V., Mallesham, B., Chakrabarti, R., & Lohray, V.B. (2003) *Bioorg. Med. Chem. Lett.* **13,** 2547.

18. Yu, X.M., Shen, G., & Blagg, B.S.J. (2004) *J. Org. Chem.* **69,** 7375.

19. Shen G., Yu, X.M., & Blagg, B.S.J. (2004) *Bioorg. Med. Chem. Lett.* **14,** 5903.

20. Pike, C.J., Walencewick-Wasserman, A.J., Kosmoski, J., Cribbs, D.H., Glabe, C.G., & Cotman, C.W. (1995) *J. Neurochem.* **64,** 253-265.

21. Michaelis, M.L., Ansar, S., Chen, Y., Reiff, E.R., Seyb, K.I., Himes, R.H., Audus, K.L., Georg, G.I. (2005) *J. Pharmacol. Exp. Ther.* **312,** 659-668.

22. Michaelis, M.L., Ranciat, N., Chen, Y., Bechtel, M., Ragan, R., Hepperle, M., Liu, Y. and Georg, G.I. (1998) *J. Neurochem.* **70,** 1623-1627.

23. Csermely, P., Schnaider, T., Soti, C., Prohaszka, Z., & Nardai, G. (1998) *Pharmacol. Ther.* **79,** 129-168.

24. Dai, C., Whitesell, W. (2005) *Future Oncol.* **1**, 529-540.

25. Schinkel, A.H., Wagenaar, E., Mol, C.A.A.M, van Deemter, L. (1996) *J. Clin Invest.* **97**, 2517.

26. van Asperen, J., Mayer, U., van Tellingen, O., Beijnen, J.H. (1997) *J Pharm Sci*. **86**, 881.

27. Audus, K.L., Borchardt, R.T. (1986) *Pharm Res* **3**, 81.

28. Michaelis, M.L. (2003) *Sci. Med.* **9,** 214-226.

29. Dickey, C.A., Eriksen, J., Kamal, A., Burrows, F., Kashibhatla, S., Eckman, C.B., Hutton, M., Petrucelli, L. (2005) *Curr. Alz. Res.* **2,** 231-238.

30. Shimura, H., Miura-Shimura, Y., Kosik, K.S. (2004) *J. Biol. Chem.* **279,** 4869-4876.

31. Salehi, A.H., Morris, S.J., Ho, W-C., Dickson, K.M., Doucet, G., Milutinovic, S., Durkin, J., Gillard, J.W., Barker, P.A. (2006) *Chem. Biol.* **13,** 213-223.

32. Pardridge, W. (2003) *Mol. Inter.* **3,** 90-105.

33. Ajay, Bemis, G.W., Murcko, M.A. (1999) *J. Med. Chem.* **42,** 4942-4951.

34. Ghose, A.K., Viswanadhan, V.N., Wendoloski, J.J. (1999) *J. Comb. Chem.* **1,** 55-68.

35. Zhang, B., Maiti, A., Shively, S., Lakhani, F., McDonald-Jones, G., Bruce, J., Lee, E.B., Xie, S.X., Joyce, S., Li., C. (2005) *Proc. Natl. Acad. Sci. USA* **102,** 227-231.

36. Michaelis, M.L., Walsh, J.L., Pal, R., Hurlbert, M., Hoel, G., Bland, K., Foye, J. and Kwong, W.H. (1994) *Brain Res.* **661,** 104-116.

37. Zaidi, A., Michaelis, M.L. (1999) *Free Radic. Biol. Med.* **27,** 810-821.

38. Zaidi, A., Barron, L., Sharov, V.S., Schoneich, C. Michaelis, E.K., Michaelis, M.L. (2003) *Biochem.* **42,** 12001-12010.

39. Silverstein, P.S., Karunaratne, D.N., Audus, K.A. (2003) Current Protocols in Pharmacology. 7.7.1.

40. Audus, K.L., Ng, L., Wang, W., Borchardt, R.T. (1996) Plenum: New York, 239.

41. Seyb, K.I., Ansar, S., Bean, J., Michaelis, M.L. (2006) *J. Mol. Neurosci.* **28**, 111-123.

Figure 1.

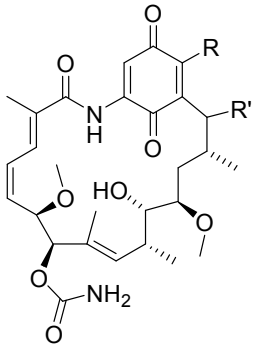

R = OMe, R' = H, **GA**
R = NHallyl, R' = H, **17-AAG**

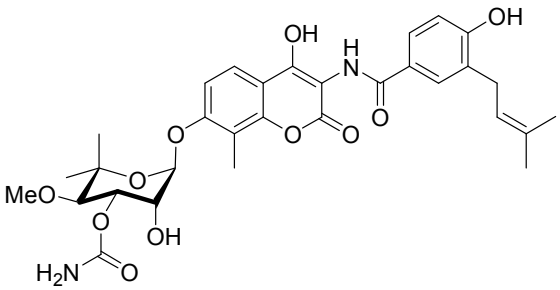

Novobiocin

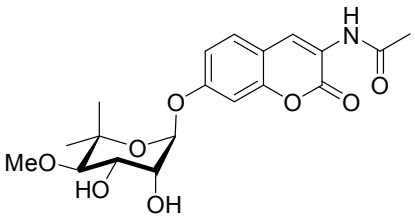

A4

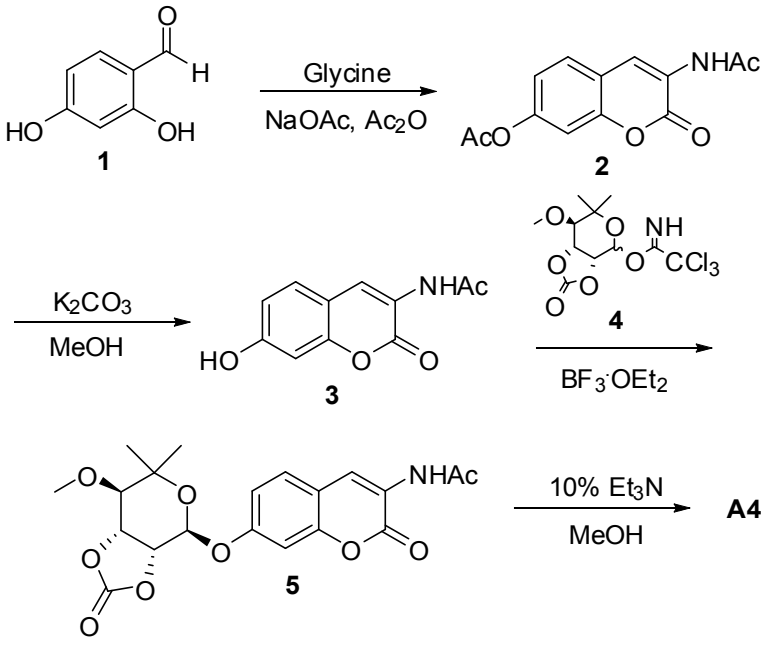

Scheme 1. Synthesis of **A4**.

Figure 2.

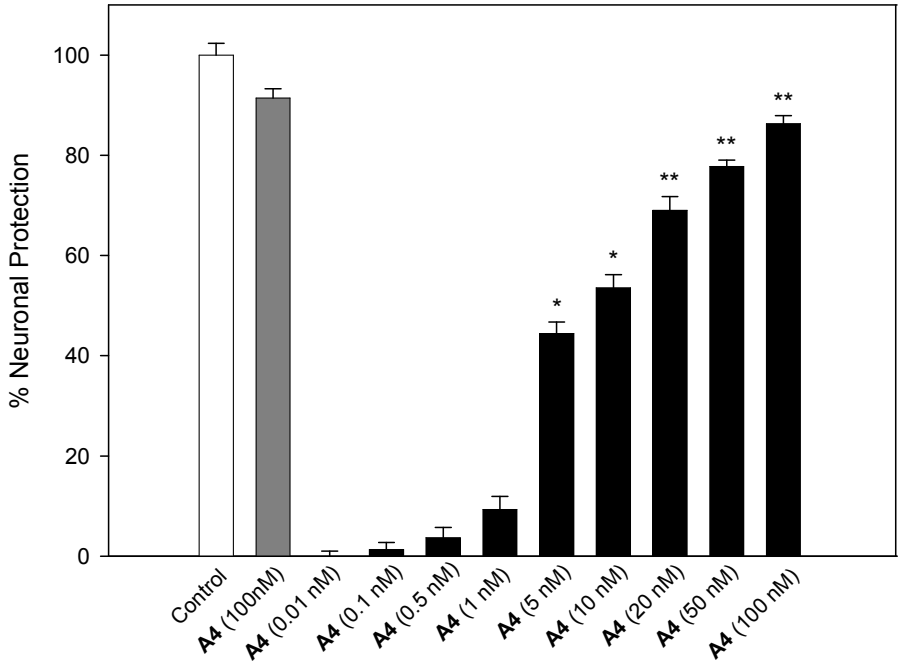
% Neuronal Protection
100
80
60
40
20
0
*
*
**
**
**
Control
A4 (100nM)
A4 (0.01 nM)
A4 (0.1 nM)
A4 (0.5 nM)
A4 (1 nM)
A4 (5 nM)
A4 (10 nM)
A4 (20 nM)
A4 (50 nM)
A4 (100 nM)

Figure 3.

(a)

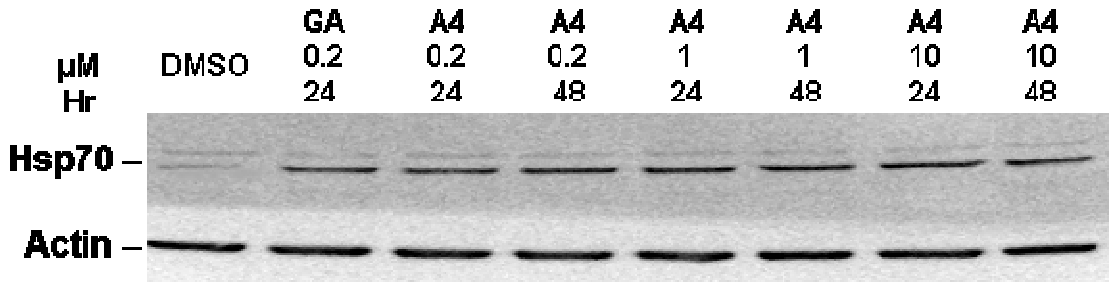
μM
Hr
DMSO
GA 0.2 24
A4 0.2 24
A4 0.2 48
A4 1 24
A4 1 48
A4 10 24
A4 10 48
Hsp70
Actin

(b)

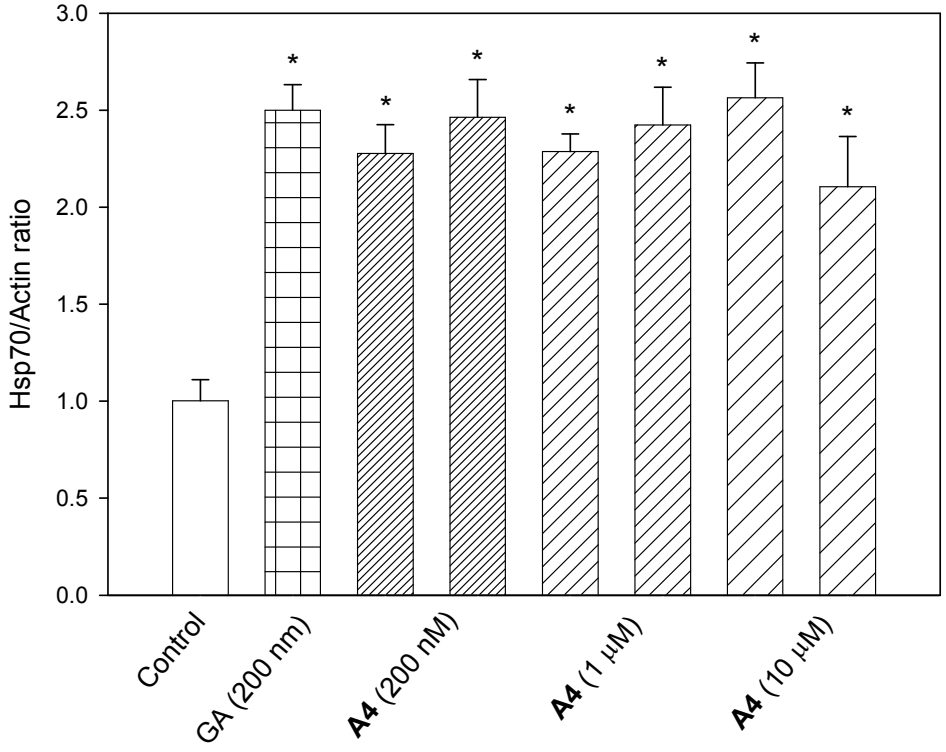
Hsp70/Actin ratio
3.0
2.5
2.0
1.5
1.0
0.5
0.0
Control
GA (200 nm)
A4 (200 nM)
A4 (1 μM)
A4 (10 μM)

Figure 4.

(a)

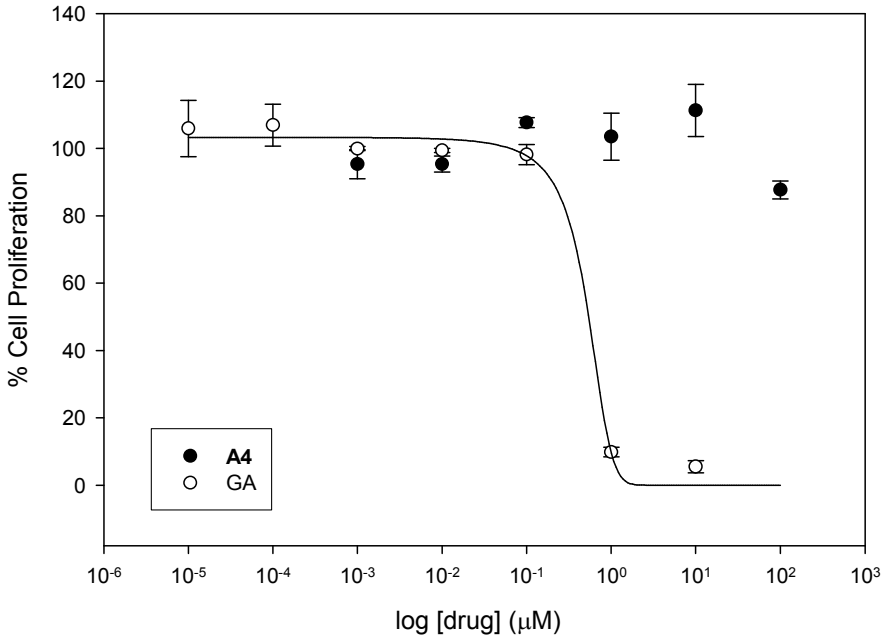
% Cell Proliferation
log [drug] (μM)
A4
GA

(b)

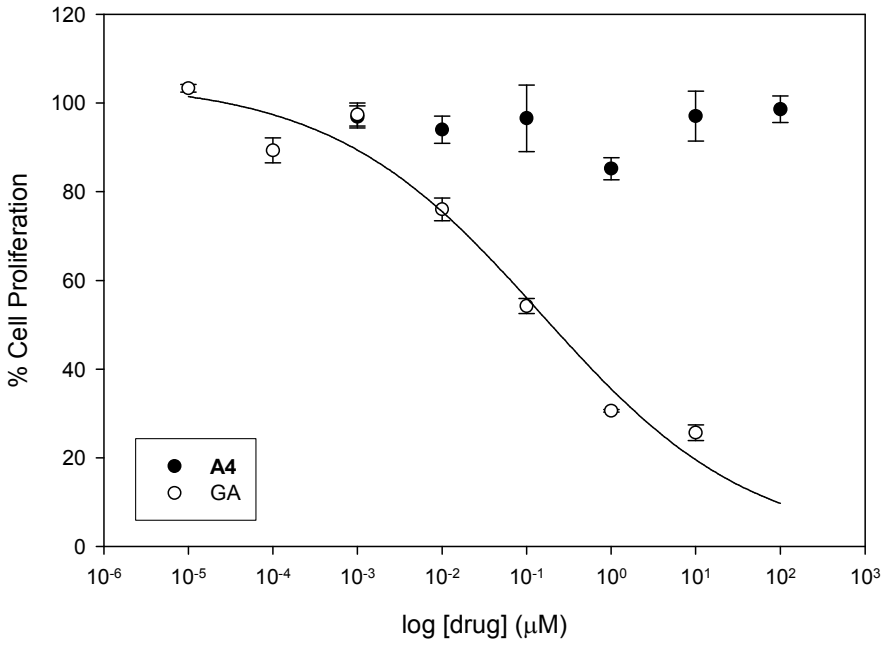
% Cell Proliferation
log [drug] (μM)
A4
GA

(c)

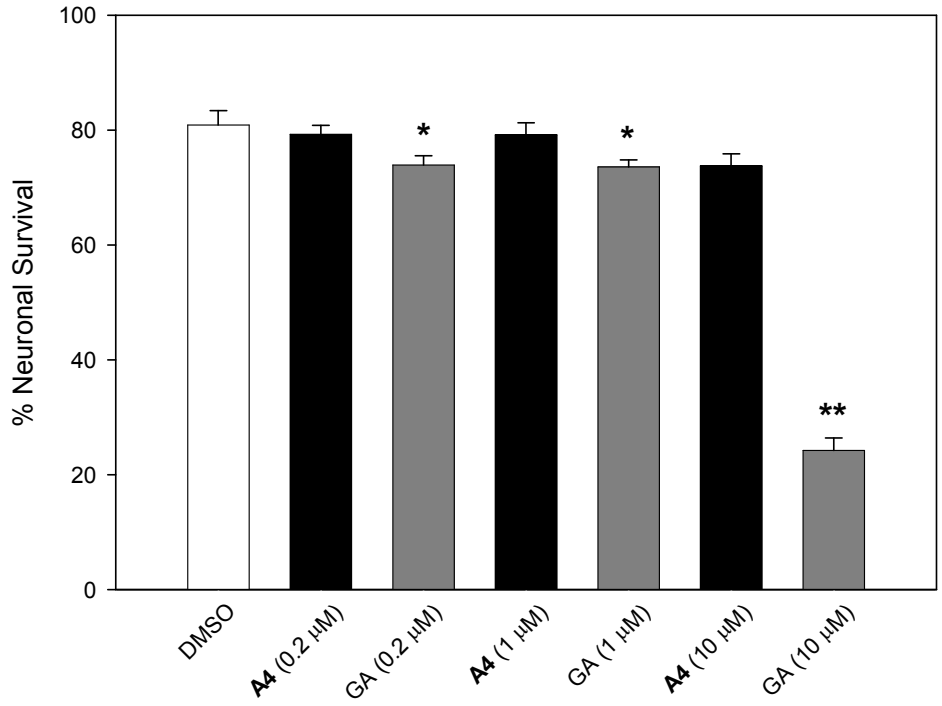
100
80
60
40
20
0
% Neuronal Survival
*
*
**
DMSO
A4 (0.2 μM)
GA (0.2 μM)
A4 (1 μM)
GA (1 μM)
A4 (10 μM)
GA (10 μM)

Figure 5.

(a)

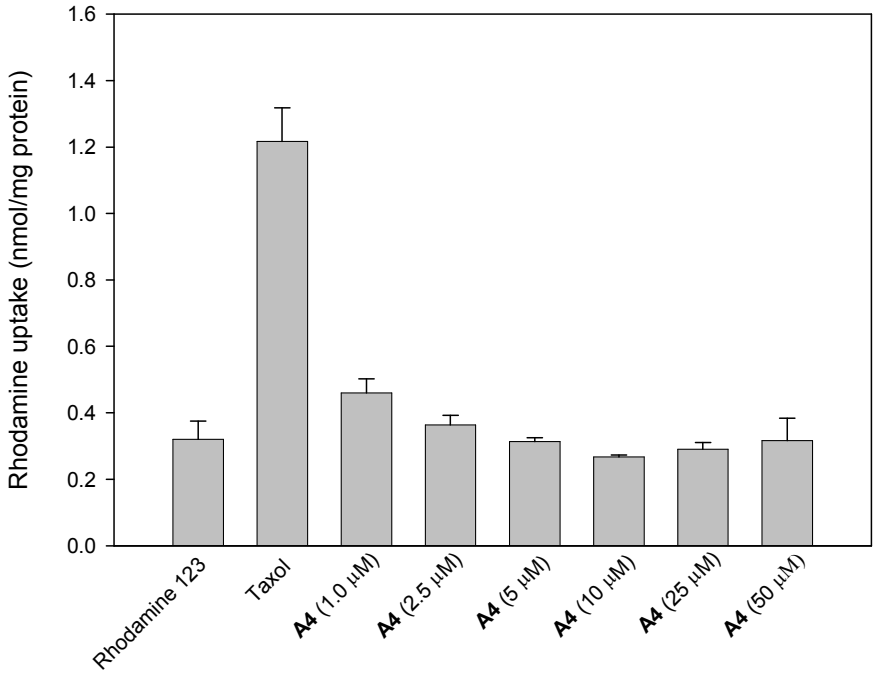
Rhodamine uptake (nmol/mg protein)
1.6
1.4
1.2
1.0
0.8
0.6
0.4
0.2
0.0
Rhodamine 123
Taxol
A4 (1.0 μM)
A4 (2.5 μM)
A4 (5 μM)
A4 (10 μM)
A4 (25 μM)
A4 (50 μM)

(b)

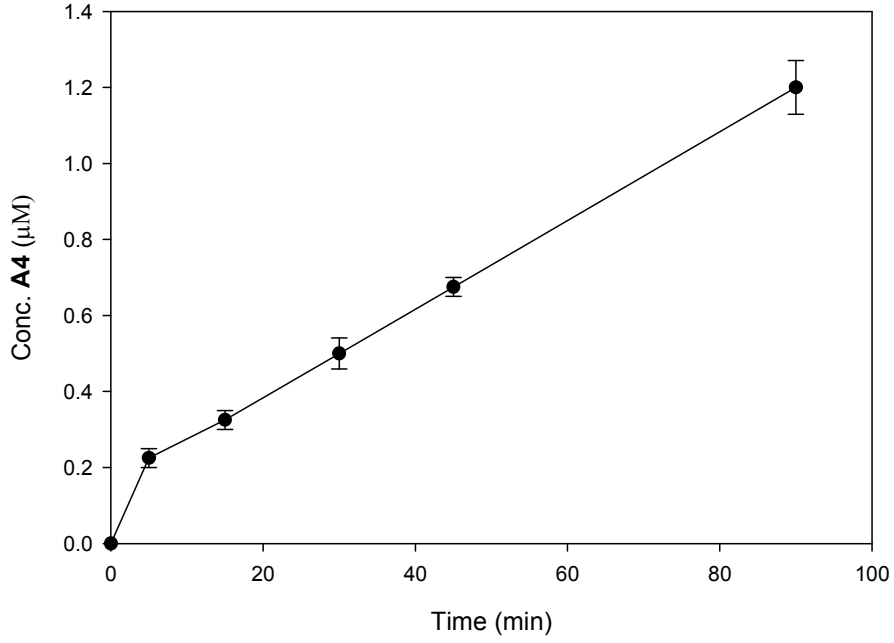
Conc. A4 (μM)
1.4
1.2
1.0
0.8
0.6
0.4
0.2
0.0
0
20
40
60
80
100
Time (min)

Figure Legends

Figure 1. Structures of Hsp90 Inhibitors. Structures of the N-terminal Hsp90 inhibitors, GA and 17-AAG, and the C-terminal inhibitors, novobiocin and **A4**.

Figure 2. Dose-dependent A4 protection against $A\beta_{25-35}$ toxicity. Neuronal cells were treated with vehicle only (clear), **A4** (100 nM, gray), or **A4** + Aβ (10 μM, black). The indicated concentrations of **A4** were added 2 h before Aβ. Cell viability was determined 48 h later as described in the methods section. *$p<0.05$ and **$p<0.01$, for Aβ alone vs. **A4** + Aβ. Data represent mean survival ± SE for three separate experiments with ~1500 cells per treatment condition. Aβ (10 μM) alone was used as 0% survival and DMSO control was used as 100% protection.

Figure 3. A4 upregulates Hsp70 in neuronal cells. (a) Primary cortical neurons were incubated with GA or **A4** for 48 h and probed for Hsp70 and actin (control). (b) The ratio between Hsp70 to actin was determined for each treatment as described (41). The first and second bars of each **A4** treatment represent 24 and 48 h, respectively. *$p<0.05$ compared to DMSO control. Each bar represents the average of four separate experiments.

Figure 4. Anti-proliferative and toxic effects of A4 and GA. MCF-7 (a) or SkBr3 (b) cells were incubated with **A4** (closed circles) or GA (open circles) at varying concentrations. Viable cells were quantitated using the MTS/PMS assay as described in the methods section. Values represent the mean ± SE for one representative experiment

performed in triplicate. Assays were replicated three times and the IC_{50} of GA correlated well with previously published values (MCF-7=133 ± 2 and SkBr3=18 ± 5 nM). In (c), neuronal cells were treated with DMSO (open bar), **A4**, or GA at the indicated concentrations, and cell viability was determined 24 h later as described in methods sections. The data represent the mean percentage ± SE of surviving neurons for three separate experiments. *$p<0.05$ for control versus GA, and **$p<0.001$ for control verus GA.

Figure 5. Efflux and Transport of A4 across BBMECs. (a) BBMECs were grown to confluency and incubated with Rhodamine 123 (5 μM) alone or **A4** (indicated concentrations) + Rhodamine 123 as described in methods section. Taxol (10 μM) was used as a positive P-gp substrate. (b) BBMECs were grown to confluency on polycarbonate membranes and **A4** (10 μM) was added to the donor chamber. Aliquots from the receiver chamber were taken at the noted time points and analyzed by RP-HPLC for **A4** permeation across the cell layer.

Appendix 2: Structures of Paclitaxel Derivatives

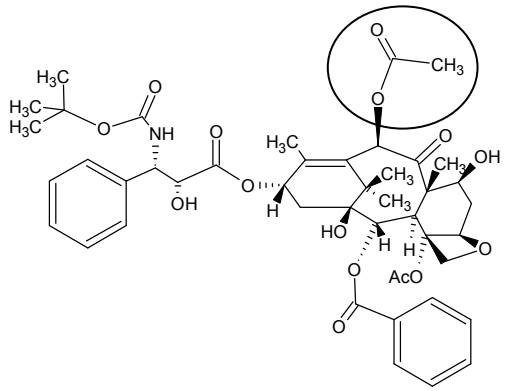

BJT2-59 (β-acetate ester, C10 position)

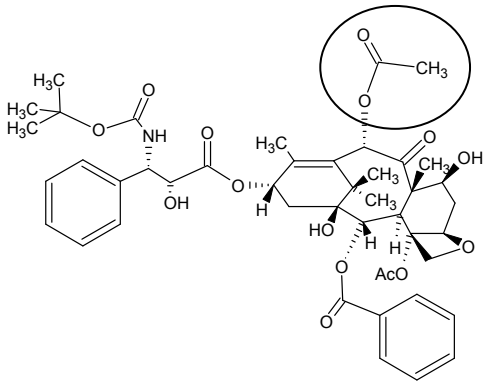

BJT1-109 (α-acetate ester, C10 position)

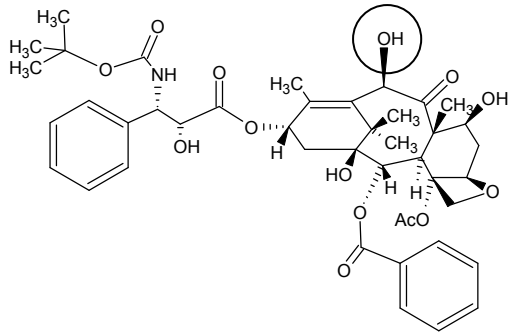

BJT1-97 (β-hydroxy, C10 position)

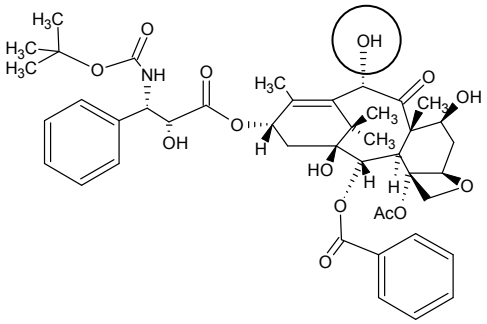

docetaxel (α-hydroxy, C10 position)

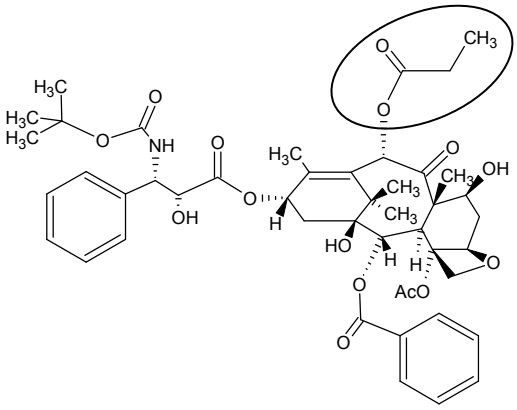

SLA269 (α - propionate, C10 position)

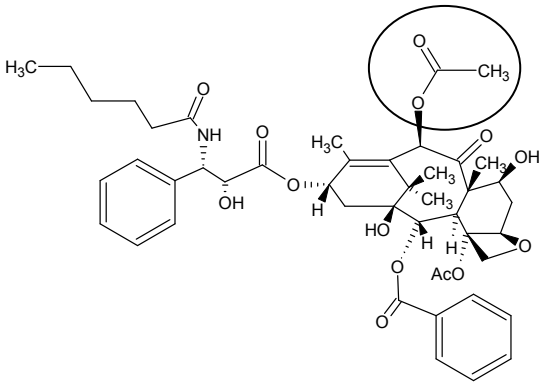

Taxol C (β-acetate ester, C10 position)

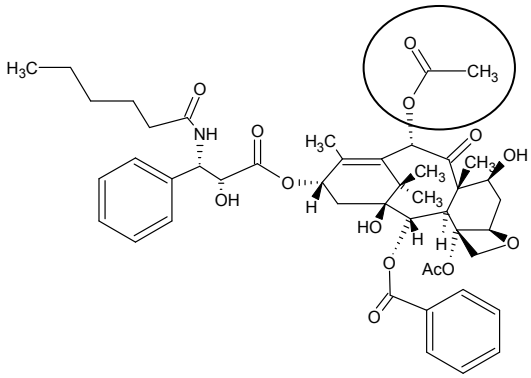

JTS1279 (α-acetate ester, C10 position)

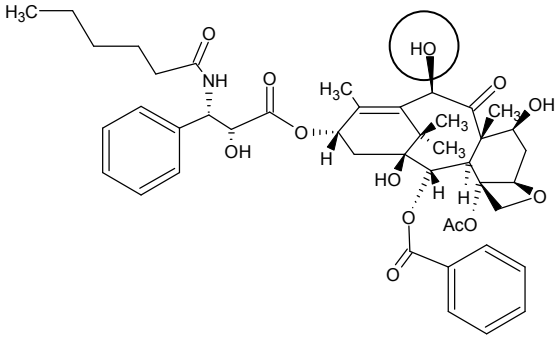

JTS6263 (β-hydroxy, C10 position)

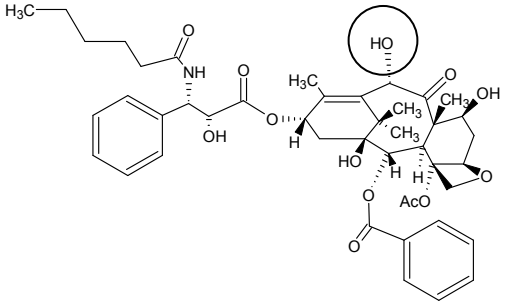

JTS6209 (α-hydroxy, C10 position)

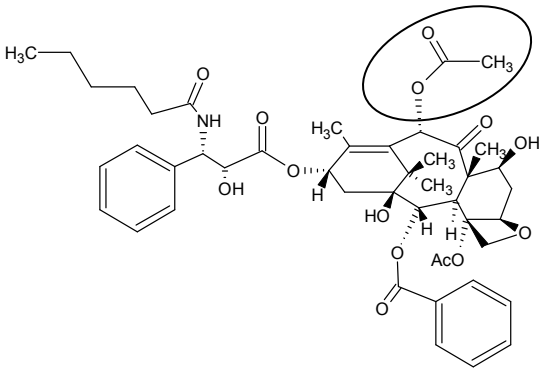

JTS6221 (α-propionate, C10 position)

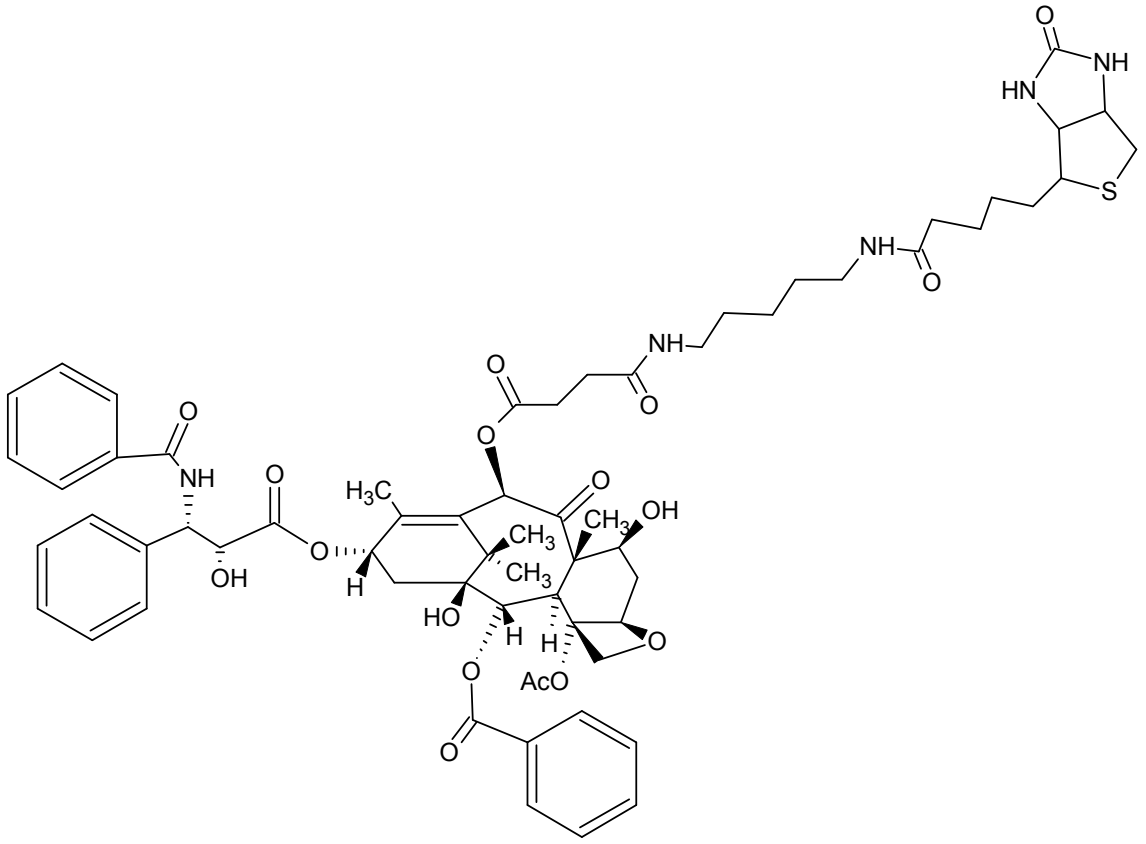

JO2-38C (biotin linked at the C10 position)

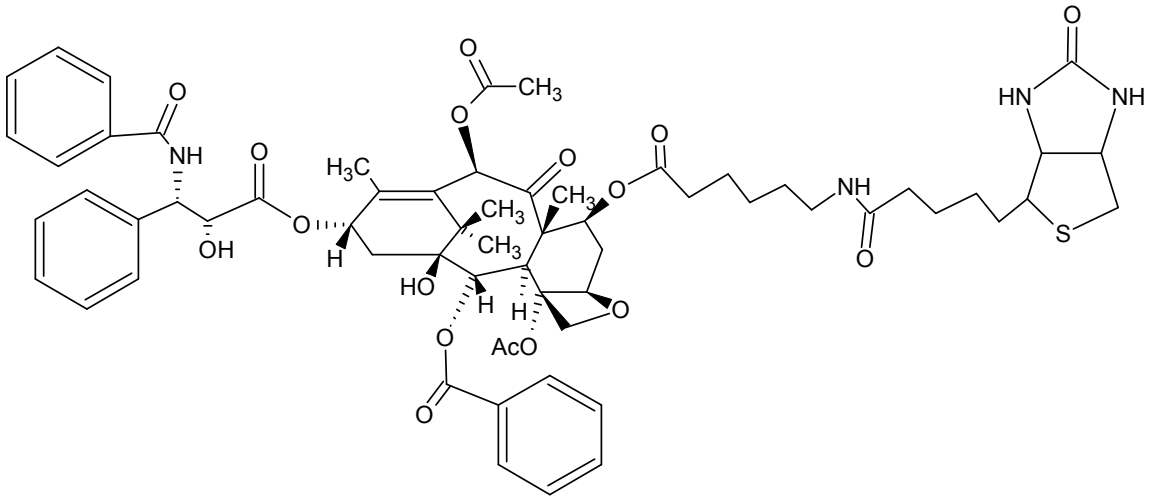

JTS4169 (biotin linked at the C7 position)